Institut für Ernährungswissenschaft
Professur für Ernährung des Menschen
Justus-Liebig-Universität Gießen

Einfluss von Anthocyanen und ihrer Metabolite auf die Migration und die Aktivierung des NLRP3 Inflammasoms in kanzerogenen Zellen

DISSERTATION

zur Erlangung des Doktorgrades (Dr. rer. nat.)
im Fachbereich Agrarwissenschaften, Ökotrophologie und Umweltmanagement der Justus-Liebig-Universität Gießen

vorgelegt von

Inken Behrendt
aus Mönchengladbach

Gießen, 2024

Mit Genehmigung des Fachbereichs Agrarwissenschaften,
Ökotrophologie und Umweltmanagement der
Justus-Liebig-Universität Gießen

Gutachter:

1. Gutachter(in): Prof. Dr. med. Mathias Fasshauer
2. Gutachter(in): Prof. Dr. Ralf Schweiggert

„Nur ein Narr macht keine Experimente“

und

„Ohne Spekulation gibt es keine neue Beobachtung“

(*Charles Darwin*)

Inhaltsverzeichnis

Abkürzungsverzeichnis **4**

Abbildungsverzeichnis **5**

Tabellenverzeichnis **6**

1. Einleitung **7**

1.1 Anthocyane: Struktur, Vorkommen und Bioverfügbarkeit 7

1.2 Tumorerkrankungen, Inflammation und Migration 11

1.3 Kardiovaskuläre Erkrankungen, Inflammation und NLRP3 Inflammasom 14

2. Fragestellung **18**

3. Publikationen **20**

3.1 Influence of Plasma-Isolated Anthocyanins and Their Metabolites on Cancer Cell Migration (HT-29 and Caco-2) In Vitro: Results of the ATTACH Study 20

3.2 Plasma anthocyanins and their metabolites prevent in-vitro migration of pancreatic cancer cells, PANC-1 in a FAK- and NF-kB dependent manner: results from the ATTACH-study a randomized, controlled, crossover trial in healthy subjects 21

3.3 Grape/blueberry anthocyanins and their gut-derived metabolites attenuate LPS/nigericin-induced inflammasome activation by inhibiting ASC speck formation in THP-1 monocytes 22

4. Diskussion **23**

4.1 Einfluss von Anthocyanen und ihrer Metabolite auf die Migration kanzerogener Zellen 23

4.2 Einfluss von Anthocyanen und ihrer Metabolite auf die Aktivierung des NLRP3 Inflammasoms 28

5. Zusammenfassung **32**

6. Abstract **34**

7. Literaturverzeichnis **36**

8. Weitere Publikationen **44**

9. Erklärung **45**

Anhang **46**

Abkürzungsverzeichnis

ASC	*apoptosis-associated speck-like protein containing a caspase activating and recruitment domain*
ATTACH	*Anthocyanins Target Tumor cell Adhesion - Cancer vs. Endothelial Cell (HUVEC)*
CD	*cluster of differentiation*
FAK	*focal adhesion kinase*
5-FU	5-Fluorouracil
HUVECs	*human umbilical vein endothelial cells*
ICAM-1	*intercellular cell adhesion molecule*
IL	Interleukin
LGI	*low-grade inflammation,* chronische, niedrig-gradige Inflammation
LPS	Lipopolysaccharide
NFκB	*nuclear factor kappa B*
NLRP3	*NOD-like receptor pyrin domain-containing protein 3*
PBMCs	*peripheral blood mononuclear cells*
SFK	*Src familiy kinase*
TLR	*Toll-like*-Rezeptor
TNF-α	Tumornekrosefaktor-α
TOFIE	*time of flight inflammasome evaluation*
VCAM-1	*vascular cell adhesion molecule 1*
VEGF	*vascular endothelial growth factor*
Y397	Tyrosin 397

Abbildungsverzeichnis

Abbildung 1 Grundstruktur der in Lebensmitteln am häufigsten vorkommenden Anthocyanidine (eigene Darstellung modifiziert nach Krga und Milenkovic 2019). 7

Abbildung 2 Potenzieller Metabolismus von Cyanidin-3-Glukosid (eigene Darstellung nach Fang 2014; Ferrars et al. 2014b; Zhu et al. 2018). 10

Abbildung 3 Transendotheliale Migration der Tumorzellen (eigene Darstellung). 12

Abbildung 4 Formierung und Aktivierung des NLRP3 Inflammasoms in humanen Monozyten (eigene Darstellung). 17

Abbildung 5 *In vitro*-Modelle zur Untersuchung des Einflusses von Anthocyanen und ihrer Metabolite auf die Migration und die Aktivierung des NLRP3 Inflammasoms in kanzerogenen Zellen (eigene Darstellung). 19

Tabellenverzeichnis

Tabelle 1 Anthocyangehalt ausgewählter Lebensmittel. 8

Tabelle 2 Übersicht der an der Tumorzellmigration beteiligten Zelladhäsionsmoleküle und ihrer Liganden (nach Blankenberg et al. 2003; Cooper und Giancotti 2019). 13

1. Einleitung

1.1 Anthocyane: Struktur, Vorkommen und Bioverfügbarkeit

Bei Anthocyanen handelt es sich um glykosylierte, wasserlösliche sekundäre Pflanzeninhaltsstoffe, die für die rote bis blau-violette Farbe vieler Obst- und Gemüsesorten verantwortlich sind. Im Gegensatz dazu stellen Anthocyanidine die zuckerfreien Aglykone der Anthocyane dar (Krga und Milenkovic 2019). Diese bestehen aus zwei phenolischen Ringen (A- und C-Ring), die über einen O-heterozyklischen (C-Ring) Ring miteinander verbunden sind (Alappat und Alappat 2020). Obwohl bisher etwa 27 natürlich vorkommende Anthocyanidine bekannt sind (Krga und Milenkovic 2019), machen Cyanidin, Delphinidin und Pelargonidin sowie deren Methylester Petunidin, Peonidin und Malvidin zusammen mehr als 90 % aller Anthocyane aus und stellen somit die bedeutsamsten in Lebensmitteln vorkommenden Anthocyanidine dar (Prior und Wu 2006). Diese unterscheiden sich sowohl in der Anzahl als auch in der Position ihrer Methyl- und Hydroxylgruppen (**Abbildung 1**) (Prior und Wu 2006; Eker et al. 2019). Zudem können Mono-, Di- und Trisaccharide, über O-glykosidische Bindungen, an das C3-Atom des C-Rings sowie das C5- bzw. C7-Atom des A-Rings substituiert werden (Prior und Wu 2006). Dabei stellen Glukose, Galaktose, Arabinose, Rhamnose und Xylose häufig substituierte Saccharide dar (Prior und Wu 2006). Diese können wiederum mit verschiedenen aromatischen (z.B. *p*-Cumarsäure, Ferulasäure und Sinapinsäure) sowie aliphatischen (z.B. Malonsäure, Bernsteinsäure, Apfelsäure und Essigsäure) Säuren acyliert werden (Eker et al. 2019), so dass bereits mehr als 700 natürlich vorkommende Anthocyane identifiziert wurden (Krga und Milenkovic 2019; Prior und Wu 2006).

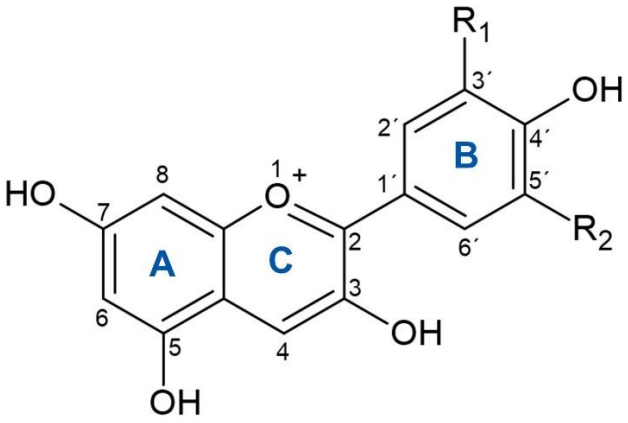

Anthocyanidin	R_1	R_2
Pelargonidin	H	H
Cyanidin	OH	H
Delphinidin	OH	OH
Petunidin	OH	OCH_3
Peonidin	OCH_3	H
Malvidin	OCH_3	OCH_3

Abbildung 1 Grundstruktur der in Lebensmitteln am häufigsten vorkommenden Anthocyanidine (eigene Darstellung modifiziert nach Krga und Milenkovic 2019). Die Strukturformel wurde mit ChemSketch (Freeware) 2023.2.3, Advanced Chemistry Development, Inc. (ACD/Labs), Toronto, ON, Canada, www.acdlabs.com erstellt.

Hohe Anthocyangehalte sind vor allem in Beerenobst (Wu et al. 2006) sowie in rot-violetten Gemüsesorten enthalten (**Tabelle 1**) (Tsutsumi et al. 2019). Allerdings tragen in Europa hauptsächlich Beeren, Trauben und Wein zur alimentären Anthocyanzufuhr bei (Zamora-Ros et al. 2011; Garcia-Larsen et al. 2018), wobei diese je nach Land sehr unterschiedlich und stark von kulturellen Unterschieden und Ernährungsgewohnheiten abhängig ist (Di Lorenzo et al. 2021). So liegt die durchschnittliche Anthocyanzufuhr in Europa schätzungsweise zwischen 9 und 28 mg/Tag (Vogiatzoglou et al. 2015).

Tabelle 1 Anthocyangehalt ausgewählter Lebensmittel.

Lebensmittel	**Anthocyangehalt pro 100 g Frischgewicht [mg Cyanidin-3-Glukosid]**
Heidelbeeren[1]	407
Brombeeren[1]	70 – 201
Himbeeren[1]	23 – 68
Erdbeeren[1]	20 – 60
Trauben[1]	39 – 187
Rotwein[1]	33 – 87
violette Karotten[2]	2 – 126

[1](Gonçalves et al. 2021), [2](Algarra et al. 2014).

Epidemiologische Studien zeigen, dass eine Anthocyan-reiche Ernährung mit einem geringeren Risiko für Herz-Kreislauf-Erkrankungen sowie für Kolonkarzinome assoziiert ist (Cassidy et al. 2016; Parmenter et al. 2021; Wang et al. 2019). Zudem konnte in zahlreichen *in vitro*- und *in vivo*-Studien die anti-oxidative, anti-inflammatorische sowie anti-kanzerogene Wirkung der Anthocyane bestätigt werden. Daher wird Anthocyanen ein hohes gesundheitsförderndes Potenzial zugeschrieben. So können diese mithilfe ihrer konjugierten Doppelbindungen und zahlreichen Hydroxylgruppen direkt als Radikalfänger fungieren und somit anti-oxidativ wirken (Gonçalves et al. 2021). Zudem konnten Kuntz et al. (2017) in einer *Cross-over*-Interventionsstudie zeigen, dass nach Aufnahme eines Anthocyan-reichen Trauben-/Heidelbeersafts, über einen Zeitraum von 2 Wochen, die Aktivität anti-oxidativer Enzyme im Plasma der Probanden signifikant zunimmt. Des Weiteren ist bekannt, dass Anthocyane intrazelluläre Signaltransduktionswege beeinflussen und somit die Sekretion pro-inflammatorischer Zytokine hemmen können (Gonçalves et al. 2021). Darüber hinaus sind Anthocyane in der Lage die Tumorprogression zu hemmen, indem sie die Proliferation der Tumorzellen inhibieren sowie den Arrest des Zellzyklus und die Einleitung der Apoptose induzieren (Gonçalves et al. 2021; Shi et al. 2021).

Allerdings ist die Bioverfügbarkeit nativer Anthocyane im Vergleich zu anderen Flavonoiden relativ gering (Krga und Milenkovic 2019). Zwar können Anthocyane, vermutlich mithilfe des Natrium-abhängigen Glukose-Transporters-1 (*sodium dependent glucose transporter-1*, SGLT-1), im oberen Intestinum als intakte Glykoside absorbiert werden, allerdings gelangen nur etwa 1-2 % der über die Nahrung aufgenommenen Anthocyane unverändert in den systemischen Kreislauf. So können sowohl nicht-mikrobielle β-Glukosidasen, wie die intestinale, membranständige Laktat-Phlorizidin-Hydrolase, als auch Enzyme der intestinalen Mikrobiota die hydrolytische Deglykosylierung der Anthocyane katalysieren (Prior und Wu 2006; Eker et al. 2019). Die dabei entstehenden Aglykone (Anthocyanidine) sind, im Vergleich zu ihren Glykosiden (Anthocyanen), bei dem im Intestinum herrschenden neutralen bis basischen pH-Wert weniger stabil. Infolge dessen kommt es zur Öffnung des C-Rings, so dass die Anthocyanidine spontan zerfallen. Dabei entstehen phenolische Säuren und Aldehyde wie z.B. 3,4-Dihydroxybenzoesäure (Protocatechusäure) und 2,4,6-Trihydroxybenzaldehyd (Phloroglucinaldehyd) (Prior und Wu 2006; Eker et al. 2019; Kay et al. 2009). Zudem werden sowohl die nativen Anthocyane als auch deren Degradationsprodukte im Fremdstoffstoffwechsel durch Phase-II-Enzyme weiter metabolisiert. Hierbei finden Sulfatierungs-, Glucuronidierungs- sowie Methylierungsreaktionen statt, wodurch die Stabilität und Wasserlöslichkeit der Anthocyane erhöht und somit ihre Verteilung und Ausscheidung beeinflusst wird (Eker et al. 2019). Der größte Teil der über die Nahrung aufgenommen Anthocyane erreicht jedoch das Kolon, wo sie von der intestinalen Mikrobiota intensiv metabolisiert werden (Kay et al. 2017). Dabei entstehen vor allem niedermolekulare, phenolische Verbindungen (**Abbildung 2**), die z.B. mithilfe epithelialer Monocarboxylat-Transporter absorbiert werden können (Krga und Milenkovic 2019; Kay et al. 2017). So konnten bereits zahlreiche Metabolite im Plasma und Urin nachgewiesen werden (Czank et al. 2013; Ferrars et al. 2014a; Mueller et al. 2017). Diese können zudem in deutlich höheren Konzentrationen im Plasma vorliegen als die nativen Verbindungen. Zudem weisen Anthocyane eine deutlich kürzere Plasmahalbwertszeit auf als ihre niedermolekularen, phenolischen Metabolite (Kay et al. 2017). Vermutlich sind daher eher langanhaltend hohe Metabolit-Konzentrationen für die gesundheitsfördernden Eigenschaften der Anthocyane verantwortlich. Somit sollten bei der Beurteilung der Bioverfügbarkeit nicht nur die nativen Anthocyane, sondern auch die Vielzahl an Degradationsprodukten, sowie an Phase I-, Phase II- und mikrobiellen Metaboliten berücksichtigt werden. Diese fiele dadurch deutlich höher aus als bisher angenommen (Kay et al. 2017).

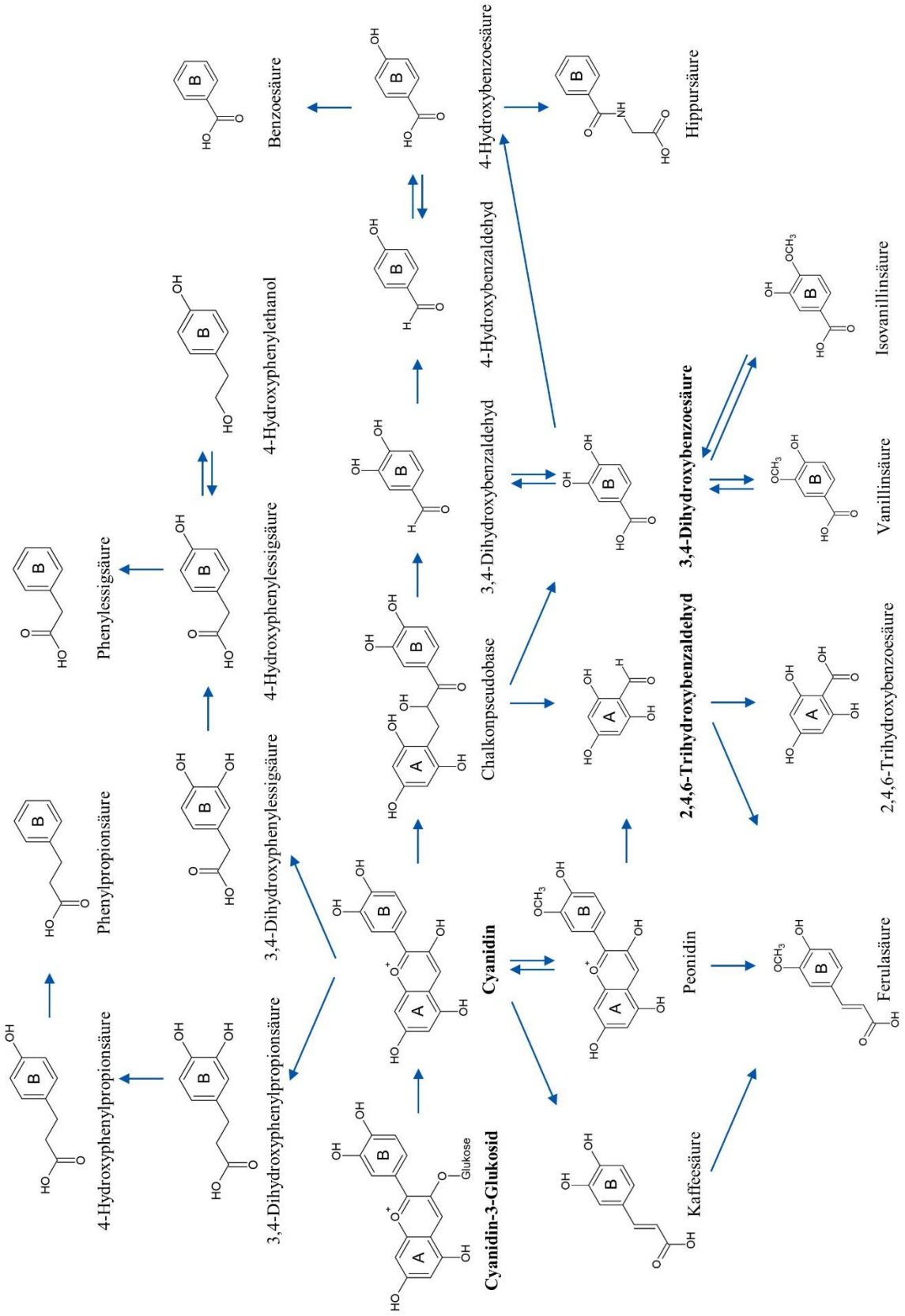

Abbildung 2 Potenzieller Metabolismus von Cyanidin-3-Glukosid (eigene Darstellung nach Fang 2014; Ferrars et al. 2014b; Zhu et al. 2018). Alle Strukturformeln wurden mit ChemSketch (Freeware) 2023.2.3, Advanced Chemistry Development, Inc. (ACD/Labs), Toronto, ON, Canada, www.acdlabs.com erstellt.

1.2 Tumorerkrankungen, Inflammation und Migration

Laut statistischem Bundesamt stellen Tumorerkrankungen, nach kardiovaskulären Erkrankungen, die zweithäufigste Todesursache in Deutschland dar. Allein im Jahr 2022 verstarben in Deutschland über 200.000 Menschen an Krebs (Statistisches Bundesamt 2024). Dabei weisen sowohl das **kolorektale Karzinom** als auch das **Pankreaskarzinom** hohe Mortalitätsraten auf, so dass sie in Deutschland die dritt- bzw. vierthäufigste tumorbedingte Todesursache bei Männern und Frauen darstellen (RKI 2023). Vor allem Patienten mit Pankreaskarzinom weisen eine äußerst ungünstige Prognose auf. Da Tumore der Bauchspeicheldrüse in frühen Stadien keine oder nur unspezifische Symptome verursachen, werden bösartige Neubildungen der Bauchspeicheldrüse häufig erst spät erkannt (RKI 2023). Zudem weisen Pankreaskarzinome ein hohes Metastasierungspotenzial auf, so dass bei mehr als 80 % der Betroffenen zum Zeitpunkt der Diagnose bereits nicht resektable oder metastasierte Pankreaskarzinome vorliegen (Guerrero et al. 2020). Dementsprechend liegt die relative **5-Jahres-Überlebensrate** für Patienten mit Pankreaskarzinom in Deutschland bei nur 11 %. Im Gegensatz dazu ist die relative 5-Jahres-Überlebensrate für Patienten mit kolorektalem Karzinom mit 64-66 % relativ hoch (RKI 2023). Allerdings bildet jeder vierte Patient mit kolorektalen Karzinom, trotz Resektion des Primärtumors, Fernmetastasen aus (Guyot et al. 2005). Vor dem Hintergrund, dass mehr als 90 % aller tumorbedingten Sterbefälle auf Metastasen zurückzuführen sind (Fares et al. 2020; Reymond et al. 2013), stellt die Inhibierung der Metastasierung einen wichtigen therapeutischen Ansatzpunkt dar.

Bei der Metastasierung von Tumorzellen handelt es sich um einen komplexen, mehrstufigen Prozess. Zunächst proliferieren die Zellen des Primärtumors und infiltrieren das umliegende Gewebe, indem sie die extrazelluläre Matrix mithilfe von Enzymen wie Matrix-Metalloproteasen lysieren (Invasion). Daraufhin lösen sich einzelne oder mehrere Zellen aus dem Primärtumor heraus und gelangen intravasal in den systemischen Blutkreislauf (Intravasation). Die im Blut zirkulierenden Tumorzellen adhärieren anschließend an das Endothel und migrieren in distale Gewebe (**Extravasation**), wo sie sich als Sekundärtumor manifestieren (**Abbildung 3**) (Fares et al. 2020; Reymond et al. 2013).

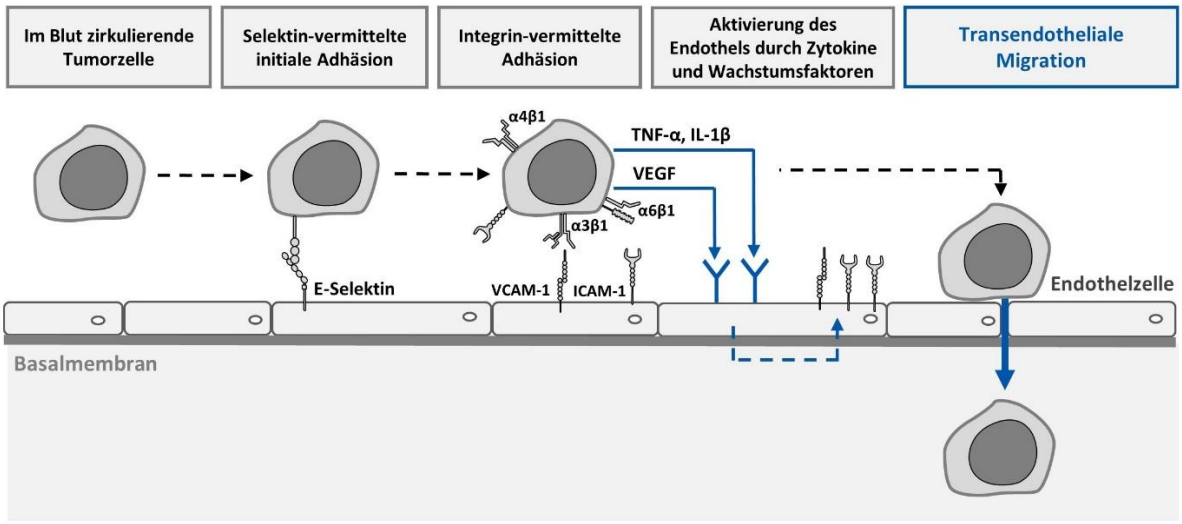

Abbildung 3 Transendotheliale Migration der Tumorzellen (eigene Darstellung). Die initiale, noch recht lose, Adhäsion im Blut zirkulierender Tumorzellen an das Endothel wird in erster Linie durch E-Selektin vermittelt, welches von den Endothelzellen exprimiert wird. Anschließend wird durch die Interaktion von α/β-Integrinen und Integrin-Liganden eine festere Bindung zwischen den Endothel- und Tumorzellen ausgebildet. Zudem sezernieren die Tumorzellen Wachstumsfaktoren (VEGF) sowie pro-inflammatorische Zytokine (TNF-α, IL-1β), die eine lokale, niedrig-gradige Inflammation induzieren. Infolgedessen kommt es zur Aktivierung des Endothels und zur vermehrten Expression Endothel-assoziierter Zelladhäsionsmoleküle wie ICAM-1. Zudem wird die Stabilität der endothelialen Zell-Zell-Kontakte herabgesetzt, wodurch die transendotheliale Migration (Extravasation) der Tumorzellen erleichtert wird (Fares et al. 2020; Reymond et al. 2013; Sulzmaier et al. 2014).

ICAM, *intercellular adhesion molecule 1*; IL-1β, Interleukin-1β; TNF-α, Tumornekrosefaktor-α; VCAM, *vascular cell adhesion molecule 1*; VEGF, *vascular endothelial growth factor.*

Bei diesem Prozess spielen pro-inflammatorische Zytokine und Wachstumsfaktoren, die von den Tumorzellen sekretiert werden, eine wichtige Rolle. Diese können sowohl autokrin auf die Tumorzellen selbst wie auch parakrin auf die Endothelzellen wirken. Infolgedessen kommt es zur Aktivierung intrazellulärer Signaltransduktionswege wie dem **NFκB** (*nuclear factor kappa B*)-**Signalweg** (Krga und Milenkovic 2019; Liu et al. 2017). NFκB-Proteine (NFκB1 (p50), NFκB2 (p52), RelA (p65), RelB und c-Rel) stellen induzierbare Transkriptionsfaktoren dar, die die Expression zahlreicher inflammatorischer Gene regulieren. Diese NFκB-Proteine liegen im Zytoplasma an inhibitorische κB-Proteine wie z.B. IκBα gebunden vor, wodurch deren Translokation in den Nukleus inhibiert wird (Liu et al. 2017). Allerdings können Zytokine und Wachstumsfaktoren die Aktivierung des IκB-Kinase-Komplexes induzieren, welcher wiederum die Phosphorylierung von IκBα katalysiert. Infolgedessen kommt es zur Ubiquitinierung und anschließenden Degradation von IκBα durch das Proteasom. Daraufhin kann die Translokation von NFκB-Heterodimeren, wie p50/RelA, in den Nukleus stattfinden, wo diese die vermehrte Expression von pro-inflammatorischen Zytokinen sowie Zelladhäsionsmolekülen induzieren (Krga und Milenkovic 2019; Liu et al. 2017). Insbesondere

Zelladhäsionsmoleküle spielen eine wichtige Rolle bei der **Migration** von Tumorzellen (Reymond et al. 2013; Makrilia et al. 2009). Diese werden sowohl von den Tumorzellen als auch von Endothelzellen exprimiert, wobei sich das Muster und Ausmaß der Expression zwischen den beiden Zelltypen unterscheidet. Endothelzellen exprimieren vor allem Zelladhäsionsmoleküle die zur Familie der Selektine (E-Selektin) und Immunglobulin-Superfamilie (ICAM-1 (*intercellular cell adhesion molecule*) und VCAM-1 (*vascular cell adhesion molecule*)) gehören (Blankenberg et al. 2003). Diese dienen wiederum als Liganden für **α/β-Integrine** (Blankenberg et al. 2003), die auf der Oberfläche der Tumorzellen vermehrt exprimiert werden (Alday-Parejo et al. 2019). Eine Übersicht der an der Tumorzellmigration beteiligten Zelladhäsionsmoleküle sowie deren Liganden ist in **Tabelle 2** dargestellt.

Tabelle 2 Übersicht der an der Tumorzellmigration beteiligten Zelladhäsionsmoleküle und ihrer Liganden (nach Blankenberg et al. 2003; Cooper und Giancotti 2019).

Zelladhäsionsmoleküle	CD-Nomenklatur	Ligand
Integrine		
Integrin-α3	CD49c	Fibronektin, Laminin
Integrin-α4	CD49d	VCAM-1, Fibronektin
Integrin-α6	CD49f	Laminin
Integrin-β1	CD29	VCAM-1, Laminin, Fibronektin
Integrin-β2	CD18	ICAM-1
Integrin-β4	CD104	Laminin
Immunglobuline		
ICAM-1	CD54	Integrin-β2
VCAM-1	CD106	Integrin-β1,Integrin-β2, Integrin-α4

CD, *cluster of differentiation.*

Bei Integrinen handelt es sich um heterodimere, transmembrane Glykoproteine, die aus einer α- sowie einer β-Untereinheit bestehen (Pan et al. 2018). Sie spielen eine zentrale Rolle für die Metastasierung von Tumorzellen (Reymond et al. 2013; Alday-Parejo et al. 2019), da sie sowohl die Adhäsion von Tumorzellen an Proteine der extrazellulären Matrix (Fibronektin, Laminin und Kollagen) als auch Zell-Zell-Interaktionen vermitteln (Alday-Parejo et al. 2019; Pan et al. 2018). Infolge dessen kommt es zur Aktivierung verschiedener intrazellulärer Signalwege (Pan et al. 2018). In diesem Zusammenhang ist insbesondere der **FAK-SFK-Signalweg** (*focal adhesion kinase* (FAK)-*Src family kinase* (SFK) *signaling*) zu nennen. Die Autophosphorylierung der nicht Rezeptor Tyrosin Kinase FAK an Tyrosin 397 (Y397) (Yu et al. 2022) ermöglicht die Bindung der Src Kinase, die wiederum die Hyperphosphorylierung der FAK katalysiert und somit zu deren vollständigen Aktivierung beiträgt (Dawson et al. 2021; Zhao und Guan 2011). Der sich gegenseitig aktivierende FAK-Src-Komplex reguliert

verschiedene zelluläre Funktionen, indem er durch Phosphorylierung weiterer Effektorproteine die Aktivierung zahlreicher *downstream* Signaltransduktionswege initiiert und somit die Tumorproliferation und -progression fördert (Zhao und Guan 2011). So konnte bereits für verschiedene Tumore, wie Pankreas- und Kolonkarzinome, eine gesteigerte Expression und/oder Aktivierung der FAK beobachtet werden (Yu et al. 2022; Zhou et al. 2017). Zudem ist die Überexpression bzw. Aktivierung der FAK mit dem Invasions- und Metastasierungspotenzial, einem geringeren Ansprechen auf Chemotherapeutika sowie einer schlechteren klinischen Prognose assoziiert (Yu et al. 2022; Zhao und Guan 2011). Allerdings konnte bereits gezeigt werden, dass Anthocyane die Invasion und Migration von Brustkrebszellen hemmen, indem sie die Aktivierung des FAK-SFK-Signalwegs inhibieren (Zhou et al. 2017). Ähnliche Effekte konnten auch schon für Delphinidin in Kolonkarzinomzellen gezeigt werden. Zudem hemmte Delphinidin konzentrationsabhängig die Expression der Integrine-αV und -β3 (Huang et al. 2019). Allerdings wurden in diesen Untersuchungen **pharmakologische Konzentrationen** eingesetzt. Interessanterweise konnten jedoch Kuntz et al. (2017) erstmals zeigen, dass Anthocyane und deren Metabolite, die 60 Minuten nach Aufnahme eines Anthocyan-reichen Trauben-/Heidelbeersafts aus dem Plasma gesunder Probanden isoliert wurden, in physiologischen Konzentrationen, die Tumorzellmigration von Pankreaskarzinomzellen (PANC-1) hemmen. Möglicherweise könnten die beobachteten anti-migratorischen Effekte auf eine verminderte Expression von Zelladhäsionsmolekülen auf den Tumorzellen zurückzuführen sein. Allerdings ist bisher unklar, inwiefern physiologische Konzentrationen an Anthocyanen sowie deren Metaboliten die Expression von Zelladhäsionsmolekülen auf Tumorzellen und infolgedessen die Tumorzellmigration beeinflussen.

1.3 Kardiovaskuläre Erkrankungen, Inflammation und NLRP3 Inflammasom

Der rapide Anstieg der Adipositasprävalenz in den letzten Dekaden ist gesellschaftlich problematisch, da Übergewicht und Adipositas zu den Hauptrisikofaktoren für eine Vielzahl an nicht übertragbaren Erkrankungen – insbesondere kardiovaskulären Erkrankungen – gehören (Kluge 2022). Charakteristisch für diese vaskulären Erkrankungen ist eine **chronische, niedrig-gradige Inflammation** (*low-grade inflammation,* LGI), die häufig mit Übergewicht und Adipositas assoziiert ist (Ngamsamer et al. 2022; Henein et al. 2022). Allerdings sind die zu Grunde liegenden Mechanismen für die *sub*-klinisch erhöhten Inflammationsmarker bisher nicht eindeutig geklärt. Neben der Beteiligung hypertropher Adipozyten am

Inflammationsgeschehen scheint vor allem die Aktivierung zirkulierender Monozyten zur LGI beizutragen. So konnte bereits gezeigt werden, dass klassische Monozyten adipöser Risikopatienten vermehrt pro-inflammatorische Zytokine sekretieren (Henein et al. 2022; Ghanim et al. 2004), die wiederum weitere Zellen wie Endothel- und Immunzellen aktivieren und somit zu einer sich potenzierenden inflammatorischen Antwort führen (Molla et al. 2020). Zudem deuten neuere Erkenntnisse darauf hin, dass auf mechanistischer Ebene, eine übermäßige Aktivierung des *NOD-like receptor pyrin domain-containing protein 3* (NLRP3) Inflammasoms, zur Entstehung der LGI beiträgt (Ngamsamer et al. 2022; Ralston et al. 2017).

Beim **NLRP3 Inflammasom** handelt es sich um einen zytosolischen Multiproteinkomplex, der vor allem von myeloiden Zellen des angeborenen Immunsystems exprimiert wird (Gritsenko et al. 2020; Baldrighi et al. 2017). Die Formierung und Aktivierung des NLRP3 Inflammasoms führt zur Sekretion pro-inflammatorischer Zytokine und somit zu einer schnellen inflammatorischen Antwort, die für die Abwehr von Pathogenen entscheidend ist (Gritsenko et al. 2020; Vetrani et al. 2022). Allerdings begünstigen metabolische Veränderungen, bei übergewichtigen/adipösen Risikopatienten, eine übermäßige Aktivierung des NLRP3 Inflammasoms und somit die vermehrte Sekretion pro-inflammatorischer Zytokine. In diesem Zusammenhang konnte bereits an Mäusen gezeigt werden, dass eine fettreiche Ernährung zur gesteigerten Aktivierung des NLRP3 Inflammasoms im Lebergewebe führt (Wang et al. 2017). Zudem konnte bei Patienten mit Diabetes mellitus Typ 2 eine erhöhte Aktivierung des NLRP3 Inflammasoms in PBMCs (*peripheral blood mononuclear cells*) beobachtet werden, was mit einer vermehrten Interleukin-1β (IL-1β) und IL-18 Sekretion einherging (Lee et al. 2013). Diese Fehlregulation der Inflammasomaktivierung scheint somit – auf mechanistischer Ebene – zur Entstehung der LGI und somit zur Pathogenese inflammatorischer Erkrankungen beizutragen (Grebe et al. 2018).

Interessanter Weise scheint die Fehlregulation der Inflammasomaktivierung auch die Tumorprogression zu fördern (Pretre et al. 2022; Sharma und Kanneganti 2021). In diesem Zusammenhang spielt vor allem die Sekretion von IL-1β, welches sowohl von den Tumorzellen selbst als auch von Immunzellen in der Tumormikroumgebung sezerniert werden kann, eine wichtige Rolle (Sharma und Kanneganti 2021). So konnte bereits gezeigt werden, dass durch IL-1β die Expression endothelialer Zelladhäsionsmoleküle gesteigert und so die Metastasierung von Tumorzellen gefördert wird (Li et al. 2021b). Zudem konnte durch Blockierung des IL-1β-Rezeptors, mithilfe von Antagonisten, sowohl das Wachstum als auch die Metastasierung von Tumorzellen gehemmt werden (Sharma und Kanneganti 2021). Des Weiteren sind

verschiedene *Single Nucleotide Polymorphisms* des NLRP3-Gens mit einigen Tumorerkrankungen, wie z.B. Pankreaskarzinomen, assoziiert (Pretre et al. 2022; Sharma und Kanneganti 2021). Darüber hinaus zeigen Transkriptomanalysen NLRP3-Inflammasom assoziierter Gene, dass diese im Tumorgewebe vermehrt exprimiert werden (Pretre et al. 2022). Die genaue Bedeutung des NLRP3 Inflammasoms für die Tumorprogression und Metastasierung ist jedoch bisher nicht eindeutig geklärt (Li et al. 2021b).

Die kanonische Aktivierung des NLRP3 Inflammasoms erfolgt typischerweise in zwei Schritten und führt zur Formierung eines einzelnen makromolekularen Multiproteinkomplexes. Dieser aus dem Sensorprotein NLRP3, dessen Adaptormolekül ASC (*apoptosis-associated speck-like protein containing a caspase activating and recruitment domain*) sowie der inaktiven pro-Caspase-1 bestehende Multiproteinkomplex wird auch als **ASC Speck** bezeichnet (Hoss et al. 2017). Der erste Schritt der Inflammasomaktivierung (*Priming*) wird sowohl durch systemisch erhöhte Konzentrationen pro-inflammatorischer Zytokine (IL-1β und Tumornekrosefaktor-α (TNF-α)) (Baldrighi et al. 2017), wie sie bei übergewichtigen/adipösen Risikopatienten bereits beobachtet wurden, als auch durch bakterielle Bestandteile wie Lipopolysaccharide (LPS), deren Konzentration in der Zirkulation übergewichtiger Risikopatienten ebenfalls erhöht ist (Vetrani et al. 2022), vermittelt. Durch die Bindung dieser Liganden an Zytokin- bzw. *Toll-like*-Rezeptoren (TLR) wird unter anderem die Aktivierung des NFκB-Signalwegs induziert, wodurch wiederum die Transkription von NLRP3 und pro-IL-1β gesteigert wird (Groslambert und Py 2018). Diesbezüglich konnte bereits beobachtet werden, dass die Expression des TLR-4 auf der Oberfläche klassischer Monozyten adipöser Risikopatienten höher ist als bei Normalgewichtigen (Devêvre et al. 2015; Mattos et al. 2016). Dies könnte zur verstärkten Induktion des *Priming*-Schrittes und somit zur vermehrten Sekretion pro-inflammatorischer Zytokine bei Risikopatienten beitragen. Die Aktivierung des NLRP3 Inflammasoms erfolgt jedoch erst durch ein zweites unabhängiges Signal, welches bei übergewichtigen/adipösen Risikopatienten durch den infolge von Übergewicht und fettreicher Ernährung entstehenden metabolischen Stress vermittelt werden kann. Dieses Signal führt zur Konformationsänderung des NLRP3 Proteins, wodurch die Formierung des ASC Specks ermöglicht wird. Die anschließende autoproteolytische Aktivierung der pro-Caspase-1, welche die Reifung der pro-inflammatorischen Zytokine IL-1β und IL-18 katalysiert, führt zur Freisetzung dieser Zytokine, die – wie bereits oben beschrieben – zur Aktivierung weiterer Immunzellen und somit zu einer sich potenzierenden inflammatorischen Antwort beitragen (**Abbildung 4**) (Baldrighi et al. 2017; Vetrani et al. 2022; Groslambert und Py 2018).

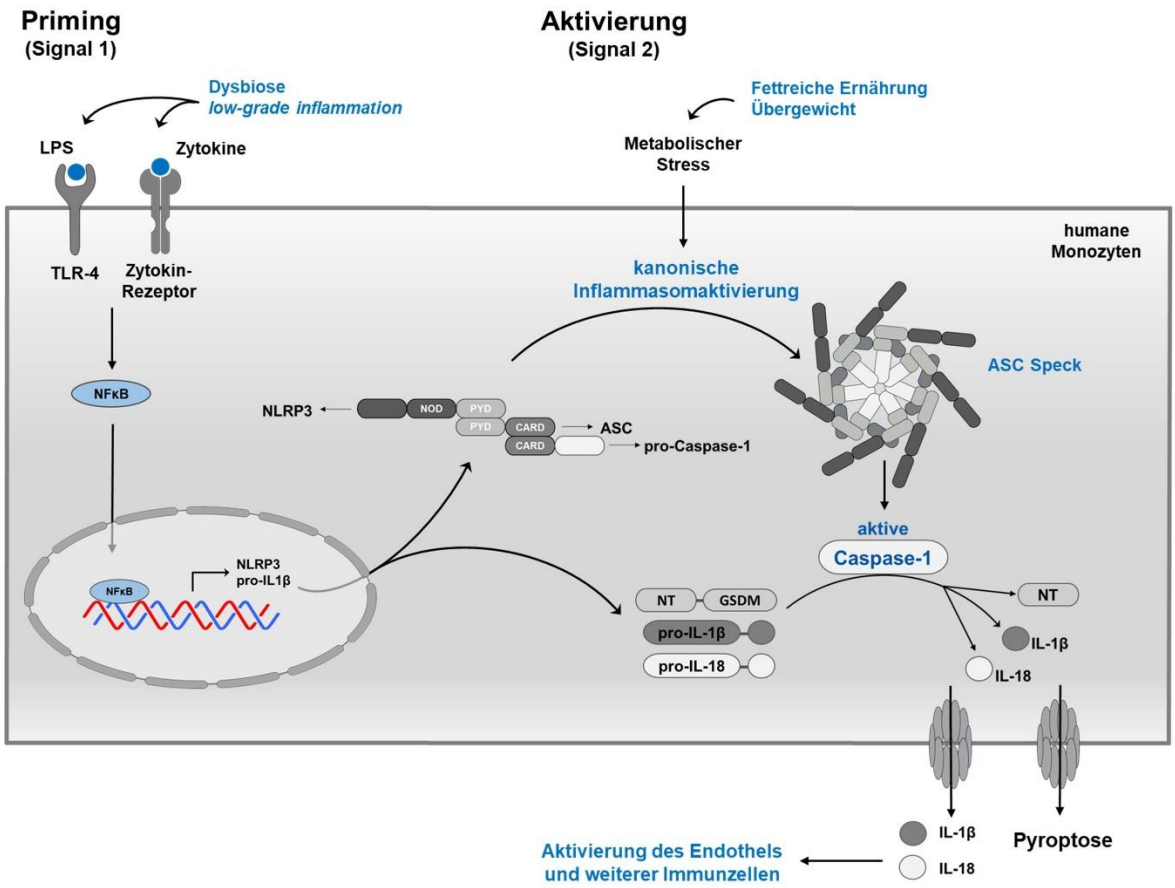

Abbildung 4 Formierung und Aktivierung des NLRP3 Inflammasoms in humanen Monozyten (eigene Darstellung). Der erste Schritt (*Priming*) der Inflammasomaktivierung kann sowohl durch inflammatorische Zytokine als auch durch Lipopolysaccharide vermittelt werden. Durch die Bindung dieser Stimuli an Zytokin- bzw. *Toll-like*-Rezeptoren, wird die Aktivierung des NFκB-Signalwegs induziert, wodurch wiederum die NLRP3 und pro-IL-1β Expression gesteigert wird. Ein zweites unabhängiges Signal, welches durch den infolge von fettreicher Ernährung und Übergewicht auftretenden metabolischen Stress vermittelt werden kann, führt zur Formierung des ASC Specks. Hierdurch kommt es zur Aktivierung der pro-Caspase-1, welche daraufhin die Spaltung von pro-IL-1β und pro-IL-18 katalysiert. Zudem löst die kanonische Aktivierung des NLRP3 Inflammasoms eine spezielle Form des Zelltodes aus, die als Pyroptose bezeichnet wird. Dabei spaltet die aktive Caspase-1 das Protein Gasmerdin D, dessen N-terminales Fragment Poren in der Zellmembran formt. Der Verlust der Zellintegrität führt zur Freisetzung inflammatorischer Zytokine sowie weiterer *damage-associated molecular patterns*, die wiederum zur Aktivierung des Endothels sowie weiterer Immunzellen beitragen und somit zu einer sich potenzierenden inflammatorischen Antwort führen (Baldrighi et al. 2017).

ASC, apoptosis-associated speck-like protein containing a CARD domain; GSDM, Gasdermin D; IL, Interleukin; LPS, Lipopolysaccharide; NLRP3, NOD-like receptor pyrin domain-containing protein 3; NT, N-terminales Ende; TLR, Toll-like-Rezeptor.

Somit stellt die Inhibierung dieses inflammatorischen Geschehens einen wichtigen präventiven Ansatzpunkt dar, um die LGI und die Entstehung inflammatorischer Erkrankungen in einem sehr frühen *sub*-klinischen Stadium zu hemmen. Möglicherweise könnten diese, bei übergewichtigen/adipösen Risikopatienten, fehlregulierten Prozesse der Inflammasomaktivierung durch Anthocyane und deren Metabolite positiv beeinflusst werden. Allerdings ist der Einfluss von Anthocyanen und insbesondere ihrer Metabolite auf die Aktivierung des NLRP3 Inflammasoms in humanen Monozyten bisher unklar.

2. Fragestellung

Anthocyanen wird ein hohes gesundheitsförderndes Potenzial zugeschrieben. Allerdings ist die Bioverfügbarkeit nativer Anthocyane relativ gering. Nur etwa 1-2 % der über die Nahrung aufgenommenen Anthocyane gelangen unverändert in den systemischen Kreislauf, da diese sowohl im Gastrointestinaltrakt als auch in der Leber intensiv metabolisiert werden. Dabei entsteht eine Vielzahl an phenolischen Metaboliten, die vermutlich in einem höheren Ausmaß zur biologischen Wirksamkeit der Anthocyane beitragen als die nativen Verbindungen selbst. Ziel dieser Dissertation war es daher, das anti-migratorische und anti-inflammatorische Potenzial von **Anthocyanen sowie deren Metaboliten** in kanzerogenen Zellen zu untersuchen. Dabei sollten im Rahmen dieser Dissertation die folgenden zwei Hauptfragestellungen untersucht werden:

1. Welchen Einfluss haben Anthocyane und ihre Metabolite auf die Migration kanzerogener Zellen?
2. Welchen Einfluss haben Anthocyane und ihre Metabolite auf die Aktivierung des NLRP3 Inflammasoms?

Für die Beantwortung der ersten Fragestellung wurde bereits im Vorfeld eine randomisierte, Placebo-kontrollierte *Cross-over*-Interventionsstudie durchgeführt, im Rahmen derer junge, gesunde Probanden, über einen Zeitraum von 4 Wochen, täglich 330 mL eines Anthocyan-reichen Trauben-/Heidelbeersafts (80 % Traubensaft, Sorte *Accent,* 20 % Heidelbeersaft) bzw. 330 mL eines Anthocyan-reduzierten Placebosafts zu sich nahmen. Sowohl vor als auch nach der jeweiligen Intervention wurden Blutproben gewonnen und die Anthocyane sowie deren Metabolite mittels Festphasenextraktion aus dem Plasma isoliert. Anschließend wurde im **ersten Teil** dieser Dissertation, mithilfe von *in vitro*-Migrationsmodellen (Boyden Kammer), der Einfluss der aus dem Plasma isolierten Anthocyane sowie deren Metabolite auf die Migration von Kolon- (HT-29 und Caco-2) und Pankreaskarzinomzellen (PANC-1 und AsPC-1) untersucht. Da Zelladhäsionsmoleküle an der Tumoradhäsion und -migration beteiligt sind, wurde in der vorliegenden Arbeit ebenfalls untersucht, inwiefern die Expression dieser durch aus dem Plasma isolierte Anthocyane sowie deren Metabolite beeinflusst wird. Dazu wurde die Expression der Zelladhäsionsmoleküle auf den Tumor- und Endothelzellen durchflusszytometrisch analysiert. Da die Behandlung mit Chemotherapeutika eine wichtige Säule der Tumortherapie darstellt, wurde ebenfalls untersucht, inwiefern aus dem Plasma isolierte Anthocyane sowie deren Metabolite die Wirkung des Chemotherapeutikums 5-

Fluorouracil (5-FU), welches häufig im Rahmen konventioneller Behandlungsregime eingesetzt wird, beeinflussen.

Für die Beantwortung der zweiten Fragestellung wurde im **zweiten Teil** dieser Dissertation zunächst ein *in vitro*-Modell etabliert, um den Einfluss von Anthocyanen und ihrer Metabolite auf die Aktivierung des NLRP3 Inflammasoms in THP-1 Monozyten zu untersuchen. Hierzu wurden die Zellen zunächst mit LPS stimuliert (*Priming*) und/oder die Aktivierung des NLRP3 Inflammasoms mit Nigericin induziert. Nach erfolgreicher Validierung dieses Modells, wurde der Einfluss von Anthocyanen und ihrer Metabolite auf die Aktivierung des NLRP3 Inflammasoms untersucht. Dazu wurden die monozytären THP-1 Zellen mit einem Anthocyan-reichen Trauben-/Heidelbeerextrakt oder mit phenolischen Metaboliten präinkubiert, bevor das NLRP3 Inflammasom – wie bereits beschrieben – mit LPS und/oder Nigericin aktiviert wurde. Die Expression von ASC und NLRP3 sowie die Formierung der ASC Specks wurde durchflusszytometrisch bestimmt. Zudem wurde die Caspase-1-Aktivität in THP-1 Monozyten mithilfe eines Biolumineszenz-basierten Assays gemessen und die Sekretion von IL-1β sowie IL-18 in den Zellkulturüberstand mittels ELISA erfasst.

Eine Übersicht der zur Untersuchung der beiden Hauptfragestellungen verwendeten *in vitro*-Modelle ist in **Abbildung 5** dargestellt.

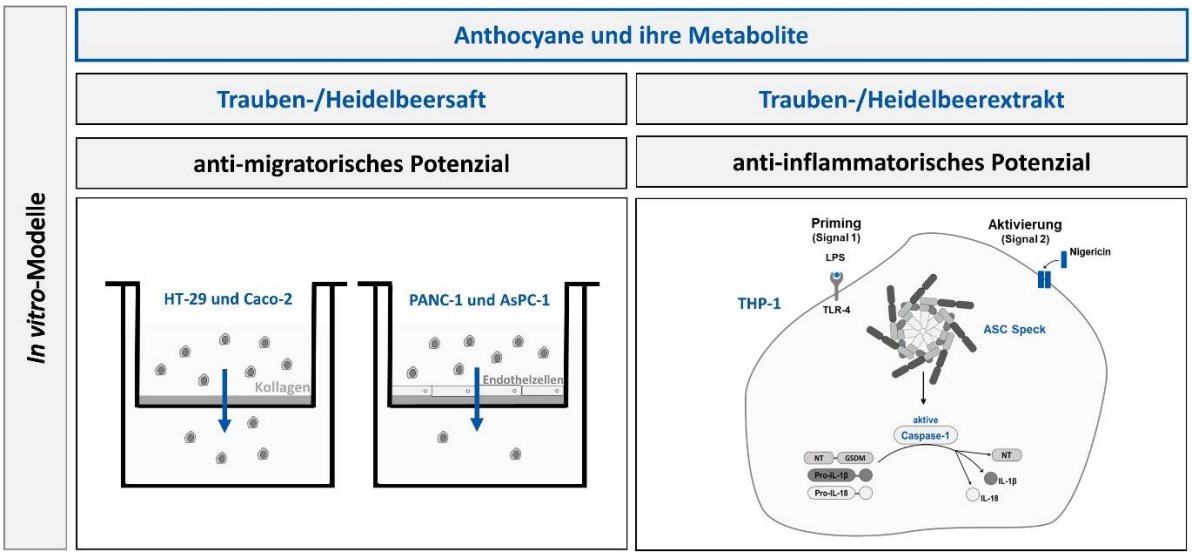

Abbildung 5 *In vitro*-Modelle zur Untersuchung des Einflusses von Anthocyanen und ihrer Metabolite auf die Migration und die Aktivierung des NLRP3 Inflammasoms in kanzerogenen Zellen (eigene Darstellung).

3. Publikationen

3.1 Influence of Plasma-Isolated Anthocyanins and Their Metabolites on Cancer Cell Migration (HT-29 and Caco-2) In Vitro: Results of the ATTACH Study

Behrendt I, Röder I, Will F, Mostafa H, Gonzalez-Dominguez R, Meroño T, Andres-Lacueva C, Fasshauer M, Rudloff S, Kuntz S. *Antioxidants* **2022**, 11, 1341. doi:10.3390/antiox11071341.

Journal impact factor: 7.0

Abstract: Cancer mortality is mainly due to metastasis. Therefore, searching for new therapeutic agents suppressing cancer cell migration is crucial. Data from human studies regarding effects of anthocyanins on cancer progression, however, are scarce and it is unclear whether physiological concentrations of anthocyanins and their metabolites reduce cancer cell migration in vivo. In addition, interactions with chemotherapeutics like 5-fluorouracil (5-FU) are largely unknown. Thus, we combined a placebo-controlled, double-blinded, cross-over study with in vitro migration studies of colon cancer cell lines to examine the anti-migratory effects of plasma-isolated anthocyanins and their metabolites (PAM). Healthy volunteers (n = 35) daily consumed 0.33 L of an anthocyanin-rich grape/bilberry juice and an anthocyanin-depleted placebo juice for 28 days. PAM were isolated before and after intervention by solid-phase extraction. HT-29 and Caco-2 cells were incubated with PAM in a Boyden chamber. Migration of HT-29 cells was significantly inhibited by PAM from juice but not from placebo. In contrast, Caco-2 migration was not affected. Co-incubation with 5-FU and pooled PAM from volunteers (n = 10), which most effectively inhibited HT-29 migration, further reduced HT-29 migration in comparison to 5-FU alone. Therefore, PAM at physiological concentrations impairs colon cancer cell migration and may support the effectiveness of chemotherapeutics.

Keywords: anthocyanins; migration; intervention study; colon cancer; 5-fluorouracil; grapes; bilberry; antioxidant capacity; juice

Anhang A: *Supplemental Material*

antioxidants

Article

Influence of Plasma-Isolated Anthocyanins and Their Metabolites on Cancer Cell Migration (HT-29 and Caco-2) In Vitro: Results of the ATTACH Study

Inken Behrendt [1,*], Isabella Röder [2], Frank Will [2], Hamza Mostafa [3,4], Raúl Gonzalez-Dominguez [3,4], Tomás Meroño [3,4], Cristina Andres-Lacueva [3,4], Mathias Fasshauer [1], Silvia Rudloff [5] and Sabine Kuntz [1]

[1] Department of Nutritional Science, Human Nutrition, Justus-Liebig-University, 35390 Giessen, Germany; mathias.fasshauer@ernaehrung.uni-giessen.de (M.F.); sabine.kuntz@nutr.jlug.de (S.K.)
[2] Department of Beverage Research, Hochschule Geisenheim University, 65366 Geisenheim, Germany; isabella.roeder@googlemail.com (I.R.); frank.will@hs-gm.de (F.W.)
[3] Biomarkers and Nutrimetabolomics Laboratory, Department of Nutrition, Food Sciences and Gastronomy, Food Innovation Network (XIA), Nutrition and Food Safety Research Institute (INSA), Facultat de Farmàcia i Ciències de l'Alimentació, Universitat de Barcelona (UB), 08028 Barcelona, Spain; hamza_mohamedamin@ub.edu (H.M.); raul.gonzalez@ub.edu (R.G.-D.); tomasmerono@ub.edu (T.M.); candres@ub.edu (C.A.-L.)
[4] Centro de Investigación Biomédica en Red de Fragilidad y Envejecimiento Saludable (CIBERFES), Instituto de Salud Carlos III, 28029 Madrid, Spain
[5] Department of Nutritional Science and Department of Pediatrics, Justus-Liebig-University, 35392 Giessen, Germany; silvia.rudloff@ernaehrung.uni-giessen.de
* Correspondence: inken.behrendt@ernaehrung.uni-giessen.de

Citation: Behrendt, I.; Röder, I.; Will, F.; Mostafa, H.; Gonzalez-Dominguez, R.; Meroño, T.; Andres-Lacueva, C.; Fasshauer, M.; Rudloff, S.; Kuntz, S. Influence of Plasma-Isolated Anthocyanins and Their Metabolites on Cancer Cell Migration (HT-29 and Caco-2) In Vitro: Results of the ATTACH Study. *Antioxidants* **2022**, *11*, 1341. https://doi.org/10.3390/antiox11071341

Academic Editor: Hae-Jeung Lee

Received: 31 May 2022
Accepted: 5 July 2022
Published: 8 July 2022

Abstract: Cancer mortality is mainly due to metastasis. Therefore, searching for new therapeutic agents suppressing cancer cell migration is crucial. Data from human studies regarding effects of anthocyanins on cancer progression, however, are scarce and it is unclear whether physiological concentrations of anthocyanins and their metabolites reduce cancer cell migration in vivo. In addition, interactions with chemotherapeutics like 5-fluorouracil (5-FU) are largely unknown. Thus, we combined a placebo-controlled, double-blinded, cross-over study with in vitro migration studies of colon cancer cell lines to examine the anti-migratory effects of plasma-isolated anthocyanins and their metabolites (PAM). Healthy volunteers (n = 35) daily consumed 0.33 L of an anthocyanin-rich grape/bilberry juice and an anthocyanin-depleted placebo juice for 28 days. PAM were isolated before and after intervention by solid-phase extraction. HT-29 and Caco-2 cells were incubated with PAM in a Boyden chamber. Migration of HT-29 cells was significantly inhibited by PAM from juice but not from placebo. In contrast, Caco-2 migration was not affected. Co-incubation with 5-FU and pooled PAM from volunteers (n = 10), which most effectively inhibited HT-29 migration, further reduced HT-29 migration in comparison to 5-FU alone. Therefore, PAM at physiological concentrations impairs colon cancer cell migration and may support the effectiveness of chemotherapeutics.

Keywords: anthocyanins; migration; intervention study; colon cancer; 5-fluorouracil; grapes; bilberry; antioxidant capacity; juice

1. Introduction

Colorectal cancer (CRC) is one of the most common cancer types worldwide. In 2020, more than one million patients were newly diagnosed and ~600,000 CRC deaths occurred [1]. However, CRC incidence shows distinct geographic variations, with higher incidence rates in industrialized countries revealing Western lifestyle, and particularly Western diet, as major modifiable risk factors [2,3]. Although the 5-year relative survival rate for CRC patients with localized disease is about 90% [4], metastasis is associated with poor outcomes. In CRC patients with metastasis, the 5-year relative survival rate

dramatically declines to 14% [4]. Therefore, CRC is the second leading cause of cancer death globally [1] and searching for new therapeutic agents to impair tumor progression and metastasis is critical.

Carcinogenesis and metastasis are associated with oxidative stress that is characterized by excessive levels of reactive oxygen species (ROS) [5]. ROS are highly reactive and capable of damaging macromolecules such as DNA, proteins, and lipids, as well as cellular structures, thus promoting malignant transformation [5,6]. In addition, mitochondrial dysfunction and high ROS levels increment the migratory and invasive potential of several cancer cell lines [7–9]. Therefore, antioxidants are hypothesized as chemopreventive and chemotherapeutic agents [6]. In recent years, several plant-derived phytochemicals, particularly polyphenols, have attracted remarkable attention for their potential to prevent tumor initiation, promotion, and progression, due to their low cost, low toxicity, and the undesirable adverse side effects of chemotherapeutical drugs [10]. Anthocyanins, a subgroup of flavonoids, belong to the most prevalent group of polyphenols in fruits [11] and are responsible for their orange to bluish-red color [12–14]. Pelargonidin, cyanidin, delphinidin, peonidin, petunidin, and malvidin are the predominant dietary anthocyanidins. These six anthocyanidins account for more than 90% of all yet identified anthocyanins [15]. However, anthocyanins in fruits are primarily present as glycosides or acylated glycosides. Berries such as blueberries, blackberries, raspberries, cranberries, and grapes show anthocyanin contents between 21 and 390 mg per 100 g fresh weight [16] with peonidin and cyanidin being the major anthocyanins in grapes and berries, respectively [17]. It is well known, that due to their structural polyphenolic characteristics, anthocyanins exhibit a high antioxidative potential, e.g., because of their capability for donating electrons [18], scavenging ROS [19,20], preventing ROS-induced oxidative damage or influencing antioxidative enzyme expression [21,22]. In epidemiological studies, total dietary anthocyanin intake is inversely associated with CRC [18,23,24]. In addition, numerous in vitro and in vivo studies reveal that anthocyanins are able to decelerate CRC promotion and progression by several mechanisms such as triggering cell cycle arrest and apoptosis or inhibiting proliferation and invasion by different signaling pathways [10,17], whereas studies regarding the anti-migratory effects of anthocyanins on colon cancer cells are scarce [25–27]. Nonetheless, it is also known that the bioavailability of anthocyanins is relatively low and native anthocyanins are only detectable at very low concentrations in the systemic circulation [28,29]. Anthocyanins which are not absorbed in the duodenum reach the lower gastrointestinal tract where they are metabolized by the gut microbiota. Recently, it has been shown that microbially metabolized anthocyanin compounds account for the majority of absorbed berry phenols [30]. Moreover, these anthocyanin metabolites also show bioactive properties and seem to be more effective than native anthocyanins to reduce Caco-2 cell proliferation [17]. In this context, we have recently shown for the first time that physiological concentrations of anthocyanins and their metabolites isolated from the plasma of healthy volunteers after a single dose of an anthocyanin-rich juice were able to reduce tumor cell migration of the pancreatic cancer cell line PANC-1 in vitro [31]. This was accompanied by a significant reduction in ROS levels and decreased matrix metalloproteinases (MMP-2 and MMP-9), as well as NF-κB, mRNA expression [31]. Despite the common concept of antioxidants as tumor suppressors, recent evidence indicates that antioxidants may also act as tumor promotors, especially in metastasis [6]. Therefore, the role of ROS and antioxidants such as anthocyanins during metastasis are still not fully understood [32]. Similarly, the prognostic importance of enzymatic and non-enzymatic biomarkers of oxidative stress in colorectal cancer progression and metastasis is still unclear. In CRC patients biomarkers of oxidative stress are significantly increased, whereas the total antioxidant capacity (TAC) is significantly lower compared with healthy controls [5,33]. Thus, CRC patients may be more vulnerable to oxidative stress and administering of anthocyanins might improve the antioxidant capacity, overall health, and the outcome for CRC patients.

Therefore, the primary outcome of the present study was to determine whether physiological concentrations of anthocyanins and their metabolites, isolated from plasma of healthy volunteers after long-term consumption of an anthocyanin-rich grape/bilberry juice, impair the migratory potential of two colon cancer cell lines, HT-29 and Caco-2, in vitro. Although both cell lines were isolated from adenocarcinoma and exhibit epithelial phenotypes [34–36], HT-29 and Caco-2 cells were chosen due to their varying grade of differentiation [37] and their different migratory, as well as metastatic, potential [36]. We further aimed to investigate whether possible anti-migratory effects were associated with alterations of antioxidant status parameters in the plasma or urine of the volunteers (secondary outcome).

2. Materials and Methods

2.1. Preparation and Characterization of the Anthocyanin-Rich Juice and the Anthocyanin-Depleted Placebo

The anthocyanin-rich juice and the anthocyanin-depleted placebo were produced at the Hochschule Geisenheim University (Department of Beverage Research, Geisenheim, Germany) and were similar to the juices for the ANTHONIA study with minor modifications [21,38]. Briefly, juices were made from 80% red grape juice (grape variety *Accent*) and 20% bilberry juice (Heidelbeersaft blank BIO (Bayernwald KG, Hengersberg, Germany). Grapes were extracted in a press and the resulting juice was separated, blended with the bilberry juice, pasteurized, and hot-filled into 0.33 L brown glass bottles. Placebo juice was obtained by passing the juice through SP70 Sepabeads® absorber resin (Resindion S.r.l., Binasco, Italy). Both juices were analyzed directly after membrane filtration (0.45 µm) for basic analytical parameters such as total phenolics, concentrations of anthocyanins, and TEAC (Trolox equivalent antioxidative capacity) as described elsewhere [39]. Anthocyanins were analyzed by LC–MS as previously described [21]. Quantitation was carried out in duplicate using peak areas detected at 520 nm and based on external calibration via the reference substance cyanidin-3-O-glucoside (0.1–100 mg/L; linearity of calibration, $r^2 = 0.9999$). For cyanidin-3-O-glucoside, the limit of detection was 0.01 mg/L and the limit of quantitation was 0.04 mg/L.

2.2. Study Design and Study Subjects

The randomized, placebo-controlled, double blinded, cross-over ATTACH study (Anthocyanins Target Tumor cell Adhesion—Cancer vs. Endothelial Cell (HUVEC) Interactions study) was carried out at the Department of Nutritional Science, Justus Liebig University, Giessen (Germany) between April and August 2019. Sample size was calculated based on the results of our previous published migration study [31] with a β- and α-error of 0.8 and 0.05 and a drop-out rate of 20%. Calculations were made with Stata Version 15.1 (StataCorp LLC, College Station, TX, USA) from ASKNET solutions AG (Karlsruhe, Germany). In total, 45 healthy students from the Justus Liebig University, Giessen were recruited and due to exclusion criteria (drugs and antibiotics in the last 3 months before the study, vitamin and mineral supplementation, as well as intestinal or cardiovascular diseases) 2 were excluded. After randomization 8 declined to participate due to non-compliance with the nutritional recommendations. From the 35 volunteers (female $n = 27$ and male $n = 8$), 13 were omnivores, 8 vegetarians, 2 vegans and 1 pescetarian with a mean ± SD age of 24.4 ± 2.3 years (range: 19–29 years), an initial body weight of 64.3 ± 17.9 kg (range: 49–93 kg), and a BMI of 21.7 ± 2.6 kg/m^2 (range: 18.4–27.6 kg/m^2). Baseline characteristics did not change during the total study period. Of the 35 subjects, 34 collected all samples (blood and urine), whereas one subject had an incomplete urine sample collection.

Volunteers received the beverages, denoted as "one" or "two", weekly at the Department of Nutritional Science. The beverages were filled in brown bottles to ensure blinding and distributed weekly to the volunteers by the lab personal. Participants were instructed to daily consume 0.33 L of the anthocyanin-rich juice or the anthocyanin-depleted placebo for 28 days. They were instructed to keep the juices cool and to avoid their exposure to

direct light. Thus, after a 7-day wash-out period, a 28-day intervention period followed, and the first phase was completed by a 14-day run-out period. After the run-out phase, the next phase started with the next beverage (Figure 1).

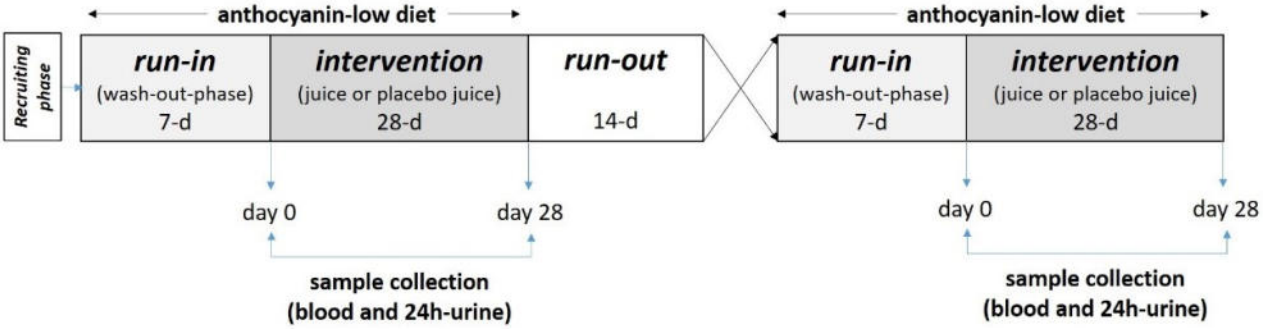

Figure 1. Study design of the ATTACH study. Participants consume the anthocyanin-rich juice and the anthocyanin-depleted placebo. Before (day 0) and after each intervention (day 28), blood and 24 h-urine samples were collected and processed for biochemical analyses (n = 35). d, day.

As phenolic compounds including anthocyanins are present in many foodstuffs and beverages, participants were explicitly counseled prior to the start of the study to follow a low phenolic/anthocyanin diet during the run-in and intervention period to avoid possible effects of other phenolics, especially anthocyanins, from the diet. Similar to our ANTHONIA study, the volunteers received a list of categorizing foodstuffs including beverages into "quantitatively limited" and "not being allowed" with slight modifications [21]. Foodstuffs were categorized according to their anthocyanin content based on data using the USDA Database for the Flavonoid Content of Selected Foods (release 3.3 (2018); http://www.ars.usda.gov/, accessed on 1 March 2019) or a database on polyphenol contents in food (Polyphenol-Explorer, release 3.0; http://www.phenol-explorer.eu/compounds, accessed on 1 March 2019) (Table S1).

Participants were also instructed to record their dietary intake over 3 days during each intervention period in order to estimate their daily energy and nutrient intakes. Dietary records were analyzed using the DGE-PC Professional software, version 1.10.0.0 (Table S2). Participants were instructed to maintain their usual physical activity.

The study protocol was approved by the local ethics committee (registration number 13/10) and according to the guidelines laid down in the Declaration of Helsinki. It is registered at DRKS (Deutsche Register Klinischer Studien) with the registration number DRKS00014767. Written informed consent was obtained from all included participants and data collection was conducted by the Department of Nutritional Science (Giessen, Germany).

2.3. Collection of Plasma and Urine Samples

Sample collection occurred before and after the two intervention periods. After an initial 7-day run-in period, participants were instructed to collect their 24 h-urine and blood was drawn by venipuncture into tubes with EDTA as anticoagulant (Sarstedt & Co., Nuembrecht, Germany). Plasma was separated immediately by centrifugation (1200× g for 15 min; 4 °C). The supernatant was divided into aliquots and stored at −80 °C until assayed (day 0). Volunteers again collected their 24 h-urine at the end of the intervention and consumed the juice after an overnight fast together with breakfast on the last day of the intervention period. Plasma samples were collected 6 h after juice ingestion (day 28).

2.4. Isolation of Plasma Anthocyanins and Their Metebaolites by Solid Phase Extraction

Plasma extraction of anthocyanins and their metabolites was based on the method described recently [40]. Briefly, each aliquot (1 mL of plasma acidified with 30 µL of 50% aqueous formic acid (Lgc Promochem, Wesel, Germany)) was loaded onto an Oasis-HLB (1 mL/30 mg) SPE cartridge (Waters, Inc., Eschborn, Germany), preconditioned with

1 mL of methanol (Thermo Fischer Scientific, Langenselbold, Germany) and 1% formic acid, followed by 1 mL of acidified water (1% formic acid). The cartridge was then washed with 1 mL of acidified water, after which anthocyanins and their metabolites were eluted with 1 mL of acidified methanol. Afterwards, eluates were dried under N_2 for approximately 3 h [40]. For cell migration studies with HT-29 and Caco-2 cells, dried anthocyanins isolated from plasma as well as their metabolites (PAM) were resolved in the same volume of culture media (1 mL; pH 7.2) as the original plasma volume (1 mL).

2.5. Cell Culture

The two human colon carcinoma cell lines HT-29 (HTB-38) and Caco-2 (HTB-37) were purchased from the American Type Culture Collection (ATCC) (San Diego, CA, USA). HT-29 is a cell line with epithelial morphology that was isolated in 1964 from a primary tumor obtained from a 44-year-old female patient with colorectal cancer by J. Fogh [34]. HT-29 cells were grown in RPMI 1640 GlutaMax (Invitrogen GmbH, Darmstadt, Germany) supplemented with 1 mmol/L sodium pyruvate (Invitrogen GmbH, Darmstadt, Germany) and 10% fetal calf serum (FCS) (Invitrogen GmbH, Darmstadt, Germany). Caco-2 are epithelial cells isolated from colon tissue derived from a 72-year-old male with colorectal adenocarcinoma and has been widely used as a model of the intestinal epithelial barrier [35]. Cells were grown in DMEM (Invitrogen GmbH, Darmstadt, Germany) supplemented with 5 mM L-glutamine (Invitrogen GmbH, Darmstadt, Germany), 1 mmol/L sodium pyruvate and 10% FCS. Thus, both cell lines were isolated from colon adenocarcinomas and were most widely used for in vitro studies to compare their tumorigenicity genotype [41–43]. Both cell lines were sub-cultured twice a week, incubated at 37 °C in a humidified 5% (*v*/*v*) CO_2 atmosphere and used between passages 10 to 35. Culture medium was changed every two days.

2.6. Cell Migration of Colon Cancer Cells In Vitro

Tumor cell migration was assessed in a Boyden chamber with the use of the CytoSelect 24-well Cell Migration Assay (CellBiolabs, San Diego, CA, USA) according to earlier studies [31]. The feeder trays were coated with 100 µL of 10 µg/mL collagen (Merck GmbH, Darmstadt, Germany) and aspirated until dryness. Onto the upper side of the 24-well feeder chamber (diameter of the chamber 6.5 mm; pore size 8 µm), cells at a density of 1×10^5/mL were seeded in DMEM or RPMI 1640 GlutaMax containing 1% FCS and diluted PAM (day 0 vs. day 28), whereas DMEM or RPMI 1640 GlutaMax supplemented with 10% FCS were added to the lower chamber [41]. Cells were incubated in the feeder tray for 36 h at 37 °C. Then cells on the lower side were detached from the membrane using a cell detachment solution and afterwards lysed with a fluorescent-dye-containing buffer. The extent of migration was assessed by the intensity of the fluorescence signal, which was measured with a Synergy H1 microplate fluorescence reader (Biotek, Karlsruhe, Germany). The number of migrated cells was determined according to a calibration curve (500 to 15,000 cells). Results are expressed as median with interquartile range from $n = 35$ or $n = 34$ volunteers. A 100 mM stock of 5-FU (Sigma-Aldrich Chemie GmbH, Taufkirchen, Germany) was prepared in absolute DMSO (Merck GmbH, Darmstadt, Germany) and stored at −20 °C. The concentration of DMSO was less than 1% of drug treatment. For treatment, 5-FU was diluted in culture media and added to cultures to give the desired final concentration.

2.7. Assessment of Cell Viability by Flow Cytometry

Viability of cells was determined by flow cytometry with the Guava® ViaCount™ reagent (Luminex, MV's, Hertogenbach, Netherlands). Therefore, HT-29 cells were seeded at a density of 1×10^5 cells/mL in 24-well plates in complete medium with or without PAM from the anthocyanin-rich juice, which were isolated before or after the 28-day intervention as well as with different concentrations of 5-FU. After 36 h incubation, cells were washed twice with PBS (Invitrogen GmbH, Darmstadt, Germany) and trypsinized with

TrypLE Express (Invitrogen GmbH, Darmstadt, Germany). Cell viability and cytotoxicity were measured according to the manufacturer's instructions using a Guava® Muse® Cell Analzyer (Luminex, MV'ss, Hertogenbach, Netherlands).

2.8. Oxidative Biomarkers in Plasma and Urine Samples

Oxidative biomarkers in plasma and urine samples were measured before (day 0) and after each intervention period (day 28). Enzyme activities of superoxide dismutase (SOD), catalase (CAT), and glutathione peroxidase (GPx) were determined by colorimetric methods according to the manufacturer's instructions (Cayman Chemical Company, Ann Arbor, MI, USA) in a Synergy H1 microplate fluorescence reader (Biotek, Karlsruhe, Germany) as described previously [21]. The amount of water and lipid soluble antioxidants in plasma was assessed using the ABTS (2,2-azino-di-3-ethylbenzthiazoline sulphonate) assay (Cayman Chemical Company, Ann Arbor, MI, USA). Generation of $ABTS^+$ from ABTS by metmyoglobin is inhibited by antioxidants and yields a reduction in absorbance at 405 nm. The capacity of antioxidants to reduce $ABTS^+$ generation was compared with that of Trolox and quantified as Trolox equivalents (mmol/L TEAC) [21]. All analyses were performed in duplicate and intra-assay coefficients of the assays were <12%. The total phenolic content (TPC) in urine samples was determined after solid-phase extraction (SPE) (Oasis® MAX 96-well plate cartridges) using a rapid Folin–Ciocalteu method described earlier [44,45]. Briefly, in a thermo microtiter 96-well plate, 170 µL of Milli-Q water, 15 µL of the urine extract, 12 µL of the Folin–Ciocalteu reagent (Sigma-Aldrich Chemie GmbH, Taufkirchen, Germany) and 30 µL of 20% sodium carbonate were mixed. After 1 h of incubation at room temperature in the dark, the absorbance was measured at 750 nm using an UV/VIS Thermo Multiskan Spectrum spectrophotometer (Vantaa, Finland). Gallic acid (Sigma-Aldrich Chemie GmbH, Taufkirchen, Germany) was used as a standard and quantified as gallic acid equivalents (mg/L). All samples were processed in triplicate and the coefficient of variation (CV) was <10%. Results were multiplied by the urine output and expressed as gallic acid equivalents (GAE) in mg/24 h

2.9. Statistical Analyses

Data from the volunteers who completed all phases of the study (n = 35; n = 34) were analyzed. The outcome measures were prospectively designated as the differences in migration of HT-29 and Caco-2 cells in vitro (primary outcome) and antioxidative parameters (secondary outcome) of placebo and juice treatment before (day 0) and after (day 28) intervention. Before-treatment versus after-treatment data within groups were analyzed using a repeated measures one-way ANOVA, with Šídák's post hoc test. A mixed model with multiple comparison test (Šídák's) were used for data sets with missing values. The normality of continuous variables was assessed using Kolmogorov–Smirnov normality test. Asterisks are used in the figures to denote p values < 0.05, which were considered significant. Data were expressed as mean ± SD or as median with interquartile range (25th–75th percentile). Correlation analyses were evaluated using Spearman correlation (r) with differences between values from day 28 and day 0 after anthocyanin-rich juice intake (e.g., Δ values = values J_28-days—values J_0-days). GraphPad Prism 9 Version 9.3.1. from ASKNET solutions AG (Karlsruhe, Germany) was used for data analyses.

3. Results

3.1. Composition of the Anthocyanin-Rich Juice and the Anthocyanin-Depleted Placebo

In this cross-over, placebo-controlled intervention study, an anthocyanin-rich grape/bilberry juice was given to healthy male and female volunteers for 28 days in order to investigate the influence of PAM on cancer cell migration in vitro. To eliminate possible effects of other juice compounds, an anthocyanin-depleted placebo juice was also applied. The anthocyanin-rich juice exhibited an especially high antioxidant activity corresponding to a higher TEAC value (27 ± 1.7 mmol/L), as well as higher concentrations of total phenolics (2622 ± 56 mg/L catechin equivalents) and anthocyanins (942 ± 10 mg/L

cyanidin-3-O-equivalents) in comparison with the anthocyanin-depleted placebo (TEAC: 1.0 ± 0.04 mmol/L; total phenolics: 115 ± 5.0 mg/L catechin equivalents; anthocyanins: 6.3 ± 0.5 mg/L cyanidin-3-O-glucoside equivalents). In comparison with commercially available grape (TEAC: 10–12 mmol/L) and blueberry juices (TEAC: 13–17 mmol/L) the TEAC value of our juice was approximately 2–3-fold higher [46–48]. Regarding anthocyanins, which were the main phenolics in both beverages, the applied beverages considerably differed in their profile and contents (Table 1). Due to the high grape content, peonidin-3,5-O-diglucoside and malvidin-3,5-O-diglucoside were the most abundant anthocyanins in the juice and accounted for more than 51.5% of all anthocyanins, followed by peonidin-3-O-glucoside and malvidin-3-O-glucoside. In comparison with the juice, the placebo contained only minor amounts of anthocyanins.

Table 1. Anthocyanin composition of the anthocyanin-rich juice and the anthocyanin-depleted placebo [1].

	Anthocyanin-Rich Juice		Anthocyanin-Depleted Placebo	
Anthocyanins	**(mg/L)**	**(%)**	**mg/L**	**(%)**
peonidin-3,5-O-diglucoside	346 ± 12.5	36.8	1.7 ± 0.02	26.9
malvidin-3,5-O-diglucoside	138 ± 8.4	14.7	0.88 ± 0.06	14.0
peonidin-3-O-glucoside	83.5 ± 6.4	8.9	0.37 ± 0.01	5.9
malvidin-3-O-glucoside	63.4 ± 3.8	6.7	0.30 ± 0.01	4.7
delphinidin-3-O-glucoside	61.5 ± 2.9	6.5	0.80 ± 0.03	12.7
delphinidin-3-O-galactoside	53.6 ± 0.6	5.7	0.75 ± 0.01	11.9
delphinidin-3-O-arabinoside	53.4 ± 1.6	5.7	0.56 ± 0.02	7.4
petunidin-3-O-glucoside	43.7 ± 1.9	4.6	0.37 ± 0.02	5.8
cyanidin-3-O-arabinoside	27.2 ± 1.7	2.9	0.11 ± 0.02	1.7
cyanidin-3,5-O-diglucoside	18.2 ± 1.6	1.9	0.29 ± 0.00	4.6
malvidin-3-(6″-O-coumaryl)-5-O-diglucoside	17.1 ± 0.4	1.8	n.d.	n.d.
petunidin-3-O-galactoside	13.2 ± 0.3	1.4	0.11 ± 0.01	1.8
petunidin-3-O-arabinoside	8.8 ± 0.0	0.9	0.05 ± 0.01	0.8
malvidin-3-O-arabinoside	5.3 ± 0.0	0.6	0.02 ± 0.00	0.3
peonidin-3-O-galactoside	4.3 ± 0.0	0.5	0.01 ± 0.00	0.1
delphinidin-3,5-O-diglucoside	3.4 ± 0.0	0.4	0.09 ± 0.01	1.4
Sum	942 ± 10	100	6.3 ± 0.5	100

[1] Juices were analyzed by LC–MS ($n \geq 2$) and data are expressed as mean ± SD mg cyanidin-3-O-glucoside equivalents per L.n.d., non-detectable

3.2. Influence of Plasma Anthocyanins and Their Metabolites on HT-29 and Caco-2 Colon Cancer Cell Migration

Anthocyanins and their metabolites were extracted by SPE from plasma samples before (0 d) and after the intervention (28 d) with juice or placebo. Afterwards, dried PAM were solved in cell culture media and applied to the two colon cancer cell lines HT-29 and Caco-2. As shown in Figure 2, cancer cell migration was differently affected by incubation with PAM from both beverages. In case of HT-29 cells, PAM from the juice significantly reduced cancer cell migration from 3806 (3646–4013) to 3453 (3052–3787) cells per cavity ($p < 0.001$). In comparison, no inhibition was observed after exposure to PAM from the placebo (Figure 2a). In contrast to HT-29 cells, migration of Caco-2 cells was neither influenced by PAM from the placebo nor by PAM from the juice (Figure 2b). Therefore, this study shows that physiological concentrations of PAM significantly impair the migratory potential of HT-29 cells, whereas migration of Caco-2 cells was not affected.

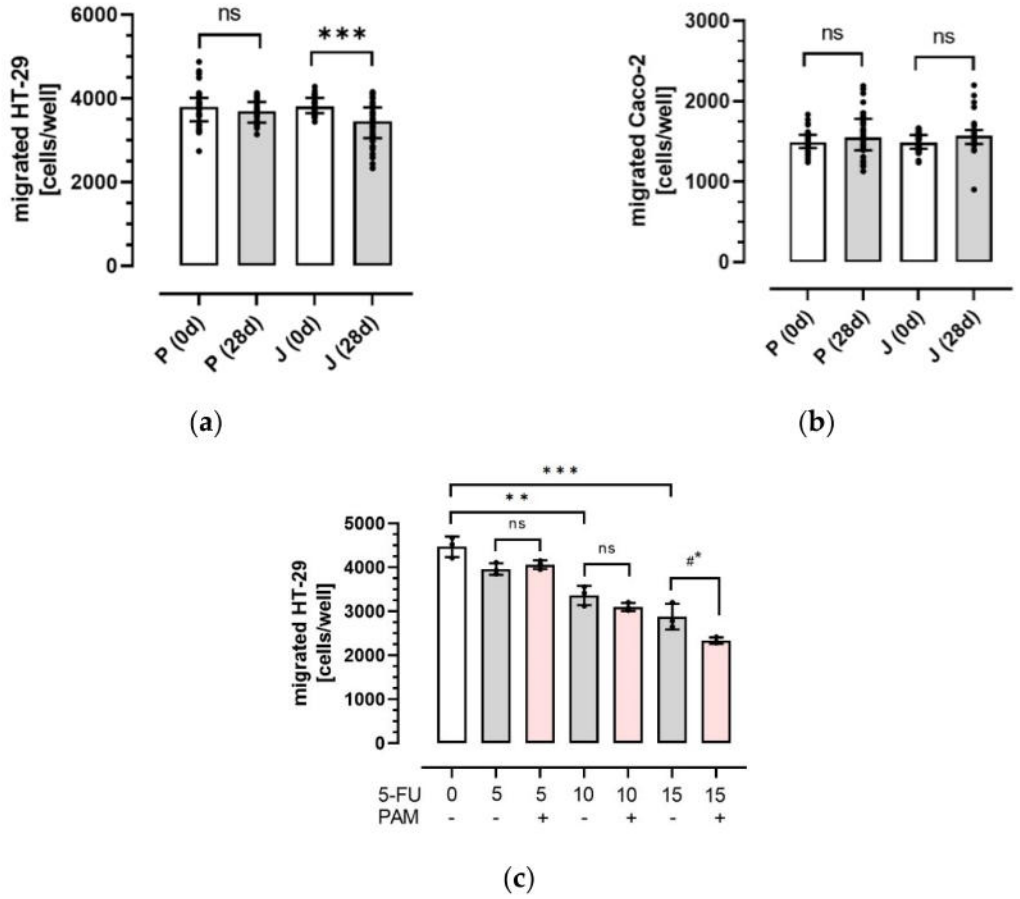

Figure 2. Migration of HT-29 and Caco-2 cells in vitro. HT-29 (**a**) and Caco-2 (**b**) cells were incubated with PAM from the anthocyanin-depleted placebo (P; $n = 34$) and anthocyanin-rich juice (J; $n = 35$) that were isolated before (0 d) and after 28-day (28 d) intervention. Migration was studied in a Boyden chamber with collagen-coated transwells. Basal cells in the lower chamber were measured after 36 h and migrated cell counts were detected fluorometrically as described in the Methods section. HT-29 cells (**c**) were exposed to indicated concentrations of 5-FU alone (5, 10, and 15 µM) and with pooled PAM ($n = 10$; most effective from (**a**)). Values are presented as aligned dot plots with median and interquartile range (25th–75th) (**a**,**b**) or means with standard deviation (**c**). Significant differences were calculated with a mixed model with multiple comparison test (Šídák's) or ANOVA with multiple comparison test (Šídák's). Values were different with ** $p < 0.01$ and *** $p < 0.001$ compared with the corresponding controls or with #* $p < 0.05$ compared with 5-FU (15 µM) alone. ns, non significant.

To examine the effect of 5-fluorouracil (5-FU) on HT-29 cell migration, various concentrations of 5-FU were applied. 5-FU is a common chemotherapeutic agent in colorectal cancer [49,50] and it is known that flavonoids can interact with chemotherapeutic agents [51]. However, possible interactions between anthocyanins and 5-FU are largely unknown. As shown in Figure 2c, HT-29 cell migration was concentration-dependently inhibited by 5-FU treatment. Compared with untreated control cells, incubation of HT-29 cells with the most effective 5-FU concentration (15 µM) significantly reduced colon cancer cell migration from 4472 ± 231 to 2882 ± 289 cells per cavity ($p < 0.001$). To further investigate, possible synergistic or even antagonistic effects of PAM on 5-FU treatment, HT-29 cells were co-incubated with 5-FU and pooled PAM from volunteers ($n = 10$) that most effectively inhibited HT-29 cancer cell migration. In comparison with 5-FU alone (15 µM), co-incubation with pooled PAM further decreased HT-29 cell migration from 2882 ± 289 to 2338 ± 71 cells per cavity ($p < 0.05$), respectively (Figure 2c). These results indicate that physiological concentrations of anthocyanins and their metabolites may promote the effects of classical chemotherapeutic agents like 5-FU.

3.3. Influence of Plasma Anthocyanins and Their Metabolites on HT-29 and Caco-2 Cell Viability

To investigate possible cytotoxic effects of PAM on colon cancer cells, HT-29 were incubated with the pooled PAM from volunteers that most effectively inhibited HT-29 cancer cell migration (n = 10). As shown in Figure 3 viability of HT-29 cells was neither affected by incubation with PAM for 36 h, nor by 5-FU in low doses (≤25 µM). In contrast, 50 µM 5-FU significantly decreased viability of HT-29 cells compared with controls. In addition, PAM showed no cytotoxic effects in non-tumor cells (Figure S1).

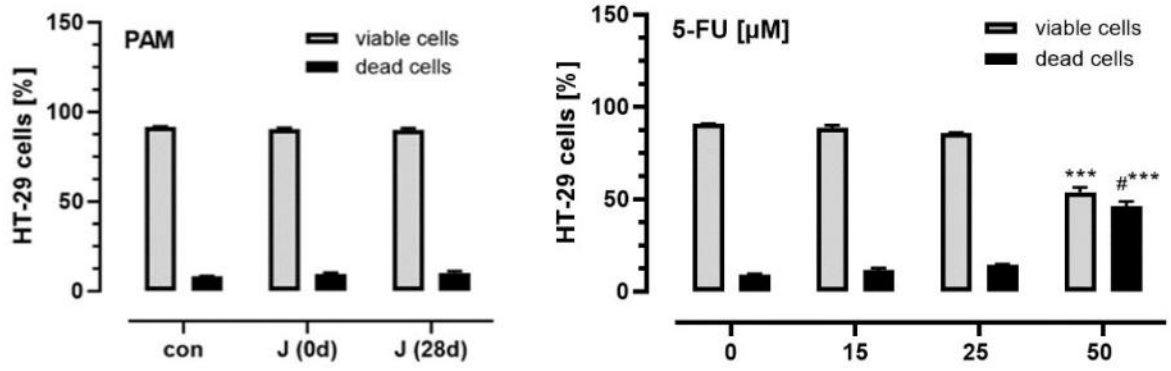

Figure 3. Effects of PAM (**a**) and 5-FU (**b**) on HT-29 cell viability. HT-29 cells were seeded at a density of 1 × 10^5 cells/mL in 24-well plates in complete medium with or without PAM from the anthocyanin-rich juice that were isolated before (J (0 d)) or after 28-day intervention (J (28 d)) or with medium alone (con), as well as with different concentrations of 5-FU. After 36 h incubation, cells were washed twice with PBS, trypsinized and cell viability was measured using a Guava® Muse® Cell Analyzer. Data are expressed as bars [%] with standard deviation. Significant differences were calculated with ANOVA with multiple comparison test. Values were different with *** $p < 0.001$ compared with viable cells of the controls (con) or with #*** $p < 0.001$ compared with dead cells of the controls (n = 2).

3.4. Effects of the Anthocyanin-Rich Juice and the Anthocyanin-Depleted Placebo on Antioxidative Biomarkers in Plasma and Urine

Biomarkers of oxidative stress are significantly increased in CRC patients, whereas TAC is significantly lower compared with healthy controls [5,33]. Thus, we aimed to investigate whether long-term consumption of an anthocyanin-rich juice improves the antioxidant status of healthy volunteers. A significant increase of median (25th–75th percentile) plasma SOD activity from 7.53 (6.27–9.55) to 9.52 (7.21–10.69) U/mL ($p < 0.001$) was observed after a 28-day intervention with the juice. In contrast, no change in plasma SOD activity was found after consumption of the placebo (Figure 4a). Similarly, after ingestion of the anthocyanin-rich juice, plasma CAT and GPx activity significantly increased from 4.92 (3.77–8.00) to 6.42 (4.33–8.24) nmol/min/mL ($p < 0.001$) and from 75.92 (69.10–90.18) to 85.22 (74.28–91.96) nmol/min/mL ($p < 0.05$), respectively. Again, CAT and GPx activity remained unchanged after placebo intake (Figure 4b,c).

The antioxidant capacity of plasma samples was estimated as TEAC comprising the antioxidative capacity of both lipophilic and hydrophilic compounds. Comparable to antioxidative enzyme activities in plasma, the median TEAC value significantly increased after ingestion of the anthocyanin-rich juice from 1.09 (1.02–1.19) to 1.21 (1.07–1.35) mmol/mL ($p < 0.001$). However, after placebo intake no significant change was observed.

(Figure 4d). In contrast to the observations for plasma antioxidative enzymes and capacity, no significant differences were found with respect to urine TPC after intake of both, placebo and juice (Figure 4e). Interestingly, heatmap analysis (Figure 4, upper panels) shows that GPx activity from vegetarians (volunteers 1–12) was higher than those of omnivores. In summary, these results show that consumption of an anthocyanin-rich juice for 28 days significantly improves the antioxidant status of healthy volunteers.

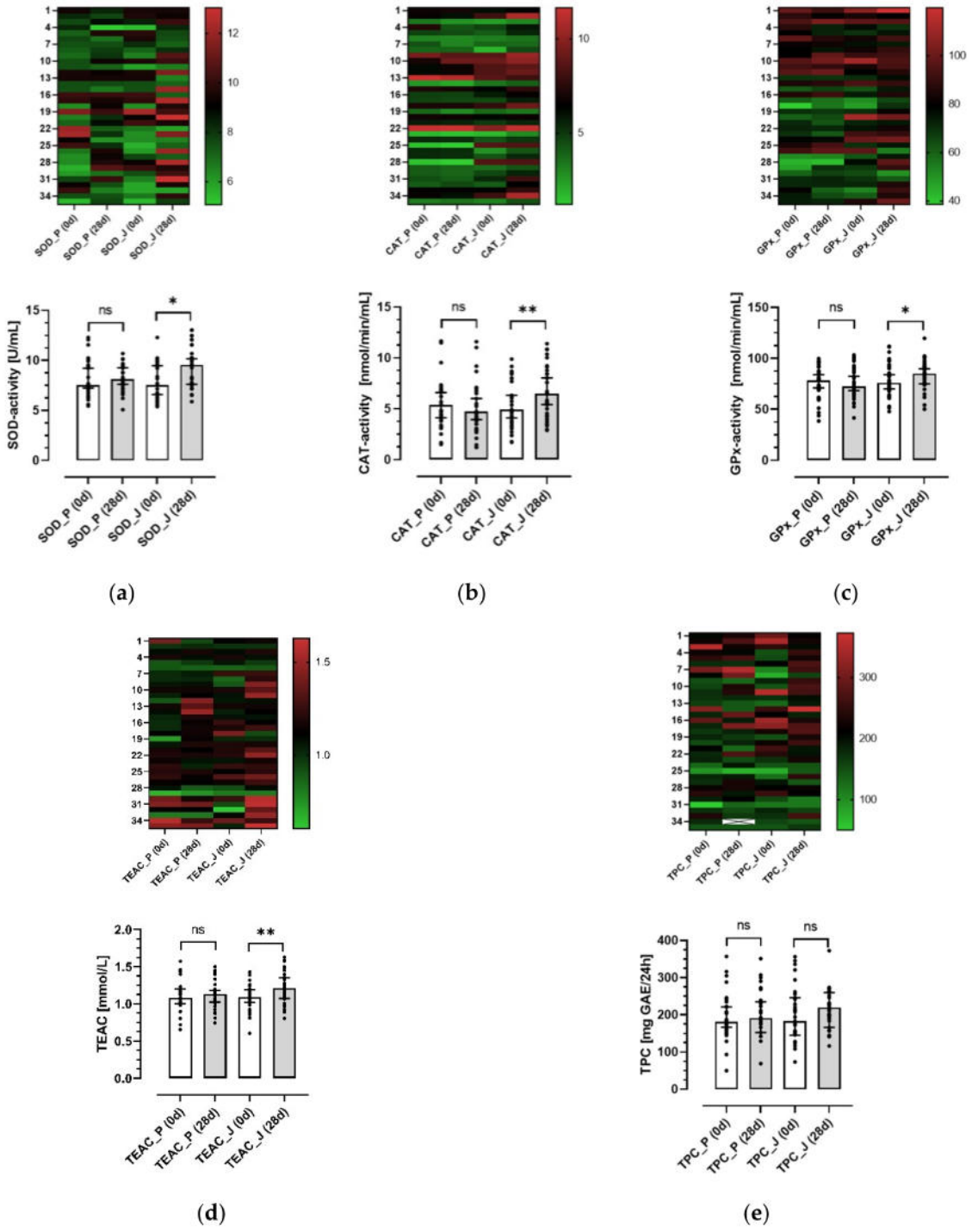

Figure 4. Effects of the anthocyanin-rich juice and the anthocyanin-depleted placebo on antioxidative parameters before and after intervention. Study participants consumed 0.33 L of the anthocyanin-depleted placebo (P) and anthocyanin-rich juice (J) over 28 days. Before (0 d) and after (28 d) intervention, blood samples were drawn and 24 h-urine samples were collected. Enzyme activities of SOD (U/mL) (**a**), CAT (nmol/min/mL) (**b**), GPx (nmol/min/mL) (**c**) as well as TEAC (mmol/mL) (**d**) were measured in plasma (n = 35). TPC (mg GAE/24 h) (**e**) was measured in urine (n = 34). Upper panel: Heatmap analyses showed single values for each participant. Lower panel: Values are presented as aligned dot blot bars with median and interquartile range (25th–75th). Significant differences were calculated with a mixed model with multiple comparison test (Šídák's) or ANOVA with multiple comparison test (Šídák's). Values after intervention were different with * $p < 0.05$, ** $p < 0.005$ to corresponding controls. ns, non significant.

3.5. Correlation between Parameters of Antioxidant Capacity and Migration

We further aimed to investigate, whether the increase in antioxidant status parameters in the plasma of healthy volunteers after 28-day consumption of the anthocyanin-rich juice was correlated with the significant decrease of HT-29 colon cancer cell migration that was observed in vitro (Figure 5). In fact, the higher the increase in SOD activity in plasma after consumption of the anthocyanin-rich juice (Figure 5a), the higher the anti-invasive effect was on HT-29 cell migration in vitro ($p < 0.05$). In contrast, no correlation was observed between other antioxidant parameters in plasma, indicating a possible link between plasma SOD activity and colon cancer metastasis.

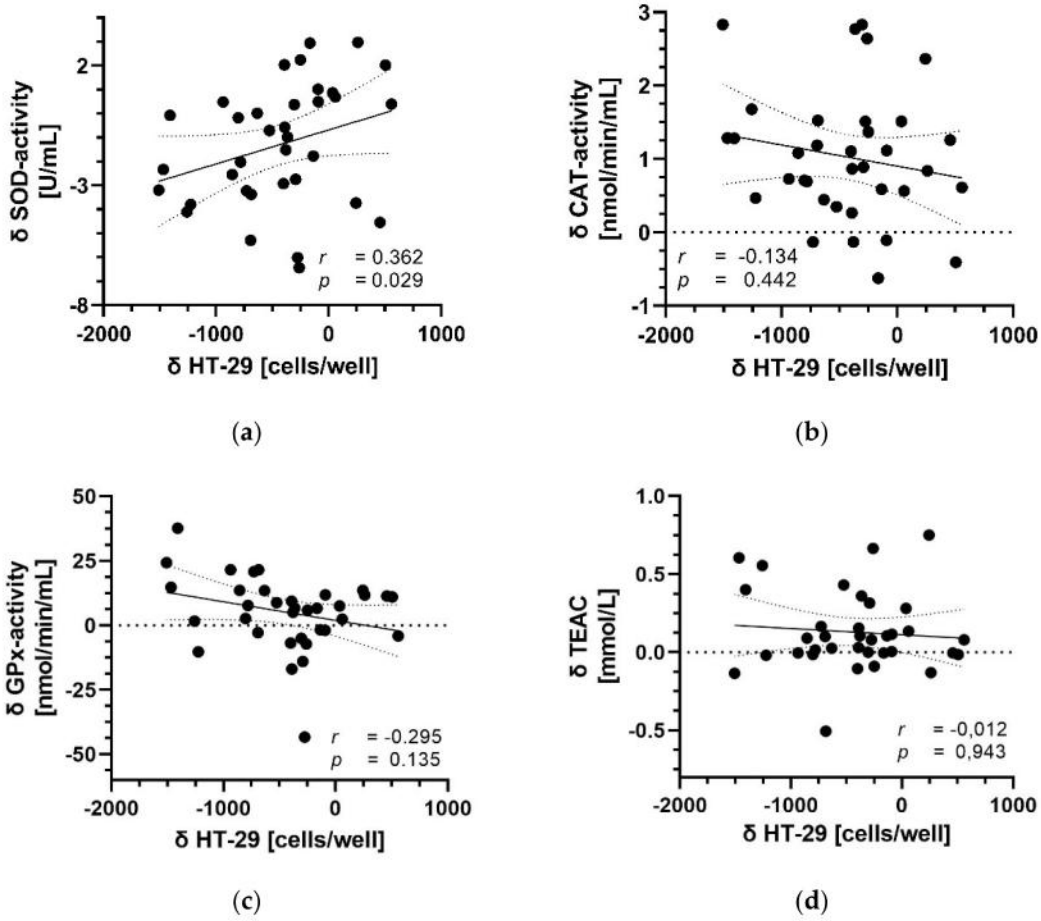

Figure 5. Scatter plots of antioxidant parameters and HT-29 migration. Correlation between HT-29 cell migration in vitro and SOD activity (**a**), CAT activity (**b**), GPx activity (**c**), and TEAC (**d**) in plasma. Correlation between the parameters were evaluated using Spearman correlation (r) with differences (δ) between values from day 28 and day 0 after anthocyanin-rich juice intake ($n = 35$).

4. Discussion

Considering that about every fourth colon cancer patient displays distant metastases after resection [52] and cancer mortality is mainly due to metastasis lesions [52,53], searching for new therapeutic agents to suppress cancer cell invasion and migration is crucial. However, data from human studies regarding the effects of anthocyanins on colon cancer progression are scarce and to date, it has not yet been clarified whether anthocyanins, particularly at physiological concentrations, have an impact on cancer cell migration in vivo. To overcome these limitations, the present study was designed to determine the anti-migratory effects of anthocyanins and their plasma metabolites on cell migration after long-term ingestion of an anthocyanin-rich grape/bilberry juice. Therefore, we combined a placebo-controlled, double-blinded, cross-over intervention study with in vitro migration

studies of two colon cancer cell lines, HT-29 and Caco-2. Healthy students daily consumed 0.33 L of an anthocyanin-rich juice in comparison to an anthocyanin-depleted placebo for 28 days. Blood samples were drawn before and after intervention. Subsequently, plasma samples were used to isolate PAM that were applied to a collagen-coated Boyden chamber for the measurement of colon cancer cell migration. To the best of our knowledge, this is the first study that showed that physiological concentrations of PAM significantly impair the migratory potential of HT-29 cells. In contrast, migration of Caco-2 cells was not affected. Although both cell lines were isolated from colon adenocarcinomas, they show differences in pheno- and genotypes, as well as in their grade of differentiation [54]. Hence, it is not surprising that undifferentiated HT-29 cells showed an obviously higher migratory potential compared with the more differentiated Caco-2 cells, which is underlined by the much higher number of migrated HT-29 cells in our experiments.

One of the most common and effective chemotherapeutic agents used for the treatment of CRC is 5-FU [50], although the benefit from 5-FU is often compromised by chemoresistance [49]. Therefore, it is vital to search for adjuvant agents and to investigate possible synergistic or even antagonistic effects of PAM on 5-FU treatment. Indeed, co-incubation of HT-29 cells with 5-FU and PAM further decreased cell migration compared with 5-FU treatment alone. Similarly, Li et al. recently reported that black raspberry anthocyanins significantly increased the anti-proliferative and anti-migratory effects of 5-FU and Celecoxib in colon cancer cell lines [55]. However, proliferation of Caco-2 cells was not affected by single treatment with black raspberry anthocyanins [55]. Accordingly, physiological concentrations of anthocyanins and their metabolites might possibly enhance the anti-migratory effect of 5-FU in Caco-2 cells. However, a possible synergistic effect of PAM and 5-FU from all volunteers was not investigated in the present study due to the limited sample material.

Metastasis is a multistep process that comprises cell migration from the primary tumor site, cell invasion, attachment to endothelial cells, extravasation, proliferation, and angiogenesis at the distal site [53,56]. Degradation of the extracellular matrix, especially collagen, mediated by proteolytic enzymes such as MMP-2 (gelatinase-A) and MMP-9 (gelatinase-B), is known to be the first step and plays a crucial role during cell migration and invasion [31,57]. While the anti-migratory and anti-invasive effects of anthocyanins have been reported for several cancer types, data regarding their impact on colon cancer cell migration are limited. The migration and invasion of HT-29 cells was significantly inhibited by an anthocyanin extract from *Vitis coignetiae Pulliat*, a member of the grape family, by suppressing MMP-2 and MMP-9 expression, which was likely due to the inhibition of NF-κB activation [25]. The inhibitory effects of anthocyanins on MMP-2 and MMP-9 expression were also shown in HCT-116 colon cancer cells [26]. Interestingly, Zhang et al., recently reported that black raspberry anthocyanins increased miR-24-1-5p expression in colon cancer cell lines, whereas miR-24-1-5p overexpression was associated with a significant decline of HCT-116 and Caco-2 migration [27]. However, these anti-invasive and anti-migratory effects were only shown at concentrations much higher than anthocyanin levels usually observed in plasma. Nevertheless, we have recently shown for the first time that physiological concentrations of anthocyanins and their metabolites isolated from the plasma of healthy volunteers are able to reduce tumor cell migration of the pancreatic cancer cell line PANC-1 in vitro [31]. This was accompanied by a significant reduction of ROS and decreased MMP-2 and MMP-9 levels, as well as NF-κB mRNA expression, suggesting that physiological concentrations of PAM may be adequate due to synergistic and additive effects. Although in the present study the underlying mechanisms remain unknown, it is most likely that inhibition of HT-29 cell migration is also attributed to suppression of the NF-κB pathway, as well as decreased expression of MMPs. In the present study the applied anthocyanin-rich juice was made from an eighty/twenty mixture of red grapes and bilberries with peonidin-3,5-O-diglucoside, malvidin-3,5-O-diglucoside, and peonidin-3-O-glucoside representing the major anthocyanins. It has been shown that peonidin-3-O-glucoside significantly inhibits MMP secretion and migration of lung cancer

cells [58]. In addition, peonidin has been reported to be the most potent anthocyanidin comparing the anti-migratory and anti-invasive capabilities of the five anthocyanidins cyanidin, malvidin, peonidin, petunidin, and delphinidin [59]. Peonidin significantly suppressed migration and invasion of highly invasive H1299 cells by about 20% even at a relatively low concentration (6.25 µM) [59]. Furthermore, synergistic anti-migratory and anti-invasive effects have been reported for a mixture comprising the five aglycons at equimolar concentrations [59]. However, this approach did not consider the impact of anthocyanin metabolites, which are much more abundant in plasma compared with native anthocyanins [38]. In addition, the bioavailability of native anthocyanins is low due to (1) their low stability and degradation at physiological pH values in the small intestine, (2) their metabolization through Phase II enzymes, and (3) their metabolism by the intestinal microbiota [60–62]. Regarding the pharmacokinetics of anthocyanins, native anthocyanins reach maximum plasma levels 30–60 min after ingestion [38]. In contrast to the ANTHONIA study [21], blood samples were drawn approximately 6 h after juice ingestion in the present study. At this time, Phase-II as well as microbiota-derived metabolites are present in the systemic circulation [63]. Therefore, the present study suggests that not only native anthocyanins but also their metabolites exert potent anti-migratory properties. However, we did not identify which anthocyanins and metabolites are responsible for the observed anti-migratory effects. Therefore, characterization of these compounds should be addressed in future studies.

Epidemiological studies indicate protective effects of dietary polyphenols against oxidation- and inflammation-related diseases such as cancer, cardiovascular diseases, diabetes mellitus, and neurodegenerative diseases [64,65]. It has been shown that the TAC of CRC patients is significantly lower compared with healthy controls [5,33]. Furthermore, CRC progression and metastasis are also associated with a significant decline in TAC, as well as lower CAT and GPx activities in serum and plasma, respectively [5,66]. Therefore, CRC patients may be more vulnerable to oxidative stress and the administering of anthocyanins might improve the antioxidant capacity, overall health, and outcome of CRC patients. Our results show that daily intake of an anthocyanin-rich juice for 28 days significantly improves plasma antioxidant capacity of healthy volunteers determined by enzymatic and non-enzymatic biomarkers. Plasma antioxidant capacity, measured as TEAC, was significantly higher after consumption of the anthocyanin-rich juice, whereas no change in TEAC was seen after ingestion of the anthocyanin-depleted placebo. Similarly, activities of the antioxidant enzymes SOD, CAT, and GPx were significantly increased after the juice, whereas the enzyme activities were not affected by the placebo. These results are in line with our recent findings from the ANTHONIA study [21]. Interestingly, GPx activity was not affected after consumption of an anthocyanin-rich grape/bilberry juice for 14 days [21]. Discrepancies in the results for GPx activity may be explained by different intervention times. In addition, there were slight differences between the grape/bilberry juices during the two studies. Both juices were made from an eighty/twenty mixture of red grapes and bilberries. Whereas in the ANTHONIA study the two grape varieties, *Dakapo* and *Accent*, were used, only the variety *Accent* was utilized in the present study, resulting in the different anthocyanin pattern of the juices. Thus, malvidin-3-O-glucoside and peonidin-3-O-glucoside were the major anthocyanin in the ANTHONIA study, whereas peonidin-3,5-O-diglucoside and malvidin-3,5-O-diglucoside represent the main anthocyanins in the present study. However, expression of the antioxidant enzymes SOD, CAT, and GPx is controlled by the redox sensitive transcription factor nuclear factor-erythroid 2 p45-related factor 2 (Nrf2) [67]. It is well known that anthocyanins, but also their gut-derived metabolites, are able to activate the Nrf2 pathway and consequently upregulate the defense against ROS and oxidative stress [68,69]. Compared with cells from the primary tumor site, metastatic cancer cells displayed higher ROS concentrations [6]. The ROS lowering effects of anthocyanins and their degradation products (gallic acid, syringic acid, protocatechuic acid, and phloroglucinol aldehyde) have been demonstrated in different colon cancer cell lines [67]. In addition, we have recently shown that physiological plasma concentrations

of PAM significantly reduce ROS generation in PANC-1 cells [31]. However, possible ROS lowering effects of PAM in HT-29 and Caco-2 cells have not been investigated in the present study. Recently, Yang et al., 2021 reported that blueberry anthocyanins significantly increased SOD activity in the lungs and livers of mice in vivo. In addition, in these organs reduced metastasis of breast cancer cells, which are known to be highly invasive, was observed [70], indicating a possible link between SOD activity and metastasis. However, to the best of our knowledge no study so far has investigated possible associations between the enzymatic and non-enzymatic antioxidant capacity in plasma and colon cancer cell migration. Interestingly, the higher the increase of SOD activity in plasma after 28 days intervention with the anthocyanin-rich juice, the higher the anti-invasive effect on HT-29 cell migration was in vitro. Although this correlation was weak, the impact of anthocyanins and their metabolites on tumor metastasis is much more complex in vivo. Besides direct effects on cancer cells, PAM may also influence other cell types such as immune cells [70] and consequently the microenvironment and migratory potential of tumor cells. To date, the role of anthocyanins during tumor migration of colon cancer patients is not fully understood and should be further investigated.

The present study has some limitations. First, participants were advised to adhere to a diet low in phenolics and anthocyanins during the run-in and intervention phase. These strong dietary limitations may not reflect a healthy and balanced diet. Furthermore, nutritional limitations were the reason for the high drop-out rate or termination of the study. Therefore, future studies should address whether the consumption of anthocyanin-rich beverages in addition to a normal diet also show health-promoting effects. Secondly, it remains to be shown which plasma anthocyanins and metabolites, as well as molecular mechanisms, are responsible for the anti-migratory effects. Finally, it could not be ruled out that the observed effects are in part mediated by other phenolic compounds also present in the anthocyanin-rich grape/bilberry juice.

5. Conclusions

To the best of our knowledge, we demonstrated for the first time that plasma-isolated anthocyanins and their metabolites significantly decrease migration of colon cancer cells in vitro. Furthermore, our data indicate that physiological concentrations of anthocyanins and their metabolites may enhance the efficacy of classical chemotherapeutic agents like 5-FU.

Supplementary Materials: The following supporting information can be downloaded at: https://www.mdpi.com/article/10.3390/antiox11071341/s1, Table S1: Foodstuffs that were restricted or not allowed during the run-in and 28-day intervention period; Table S2: Baseline characteristics and mean dietary intake of the study population during the two intervention periods (n = 34); Figure S1: Effects of PAM on HUVE cell viability.

Author Contributions: Principal investigator and conceptualization, S.K. and S.R.; migration studies, measurement of plasma antioxidant parameters and writing—original draft preparation, S.K. and I.B.; juice preparation and characterization, I.R. and F.W.; TPC analysis, H.M., T.M., R.G.-D. and C.A.-L.; writing—editing the manuscript, M.F. All authors have read and agreed to the published version of the manuscript.

Funding: This research was funded by the German Research Foundation (DFG, Deutsche Forschungsgemeinschaft) (grant # 1925/5-1) and further supported by CIBERFES, AC19/00096 funded by Instituto de Salud Carlos III and co-funded by European Regional Development Fund "A way to make Europe" and the award of the Generalitat de Catalunya's Agency AGAUR [2017SGR1546] and ICREA Academia 2018. T.M. would like to thank the "Juan de la Cierva" program from MINECO (IJCI-2017-32534). H.M. would like to thank the scholarship ajuts de personal investigador predoctoral en formació (APIF) from the University of Barcelona (Contract code: 404).

Institutional Review Board Statement: The study was conducted in accordance with the Declaration of Helsinki, and approved by the Ethics Committee of the Justus Liebig University, Giessen (registration number: 13/10; date: 7 July 2017).

Informed Consent Statement: Informed consent was obtained from all subjects involved in the study.

Data Availability Statement: The data are not publicly available due to European data protection regulations.

Acknowledgments: We are deeply grateful to all volunteers who participated in the study. The authors would also like to thank Cordula Becker, Katrin Koslowski, Sina Streichert, and Elvira Friedrich for their technical support in performing blood and urine analyses.

Conflicts of Interest: The authors declare no conflict of interest. The funders had no role in the design of the study; in the collection, analyses, or interpretation of data; in the writing of the manuscript, or in the decision to publish the results.

References

1. Sung, H.; Ferlay, J.; Siegel, R.L.; Laversanne, M.; Soerjomataram, I.; Jemal, A.; Bray, F. Global Cancer Statistics 2020: GLOBOCAN Estimates of Incidence and Mortality Worldwide for 36 Cancers in 185 Countries. *CA Cancer J. Clin.* **2021**, *71*, 209–249. [CrossRef] [PubMed]
2. Kim, J.; Lee, J.; Oh, J.H.; Chang, H.J.; Sohn, D.K.; Shin, A.; Kim, J. Circulating Interleukin-6 Level, Dietary Antioxidant Capacity, and Risk of Colorectal Cancer. *Antioxidants* **2019**, *8*, 595. [CrossRef] [PubMed]
3. O'Keefe, S.J.D. Diet, microorganisms and their metabolites, and colon cancer. *Nat. Rev. Gastroenterol. Hepatol.* **2016**, *13*, 691–706. [CrossRef] [PubMed]
4. Siegel, R.L.; Miller, K.D.; Sauer, A.G.; Fedewa, S.A.; Butterly, L.F.; Anderson, J.C.; Cercek, A.; Smith, R.A.; Jemal, A. Colorectal cancer statistics, 2020. *CA Cancer J. Clin.* **2020**, *70*, 145–164. [CrossRef] [PubMed]
5. Zińczuk, J.; Maciejczyk, M.; Zaręba, K.; Romaniuk, W.; Markowski, A.; Kędra, B.; Zalewska, A.; Pryczynicz, A.; Matowicka-Karna, J.; Guzińska-Ustymowicz, K. Antioxidant Barrier, Redox Status, and Oxidative Damage to Biomolecules in Patients with Colorectal Cancer. Can Malondialdehyde and Catalase Be Markers of Colorectal Cancer Advancement? *Biomolecules* **2019**, *9*, 637. [CrossRef] [PubMed]
6. Harris, I.; Brugge, J.S. The enemy of my enemy is my friend. *Nature* **2015**, *527*, 170–171. [CrossRef] [PubMed]
7. Porporato, P.E.; Payen, V.L.; Pérez-Escuredo, J.; De Saedeleer, C.J.; Danhier, P.; Copetti, T.; Dhup, S.; Tardy, M.; Vazeille, T.; Bouzin, C.; et al. A Mitochondrial Switch Promotes Tumor Metastasis. *Cell Rep.* **2014**, *8*, 754–766. [CrossRef]
8. LeBleu, V.S.; O'Connell, J.T.; Gonzalez Herrera, K.N.G.; Wikman, H.; Pantel, K.; Haigis, M.C.; De Carvalho, F.M.; Damascena, A.; Domingos Chinen, L.T.; Rocha, R.M.; et al. PGC-1α mediates mitochondrial biogenesis and oxidative phosphorylation in cancer cells to promote metastasis. *Nat. Cell Biol.* **2014**, *16*, 992–1003. [CrossRef]
9. Allesina, S.; Alonso, D.; Pascual, M. A General Model for Food Web Structure. *Science* **2008**, *320*, 658–661. [CrossRef]
10. Afrin, S.; Giampieri, F.; Gasparrini, M.; Forbes-Hernandez, T.Y.; Varela-López, A.; Quiles, J.L.; Mezzetti, B.; Battino, M. Chemopreventive and Therapeutic Effects of Edible Berries: A Focus on Colon Cancer Prevention and Treatment. *Molecules* **2016**, *21*, 169. [CrossRef]
11. Kumar, S.; Pandey, A.K. Chemistry and Biological Activities of Flavonoids: An Overview. *Sci. World J.* **2013**, *2013*, 162750. [CrossRef] [PubMed]
12. Jordheim, M.; Måge, F.; Andersen, Ø.M. Anthocyanins in Berries of *Ribes* Including Gooseberry Cultivars with a High Content of Acylated Pigments. *J. Agric. Food Chem.* **2007**, *55*, 5529–5535. [CrossRef] [PubMed]
13. Ramirez, J.E.; Zambrano, R.; Sepúlveda, B.; Kennelly, E.J.; Simirgiotis, M.J. Anthocyanins and antioxidant capacities of six Chilean berries by HPLC–HR-ESI-ToF-MS. *Food Chem.* **2015**, *176*, 106–114. [CrossRef]
14. Wallace, T.C.; Giusti, M.M. Anthocyanins. *Adv. Nutr. Int. Rev. J.* **2015**, *6*, 620–622. [CrossRef]
15. Fang, J. Classification of fruits based on anthocyanin types and relevance to their health effects. *Nutrition* **2015**, *31*, 1301–1306. [CrossRef] [PubMed]
16. Wu, X.; Beecher, G.R.; Holden, J.M.; Haytowitz, D.B.; Gebhardt, S.E.; Prior, R.L. Concentrations of Anthocyanins in Common Foods in the United States and Estimation of Normal Consumption. *J. Agric. Food Chem.* **2006**, *54*, 4069–4075. [CrossRef] [PubMed]
17. Shi, N.; Chen, X.; Chen, T. Anthocyanins in Colorectal Cancer Prevention Review. *Antioxidants* **2021**, *10*, 1600. [CrossRef] [PubMed]
18. Wang, X.; Yang, D.-Y.; Yang, L.-Q.; Zhao, W.-Z.; Cai, L.-Y.; Shi, H.-P. Anthocyanin Consumption and Risk of Colorectal Cancer: A Meta-Analysis of Observational Studies. *J. Am. Coll. Nutr.* **2018**, *38*, 470–477. [CrossRef]
19. Wang, S.Y.; Jiao, H. Scavenging Capacity of Berry Crops on Superoxide Radicals, Hydrogen Peroxide, Hydroxyl Radicals, and Singlet Oxygen. *J. Agric. Food Chem.* **2000**, *48*, 5677–5684. [CrossRef]
20. Yan, X.; Murphy, B.T.; Hammond, G.B.; Vinson, J.A.; Neto, C.C. Antioxidant Activities and Antitumor Screening of Extracts from Cranberry Fruit (*Vaccinium macrocarpon*). *J. Agric. Food Chem.* **2002**, *50*, 5844–5849. [CrossRef]
21. Kuntz, S.; Kunz, C.; Herrmann, J.; Borsch, C.H.; Abel, G.; Fröhling, B.; Dietrich, H.; Rudloff, S. Anthocyanins from fruit juices improve the antioxidant status of healthy young female volunteers without affecting anti-inflammatory parameters: Results from the randomised, double-blind, placebo-controlled, cross-over ANTHONIA (ANTHOcyanins in Nutrition Investigation Alliance) study. *Br. J. Nutr.* **2014**, *112*, 925–936. [CrossRef] [PubMed]
22. Bakuradze, T.; Tausend, A.; Galan, J.; Groh, I.A.M.; Berry, D.; Tur, J.A.; Marko, D.; Richling, E. Antioxidative activity and health benefits of anthocyanin-rich fruit juice in healthy volunteers. *Free Radic. Res.* **2019**, *53*, 1045–1055. [CrossRef] [PubMed]

23. Zamora-Ros, R.; Not, C.; Guino, E.; Lujan-Barroso, L.; Garcia, R.M.; Biondo, S.; Salazar, R.; Moreno, V. Association between habitual dietary flavonoid and lignan intake and colorectal cancer in a Spanish case–control study (the Bellvitge Colorectal Cancer Study). *Cancer Causes Control* **2012**, *24*, 549–557. [CrossRef] [PubMed]
24. Rossi, M.; Negri, E.; Talamini, R.; Bosetti, C.; Parpinel, M.; Gnagnarella, P.; Franceschi, S.; Dal Maso, L.; Montella, M.; Giacosa, A.; et al. Flavonoids and Colorectal Cancer in Italy. *Cancer Epidemiol. Biomark. Prev.* **2006**, *15*, 1555–1558. [CrossRef] [PubMed]
25. Yun, J.W.; Lee, W.S.; Kim, M.J.; Lu, J.N.; Kang, M.H.; Kim, H.G.; Kim, D.C.; Choi, E.J.; Choi, J.Y.; Kim, H.G.; et al. Characterization of a profile of the anthocyanins isolated from Vitis coignetiae Pulliat and their anti-invasive activity on HT-29 human colon cancer cells. *Food Chem. Toxicol.* **2010**, *48*, 903–909. [CrossRef]
26. Lee, W.S.; Shin, D.Y.; Lu, J.N.; Kim, G.-Y.; Jung, J.M.; Kang, H.S.; Choi, Y.H. Lee Anti-invasive activities of anthocyanins through modulation of tight junctions and suppression of matrix metalloproteinase activities in HCT-116 human colon carcinoma cells. *Oncol. Rep.* **2011**, *25*, 567–572. [CrossRef]
27. Zhang, H.; Guo, J.; Mao, L.; Li, Q.; Guo, M.; Mu, T.; Zhang, Q.; Bi, X. Up-regulation of miR-24-1-5p is involved in the chemoprevention of colorectal cancer by black raspberry anthocyanins. *Br. J. Nutr.* **2018**, *122*, 518–526. [CrossRef]
28. Kay, C.D.; Kroon, P.A.; Cassidy, A. The bioactivity of dietary anthocyanins is likely to be mediated by their degradation products. *Mol. Nutr. Food Res.* **2009**, *53*, S92–S101. [CrossRef]
29. Tena, N.; Martín, J.; Asuero, A.G. State of the Art of Anthocyanins: Antioxidant Activity, Sources, Bioavailability, and Therapeutic Effect in Human Health. *Antioxidants* **2020**, *9*, 451. [CrossRef]
30. Chandra, P.; Rathore, A.S.; Kay, K.L.; Everhart, J.L.; Curtis, P.; Burton-Freeman, B.; Cassidy, A. Contribution of Berry Polyphenols to the Human Metabolome. *Molecules* **2019**, *24*, 4220. [CrossRef]
31. Kuntz, S.; Kunz, C.; Rudloff, S. Inhibition of pancreatic cancer cell migration by plasma anthocyanins isolated from healthy volunteers receiving an anthocyanin-rich berry juice. *Eur. J. Nutr.* **2017**, *56*, 203–214. [CrossRef] [PubMed]
32. Sutkowy, P.; Czuczejko, J.; Małkowski, B.; Szewczyk-Golec, K.; Łopatto, R.; Maruszak, M.; Woźniak, A. Redox State and Lysosomal Activity in Women with Ovarian Cancer with Tumor Recurrence and Multiorgan Metastasis. *Molecules* **2021**, *26*, 4039. [CrossRef] [PubMed]
33. Kundaktepe, B.P.; Sozer, V.; Durmus, S.; Kocael, P.C.; Kundaktepe, F.O.; Papila, C.; Gelisgen, R.; Uzun, H. The evaluation of oxidative stress parameters in breast and colon cancer. *Medicine* **2021**, *100*, e25104. [CrossRef]
34. Von Kleist, S.; Chany, E.; Burtin, P.; King, M.; Fogh, J. Immunohistology of the Antigenic Pattern of a Continuous Cell Line from a Human Colon Tumor. *JNCI J. Natl. Cancer Inst.* **1975**, *55*, 555–560. [CrossRef]
35. Lea, T. Caco-2 Cell Line. In *The Impact of Food Bioactives on Health: In Vitro and Ex Vivo Models*; Verhoeckx, K., Cotter, P., López-Expósito, I., Kleiveland, C., Lea, T., Mackie, A., Requena, T., Swiatecka, D., Wichers, H., Eds.; Springer: Cham, Switzerland, 2015; pp. 103–111.
36. De Both, N.J.; Vermey, M.; Dinjens, W.N.; Bosman, F.T. A comparative evaluation of various invasion assays testing colon carcinoma cell lines. *Br. J. Cancer* **1999**, *81*, 934–941. [CrossRef] [PubMed]
37. Kuntz, S.; Rudloff, S.; Kunz, C. Oligosaccharides from human milk influence growth-related characteristics of intestinally transformed and non-transformed intestinal cells. *Br. J. Nutr.* **2008**, *99*, 462–471. [CrossRef]
38. Kuntz, S.; Rudloff, S.; Asseburg, H.; Borsch, C.; Fröhling, B.; Unger, F.; Dold, S.; Spengler, B.; Römpp, A.; Kunz, C. Uptake and bioavailability of anthocyanins and phenolic acids from grape/blueberry juice and smoothie In Vitro and In Vivo. *Br. J. Nutr.* **2015**, *113*, 1044–1055. [CrossRef]
39. Spormann, T.M.; Albert, F.W.; Rath, T.; Dietrich, H.; Will, F.; Stockis, J.-P.; Eisenbrand, G.; Janzowski, C. Anthocyanin/Polyphenolic–Rich Fruit Juice Reduces Oxidative Cell Damage in an Intervention Study with Patients on Hemodialysis. *Cancer Epidemiol. Biomark. Prev.* **2008**, *17*, 3372–3380. [CrossRef]
40. Urpi-Sarda, M.; Monagas, M.; Khan, N.; Llorach, R.; Lamuela-Raventós, R.M.; Jáuregui, O.; Estruch, R.; Izquierdo-Pulido, M.; Andrés-Lacueva, C. Targeted metabolic profiling of phenolics in urine and plasma after regular consumption of cocoa by liquid chromatography–tandem mass spectrometry. *J. Chromatogr. A* **2009**, *1216*, 7258–7267. [CrossRef]
41. Gagnon, M.; Zihler Berner, A.; Chervet, N.; Chassard, C.; Lacroix, C. Comparison of the Caco-2, HT-29 and the mucus-secreting HT29-MTX intestinal cell models to investigate Salmonella adhesion and invasion. *J. Microbiol. Methods* **2013**, *94*, 274–279. [CrossRef]
42. Lesuffleur, T.; Porchet, N.; Aubert, J.P.; Swallow, D.; Gum, J.R.; Kim, Y.S.; Real, F.X.; Zweibaum, A. Differential expression of the human mucin genes MUC1 to MUC5 in relation to growth and differentiation of different mucus-secreting HT-29 cell subpopulations. *J. Cell Sci.* **1993**, *106*, 771–783. [CrossRef] [PubMed]
43. Bourgine, J.; Billaut-Laden, I.; Happillon, M.; Lo-Guidice, J.-M.; Maunoury, V.; Imbenotte, M.; Broly, F. Gene Expression Profiling of Systems Involved in the Metabolism and the Disposition of Xenobiotics: Comparison between Human Intestinal Biopsy Samples and Colon Cell Lines. *Drug Metab. Dispos.* **2012**, *40*, 694–705. [CrossRef] [PubMed]
44. Medina-Remón, A.; Barrionuevo-González, A.; Zamora-Ros, R.; Andres-Lacueva, C.; Estruch, R.; Martinez-Gonzalez, M.A.; Diez-Espino, J.; Lamuela-Raventos, R.M. Rapid Folin–Ciocalteu method using microtiter 96-well plate cartridges for solid phase extraction to assess urinary total phenolic compounds, as a biomarker of total polyphenols intake. *Anal. Chim. Acta* **2009**, *634*, 54–60. [CrossRef]

45. Msc, M.R.; Cherubini, A.; Zamora-Ros, R.; Urpi-Sarda, M.; Bandinelli, S.; Ferrucci, L.; Andres-Lacueva, C. Low Levels of a Urinary Biomarker of Dietary Polyphenol Are Associated with Substantial Cognitive Decline over a 3-Year Period in Older Adults: The Invecchiare in Chianti Study. *J. Am. Geriatr. Soc.* **2015**, *63*, 938–946. [CrossRef]
46. Seeram, N.P.; Aviram, M.; Zhang, Y.; Henning, S.M.; Feng, L.; Dreher, M.; Heber, D. Comparison of Antioxidant Potency of Commonly Consumed Polyphenol-Rich Beverages in the United States. *J. Agric. Food Chem.* **2008**, *56*, 1415–1422. [CrossRef]
47. Düsman, E.; Almeida, I.; Pinto, E.; Lucchetta, L.; Vicentini, V. Influence of processing and storage of integral grape juice (*Vitis labrusca* L.) on its physical and chemical characteristics, cytotoxicity, and mutagenicity in vitro. *Genet. Mol. Res.* **2017**, *16*, gmr16029670. [CrossRef]
48. Fröhling, B.; Patz, C.-D.; Dietrich, H.; Will, F. Anthocyanins, total phenolics and antioxidant capacities of commercial red grape juices, black curant and sour cherry nectars. *Fruit Processing* **2012**, *3*, 100–104.
49. Vodenkova, S.; Buchler, T.; Cervena, K.; Veskrnova, V.; Vodicka, P.; Vymetalkova, V. 5-fluorouracil and other fluoropyrimidines in colorectal cancer: Past, present and future. *Pharmacol. Ther.* **2019**, *206*, 107447. [CrossRef]
50. Wang, N.; Yang, L.; Dai, J.; Wu, Y.; Zhang, R.; Jia, X.; Liu, C. 5-FU inhibits migration and invasion of CRC cells through PI3K/AKT pathway regulated by MARCH1. *Cell Biol. Int.* **2020**, *45*, 368–381. [CrossRef]
51. Sak, K. Chemotherapy and Dietary Phytochemical Agents. *Chemother. Res. Pract.* **2012**, *2012*, 282570. [CrossRef]
52. Guyot, F.; Faivre, J.; Manfredi, S.; Meny, B.; Bonithon-Kopp, C.; Bouvier, A.M. Time trends in the treatment and survival of recurrences from colorectal cancer. *Ann. Oncol.* **2005**, *16*, 756–761. [CrossRef] [PubMed]
53. Serala, K.; Steenkamp, P.; Mampuru, L.; Prince, S.; Poopedi, K.; Mbazima, V. In vitro antimetastatic activity of *Momordica balsamina* crude acetone extract in HT -29 human colon cancer cells. *Environ. Toxicol.* **2021**, *36*, 2196–2205. [CrossRef] [PubMed]
54. Ahmed, D.; Eide, P.W.; Eilertsen, I.A.; Danielsen, S.A.; Eknaes, M.; Hektoen, M.; Lind, G.E.; Lothe, R.A. Epigenetic and genetic features of 24 colon cancer cell lines. *Oncogenesis* **2013**, *2*, e71. [CrossRef]
55. Li, X.; Chen, L.; Gao, Y.; Zhang, Q.; Chang, A.K.; Yang, Z.; Bi, X. Black raspberry anthocyanins increased the antiproliferative effects of 5-Fluorouracil and Celecoxib in colorectal cancer cells and mouse model. *J. Funct. Foods* **2021**, *87*, 104801. [CrossRef]
56. Chavda, V.; Chaurasia, B.; Garg, K.; Deora, H.; Umana, G.E.; Palmisciano, P.; Scalia, G.; Lu, B. Molecular mechanisms of oxidative stress in stroke and cancer. *Brain Disord.* **2021**, *5*, 100029. [CrossRef]
57. Paramanantham, A.; Kim, M.J.; Jung, E.J.; Nagappan, A.; Yun, J.W.; Kim, H.J.; Shin, S.C.; Kim, G.S.; Lee, W.S. Pretreatment of Anthocyanin from the Fruit of Vitis coignetiae Pulliat Acts as a Potent Inhibitor of TNF-α Effect by Inhibiting NF-κB-Regulated Genes in Human Breast Cancer Cells. *Molecules* **2020**, *25*, 2396. [CrossRef]
58. Ho, M.-L.; Chen, P.-N.; Chu, S.-C.; Kuo, D.-Y.; Kuo, W.-H.; Chen, J.-Y.; Hsieh, Y.-S. Peonidin 3-Glucoside Inhibits Lung Cancer Metastasis by Downregulation of Proteinases Activities and MAPK Pathway. *Nutr. Cancer* **2010**, *62*, 505–516. [CrossRef]
59. Kausar, H.; Jeyabalan, J.; Aqil, F.; Chabba, D.; Sidana, J.; Singh, I.P.; Gupta, R.C. Berry anthocyanidins synergistically suppress growth and invasive potential of human non-small-cell lung cancer cells. *Cancer Lett.* **2012**, *325*, 54–62. [CrossRef]
60. Jayarathne, S.; Stull, A.J.; Park, O.; Kim, J.H.; Thompson, L.; Moustaid-Moussa, N. Protective Effects of Anthocyanins in Obesity-Associated Inflammation and Changes in Gut Microbiome. *Mol. Nutr. Food Res.* **2019**, *63*, e1900149. [CrossRef]
61. Gu, J.; Thomas-Ahner, J.; Riedl, K.; Bailey, M.; Vodovotz, Y.; Schwartz, S.J.; Clinton, S.K. Dietary Black Raspberries Impact the Colonic Microbiome and Phytochemical Metabolites in Mice. *Mol. Nutr. Food Res.* **2019**, *63*, e1800636. [CrossRef]
62. Boto-Ordóñez, M.; Urpi-Sarda, M.; Queipo-Ortuño, M.I.; Tulipani, S.; Tinahones, F.J.; Andres-Lacueva, C. High levels of Bifidobacteria are associated with increased levels of anthocyanin microbial metabolites: A randomized clinical trial. *Food Funct.* **2014**, *5*, 1932–1938. [CrossRef] [PubMed]
63. Czank, C.; Cassidy, A.; Zhang, Q.; Morrison, D.J.; Preston, T.; Kroon, P.A.; Botting, N.P.; Kay, C.D. Human metabolism and elimination of the anthocyanin, cyanidin-3-glucoside: A 13C-tracer study. *Am. J. Clin. Nutr.* **2013**, *97*, 995–1003. [CrossRef]
64. Khoo, H.E.; Azlan, A.; Tang, S.T.; Lim, S.M. Anthocyanidins and anthocyanins: Colored pigments as food, pharmaceutical ingredients, and the potential health benefits. *Food Nutr. Res.* **2017**, *61*, 1361779. [CrossRef] [PubMed]
65. Cui, L.; Liu, X.; Tian, Y.; Xie, C.; Li, Q.; Cui, H.; Sun, C. Flavonoids, Flavonoid Subclasses, and Esophageal Cancer Risk: A Meta-Analysis of Epidemiologic Studies. *Nutrients* **2016**, *8*, 350. [CrossRef] [PubMed]
66. Santiago-Arteche, R.; Muñiz, P.; Cavia-Saiz, M.; García-Girón, C.; Garcia-Gonzalez, M.; Llorente-Ayala, B.; Corral, M.J.C.-D. Cancer chemotherapy reduces plasma total polyphenols and total antioxidants capacity in colorectal cancer patients. *Mol. Biol. Rep.* **2012**, *39*, 9355–9360. [CrossRef] [PubMed]
67. Pahlke, G.; Ahlberg, K.; Oertel, A.; Janson-Schaffer, T.; Grabher, S.; Mock, H.-P.; Matros, A.; Marko, D. Antioxidant Effects of Elderberry Anthocyanins in Human Colon Carcinoma Cells: A Study on Structure–Activity Relationships. *Mol. Nutr. Food Res.* **2021**, *65*, 2100229. [CrossRef] [PubMed]
68. Lin, B.-W.; Gong, C.-C.; Song, H.-F.; Cui, Y.-Y. Effects of anthocyanins on the prevention and treatment of cancer. *J. Cereb. Blood Flow Metab.* **2016**, *174*, 1226–1243. [CrossRef]
69. Kropat, C.; Mueller, D.; Boettler, U.; Zimmermann, K.; Heiss, E.H.; Dirsch, V.; Rogoll, D.; Melcher, R.; Richling, E.; Marko, D. Modulation of Nrf2-dependent gene transcription by bilberry anthocyanins in vivo. *Mol. Nutr. Food Res.* **2013**, *57*, 545–550. [CrossRef]
70. Yang, S.; Wang, C.; Li, X.; Wu, C.; Liu, C.; Xue, Z.; Kou, X. Investigation on the biological activity of anthocyanins and polyphenols in blueberry. *J. Food Sci.* **2021**, *86*, 614–627. [CrossRef]

3.2 Plasma anthocyanins and their metabolites prevent in-vitro migration of pancreatic cancer cells, PANC-1 in a FAK- and NF-kB dependent manner: results from the ATTACH-study a randomized, controlled, crossover trial in healthy subjects

Mostafa H[1], Behrendt I[1], Meroño T, González-Domínguez R, Fasshauer M, Rudloff S, Andres-Lacueva C, Kuntz S. *Biomed. Pharmacother.* **2023**, 158, 114076. doi:10.1016/j.biopha.2022.114076.

Journal impact factor: 7.5 [1]Co-first authorship

Abstract: Pancreatic cancer is primarily considered to be a metastatic disease with a low 5-year survival rate. We aimed to detect if plasma-isolated anthocyanins and their metabolites (PAMs) modulate pancreatic cancer cells migration and to describe molecular targets of PAMs in this process. Plasma metabolites were isolated by solid-phase extraction before and after a 28-days intervention trial involving 35 healthy subjects comparing effects of a daily anthocyanin-rich juice intake *vs.* placebo. Plasma extracts were used for migration and mechanistic *in vitro* studies as well as for metabolomic analysis. Pancreatic PANC-1 and AsPC-1 were used for migration studies in a Boyden chamber co-cultured with endothelial cells. Expression of adhesion molecules on cancer and endothelial cells were determined by flow cytometry and NF-kB (nuclear factor-kappa B) p65 and focal adhesion kinase activation were measured by immunoassays. UHPLC-MS/MS metabolomics was done in plasma and urine samples. Plasma extracts isolated after the intake of the anthocyanin-rich juice significantly reduced PANC-1 migration, but not AsPC-1 migration. In PANC-1, and to a lower extent in endothelial cells, plasma extracts after juice intake decreased the expression of β1- and β4-integrins and intercellular adhesion molecule-1. Pooled plasma from volunteers with the highest inhibition of PANC-1 migration (n = 10) induced a reduction of NF-kB-p65 and FAK-phosphorylation in cancer and in endothelial cells. Concerning metabolites, 14 were significantly altered by juice intervention and PANC-1 migration was inversely associated with the increase of o-coumaric acid and peonidin-3-galactoside. PAMs were associated with lower PANC-1 cell migration opening new strategies for metastatic pancreatic cancer treatment.

Keywords: Anthocyanins; Metabolomics; Pancreatic cancer cells; Migration; Adhesion molecules

Anhang B: *Supplemental Material*

Biomedicine & Pharmacotherapy 158 (2023) 114076

Contents lists available at ScienceDirect

Biomedicine & Pharmacotherapy

journal homepage: www.elsevier.com/locate/biopha

Plasma anthocyanins and their metabolites reduce *in vitro* migration of pancreatic cancer cells, PANC-1, in a FAK- and NF-kB dependent manner: Results from the ATTACH-study a randomized, controlled, crossover trial in healthy subjects

Hamza Mostafa [a,b,1], Inken Behrendt [c,*,1], Tomás Meroño [a,b,**], Raúl González-Domínguez [a,b], Mathias Fasshauer [c], Silvia Rudloff [c,d], Cristina Andres-Lacueva [a,b], Sabine Kuntz [c]

[a] Biomarkers and Nutrimetabolomics Laboratory, Department of Nutrition, Food Sciences and Gastronomy, Food Innovation Network (XIA), Nutrition and Food Safety Research Institute (INSA), Facultat de Farmàcia i Ciències de l'Alimentació, Universitat de Barcelona (UB), 08028 Barcelona, Spain
[b] Centro de Investigación Biomédica en Red de Fragilidad y Envejecimiento Saludable (CIBERFES), Instituto de Salud Carlos III, Madrid 28029, Spain
[c] Department of Nutritional Science, Human Nutrition, Justus-Liebig-University, 35390 Giessen, Germany
[d] Department of Nutritional Science and Department of Pediatrics, Justus-Liebig-University, 35392 Giessen, Germany

ARTICLE INFO

Keywords:
Anthocyanins
Metabolomics
Pancreatic cancer cells
Migration
Adhesion molecules

ABSTRACT

Pancreatic cancer is primarily considered to be a metastatic disease with a low 5-year survival rate. We aimed to detect if plasma-isolated anthocyanins and their metabolites (PAMs) modulate pancreatic cancer cells migration and to describe molecular targets of PAMs in this process. Plasma metabolites were isolated by solid-phase extraction before and after a 28-days intervention trial involving 35 healthy subjects comparing effects of a daily anthocyanin-rich juice intake *vs.* placebo. Plasma extracts were used for migration and mechanistic *in vitro* studies as well as for metabolomic analysis. Pancreatic PANC-1 and AsPC-1 were used for migration studies in a Boyden chamber co-cultured with endothelial cells. Expression of adhesion molecules on cancer and endothelial cells were determined by flow cytometry and NF-kB (nuclear factor-kappa B) p65 and focal adhesion kinase activation were measured by immunoassays. UHPLC-MS/MS metabolomics was done in plasma and urine samples. Plasma extracts isolated after the intake of the anthocyanin-rich juice significantly reduced PANC-1 migration, but not AsPC-1 migration. In PANC-1, and to a lower extent in endothelial cells, plasma extracts after juice intake decreased the expression of ß1- and ß4-integrins and intercellular adhesion molecule-1. Pooled plasma from volunteers with the highest inhibition of PANC-1 migration (n = 10) induced a reduction of NF-kB-p65 and FAK-phosphorylation in cancer and in endothelial cells. Concerning metabolites, 14 were significantly altered by juice intervention and PANC-1 migration was inversely associated with the increase of o-coumaric acid and peonidin-3-galactoside. PAMs were associated with lower PANC-1 cell migration opening new strategies for metastatic pancreatic cancer treatment.

1. Introduction

Pancreatic cancer is predicted to become the second leading cause of cancer death within the next decade in Western countries. It is commonly associated with poor prognosis and low overall five-year survival rate (5–7%) due to the early metastatic potential of pancreatic cancer cells [1]. Indeed, more than 80% of the patients are suffering from metastases or unresectable tumors at time of diagnosis [1].

Abbreviations: CAM, Cell Adhesion Molecules; ACN, Anthocyanins; HUVEC, Human Umbilical Vein Endothelial Cells; TEER, Transepithelial electrical resistance; FAK, Focal Adhesion Kinase; ROS, Reactive Oxygen Species.

* Correspondence to: Department of Nutritional Science Human Nutrition, Justus-Liebig-University, Goethestraße 55, D-35390 Giessen, Germany.
** Correspondence to: Biomarkers and Nutritional & Food Metabolomics Research Group, Department of Nutrition, Food Science and Gastronomy, Facultat de Farmàcia i Ciències de l'Alimentació, Universitat de Barcelona (UB), Av. Joan XXIII s/n, 08028 Barcelona, Spain.
E-mail addresses: inken.behrendt@ernaehrung.uni-giessen.de (I. Behrendt), tomasmerono@ub.edu (T. Meroño).
[1] Co-first authorship

https://doi.org/10.1016/j.biopha.2022.114076
Received 6 October 2022; Received in revised form 25 November 2022; Accepted 2 December 2022
Available online 13 December 2022

Metastasis is a multistep process in which cell adhesion molecules (CAMs), such as integrins and selectins play pivotal roles [2]. Malignant cells from the primary tumor infiltrate the surrounding tissue and enter the circulation by blood vessel intravasation and extravasation into the target tissue [2,3]. Alterations in the expression of several CAMs are known to modulate the migratory and invasive potential of cancer cells [4].

Strategies to improve the health outcomes in pancreatic cancer are challenging. Not only primary prevention strategies associated with a healthy lifestyle are discussed, but also secondary prevention strategies. Epidemiological studies revealed a potential benefit of diets high in fruits and vegetables [5–7]. A group of bioactive phytochemicals responsible for 'anti-cancer' effects are anthocyanins (ACNs). ACNs could account for up to 80% of the total polyphenolic content in berries [8]. However, ACNs bioavailability is low, and large amounts of dietary ACNs are fermented by gut microbiota [9,10]. As a result, several phenolic acids and other metabolites are generated [10,11]. Whether parent ACNs or their metabolites are responsible for these 'anti-cancer' effects is not fully understood. Recently, a screening of polyphenol metabolites on HCT116 3D-spheroids revealed that the ACN-related metabolite, 3′,4′-dihydroxyphenyl-γ-valerolactone (3,4-DHPV), reduced cancer cells spheroid integrity [12] underlining the role of gut microbiota fermentation of ACNs. Furthermore, a blueberry extract decreased CAM expression in several cancer cell lines and inhibited migration of breast and prostatic cancer cell lines (MDA-MB-231 and PC-3 cells), respectively [13]. Nonetheless, only few *in vitro* studies reported changes in CAM expression in cancer and endothelial cells in response to ACNs.

Previously, we showed that 60 min after a single ACN dose, plasma extracts from volunteers inhibited migration of the pancreatic cancer cell line PANC-1 *in vitro* [14]. Furthermore, we observed a reduction of migration of the colon cancer cell line HT-29 after a daily ingestion of ACNs over 28 days [15]. Therefore, our aims were to investigate: 1) whether plasma metabolites, isolated after a 28-day intervention, would reduce migration of two pancreatic cancer cell lines (PANC-1 and AsPC-1); 2) whether expression of adhesion molecules on cancer and endothelial cells were influenced by plasma ACN metabolites; 3) which molecular mechanisms were involved; and 4) which metabolites in plasma and urine were altered during a long-term ACN intake and how they associate with the inhibitory effects on migration.

2. Materials and methods

All details on materials are given in the Supplementary Table 1.

2.1. Study design and subjects

Details on the ATTACH study (Anthocyanins Target Tumor cell Adhesion—Cancer vs. Endothelial Cell (HUVEC)) have been published previously [15]. Briefly, this was a randomised, double-blind, placebo-controlled, cross-over, 28-days intervention comparing the effects of an ACN-rich juice (J) (330 ml/day, 942 mg/L of ACNs and 2622 mg/L of total polyphenols) and an ACN-depleted (330 ml/day, 6.3 mg/L of ACNs and 115 mg/L of total polyphenols) placebo juice (P), with a 2-week wash-out and 1-week run-in period. Thirty-five young, healthy volunteers participated in the intervention. Sample size was calculated based on the results of our previous published migration study [14] with ß- and α-error of 0.8 and 0.05 and a drop-out rate of 20%. CONSORT flowchart diagram is shown in Supplementary Figure 1. Participants were randomly assigned (random-table). The study protocol was approved by the local ethic committee in Gießen (Germany) (registration number 13/10) and performed according to the guidelines laid down in the Declaration of Helsinki. Written informed consent was obtained from all participants and the trial is registered at DRKS (*Deutsche Register Klinischer Studien;* DRKS00014767). The present manuscript is reported following the CONSORT checklist Supplementary Table 2.

2.2. Blood and urine sample preparation

Blood and 24 h-urine samples were collected before (day 0) and at the end (day 28) of the two intervention periods. Blood was taken 6 h after beverages intake of day 28 into EDTA-tubes and centrifuged to separate plasma. Acidified urine samples were then stored at − 80 °C until assayed. Extraction of plasma metabolites for cell culture assays and plasma and urine sample preparation for metabolomics analysis are described in the Supplementary Data (S1 and S2).

2.3. Cell culture and functional assays

Details on cancer cell lines and endothelial cells are given in the Supplementary Data (S3 and S4).

2.4. Outcomes

2.4.1. Primary outcome

2.4.1.1. Cell migration of pancreatic cancer cells in-vitro. Tumor cell migration was assessed in a Boyden membrane chamber with the use of the CytoSelect 24-well Cell Migration Assay as described previously [14,15]. The 24-well feeder chamber (diameter of the chamber 6.5 mm; pore size 8 μm) tray was coated with 50 μL of 0.1% fibronectin and aspirated until dryness. Thereafter, HUVECs (5×10^4/ml) were seeded onto the fibronectin-coated inserts and allow to grow confluent. Two-days post-confluence, transepithelial electrical resistance (TEER) was determined before the experiments by using a Millicell® ERS volt-ohmmeter. A TEER value $\geq$ 250 Ω per cm^2 was used as an indicator for an intact endothelial layer suitable to be used for functional studies. Pancreatic cancer cells (1×10^5/ml) were seeded in Endothelial growth medium II supplemented with 2.5% fetal calf serum (FCS) containing diluted plasma extracts of the participants, whereas Endothelial growth medium II supplemented with 12.5% FCS was added to the lower basal chamber. The cells were incubated in the feeder tray for 36 h at 37 °C, and cells on the lower side were then detached from the membrane using a cell detachment solution and afterwards lysed with fluorescent dye-containing buffer. The extent of migration was assessed by the intensity of the fluorescence signal with a microplate fluorescence reader. The number of migrated cells was determined according to a calibration curve (0–7500 cells). The results are expressed as medians and IQR (25th-75th).

2.4.2. Secondary outcome

2.4.2.1. Analysis of CAMs by flow cytometry analysis. Basal and `CytoMIX´-stimulated expression of surface marker such as cell adhesion molecules (CAMs) and Vascular endothelial growth factor receptor (VEGF-R) were analyzed under pre-confluent (PANC-1 and AsPC-1) or post-confluent (HUVECs) conditions. Cells were washed twice with phosphate buffered saline (PBS) and detached with TrypLE™ Express-solution for cancer cells or accutase-solution (0.15 ml/cm^2) for endothelial cells. After the detachment, cells were centrifugated (220xg for 3 min) and supernatant was decanted. Pellet was washed twice with PBS, resuspended in cold 100 μL MACS Running Buffer (pH 7.2) for staining procedures. Results are expressed as means ± SD or median with IQR (25th-75th). More details about staining procedures are given in the Supplementary data (S5).

2.4.2.2. Cytokine quantification, detection of NF-kB p65, FAK (focal adhesion kinase) activation and reactive oxygen species (ROS) determination. Commercially available ELISAs were used to determine cytokines, activation of NF-kB p65 and FAK in the supernatants of cells and were done by the manufacturer's instructions. ROS determination and sample preparation have been described previously (14). The results are

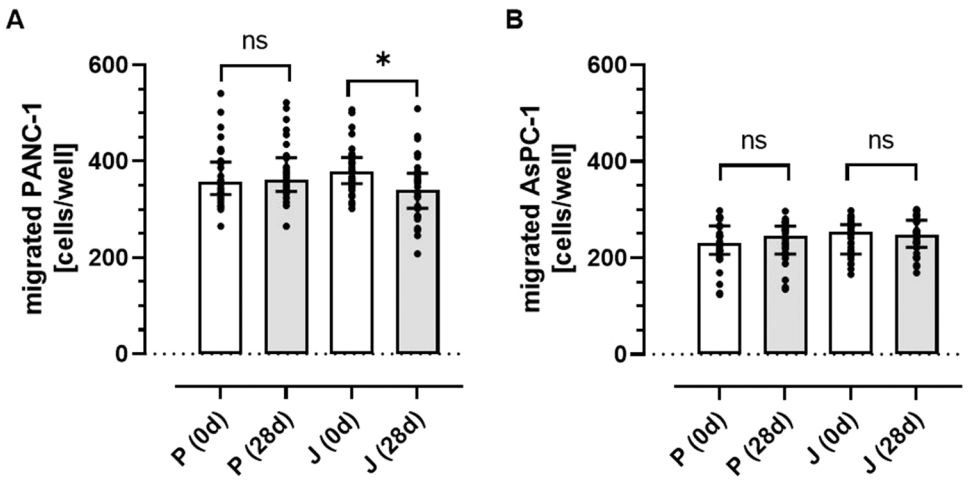

Fig. 1. Migration of PANC-1 and AsPC-1 in a Boyden chamber co-cultured with HUVECs representing endothelial cells *in vitro*. PANC-1 (A) and AsPC-1 (B) were exposed to plasma extracts from the placebo (P) and juice (J) intake before (0d) and after (28d) intervention. Migration across the endothelial layer into the lower chamber was measured after 36 h. Migration was measured fluorometrically in a Boyden chamber as described in Materials and Methods Section 2.4.1. Values are expressed as aligned dot blot with median and interquartile range (25th-75th). Significant differences were calculated with repeated measurements One-way ANOVA and values with * were different with *p-value* < 0.05 to corresponding controls (n = 34).

expressed as mean ± SD and more details are given in the Supplementary data (S6-S8).

2.4.3. Exploratory outcome

2.4.3.1. Targeted metabolomics UHPLC-MS/MS analysis. The UHPLC-MS/MS analysis has been explained previously [16]. Briefly, the analysis of plasma and urine was performed by using the 1290 Infinity UHPLC system coupled to a QTRAP 6500 mass spectrometer equipped with Ion Drive Turbo V ion source. Luna Omega Polar C18 column, 100 mm × 2.1 mm (i.d. 1.6 μm) with a porous polar C18 security guard cartridge were used to perform the chromatographic separation. More details are described in the Supplementary data (S9 and 10).

2.5. Statistical analysis

2.5.1. Cell culture data analyses

Data from the volunteers who completed all phases of the study were analyzed (n = 35). The outcome measures were prospectively designated as the differences in migration of PANC-1 and AsPC-1 *in vitro* (primary outcome) and mechanistic parameters (secondary outcome) of placebo and juice treatment before and after intervention. Before-treatment versus after-treatment data within groups were analyzed using a repeated measures one-way ANOVA with Šídák's post hoc test. The normality of continuous variables was assessed using Kolmogorov-Smirnov normality test. Asterisks are used in the figures to denote *p* values < 0.05, which were considered significant. GraphPad Prism 9 (Version 9.3.1.) was used for data analyses.

2.5.2. Metabolomics data analyses

Pre-processing of metabolomics data is described in the Supplementary Data (S10). To assess the effects of the juice intervention, we used a linear mixed model (LMM) including treatment (juice/placebo), age, and sex as fixed effects and subject as random effect. *P*-values were adjusted for multiple comparisons using the Benjamini-Hochberg false discovery rate (FDR) and results were integrated in a volcano plot. We selected as significant those metabolites with a $\log_2FC > |0.584|$ and an FDR-adjusted *p*-value < 0.05. Associations between plasma anthocyanin metabolites and migration experiments and adhesion molecules expression were tested using linear mixed models adjusted for age, sex and treatment as fixed effects, and subject as random effect. R statistical software version 4.1.3 was used for metabolomics statistical analyses.

3. Results & discussion

Thirty-five volunteers (female n = 27 and male n = 8), with a mean (± SD) age of 24.4 (± 2.3) years old, an initial body weight of 64 ± 18 kg and a BMI of 21.7 ± 2.6 kg/m^2, completed the protocol while one

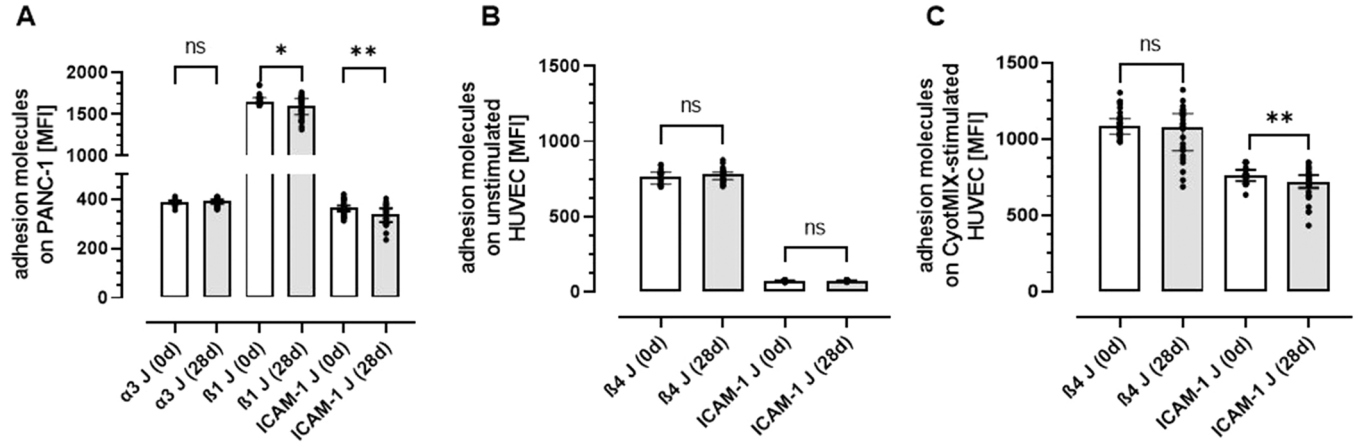

Fig. 2. Expression of CAMs on cancer cells and endothelial cells after incubation with plasma extracts from ACN-rich juice. Expression of adhesion molecules on PANC-1 (A) as well as on non-stimulated and CytoMIX-stimulated HUVECs (B and C) after incubation with plasma extracts from volunteers ingested the ACN-rich juice (J) over 28 days. CAMs were measured fluorometrically by flow cytometry as described in the Materials and Method Section 2.4.2. Values are expressed as median of main fluorescence intensity (MFI) with interquartile range (25th–75th). Significant differences were calculated with repeated measurements One-way ANOVA and values with * , * * and * ** were different with *p-value* < 0.05, *p-value* < 0.01 and *p-value* < 0.001 to corresponding controls (n = 34).

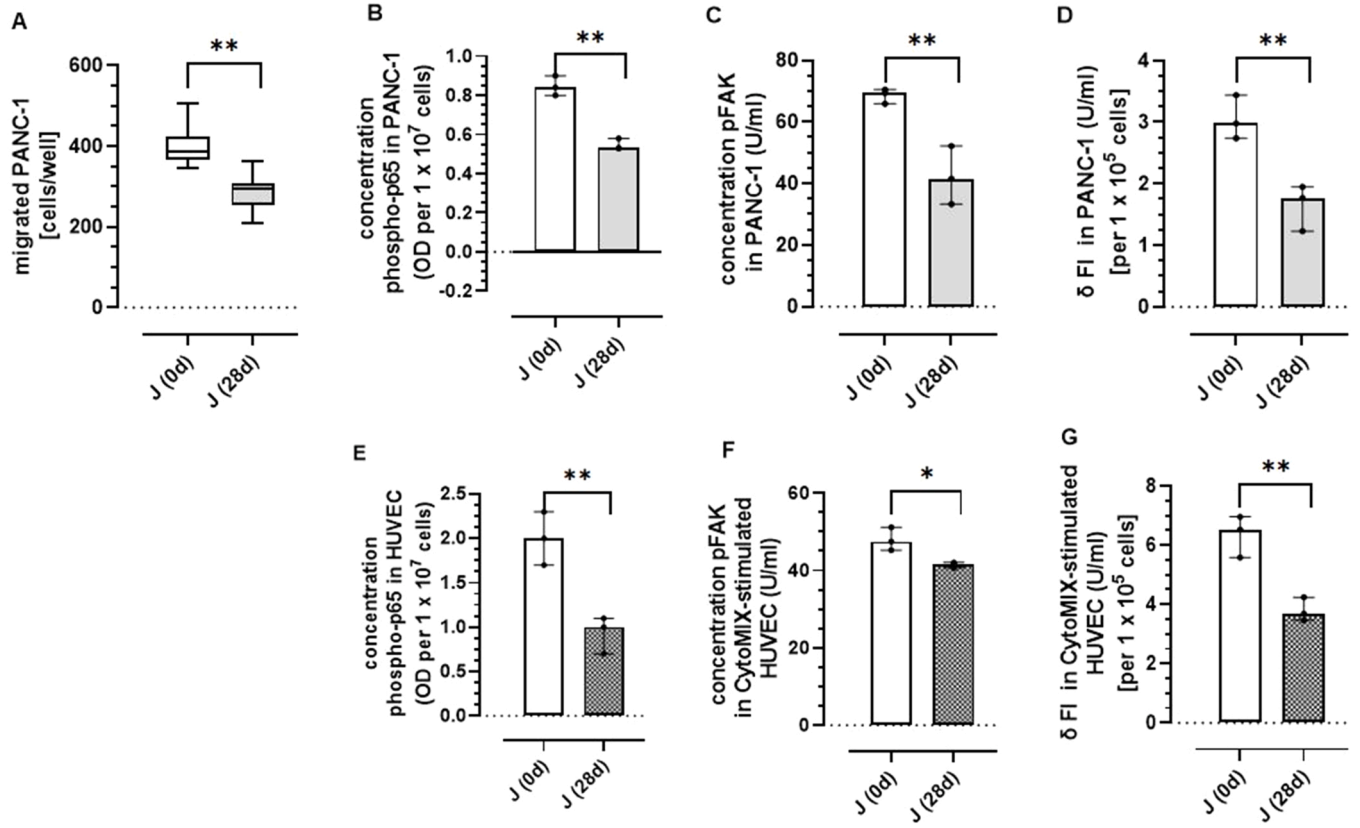

Fig. 3. Molecular Targets of plasma extracts previous and after juice intervention in PANC-1 and HUVECs. (A). PANC-1 migration across the endothelial layer into the lower chamber of co-culture model were measured after 36 h with pooled plasma metabolites of the 10 samples with the highest percentage of migration reduction). (B-G) PANC-1 and ĆytoMIX´-stimulated HUVECs were seeded onto 6-well plates and incubated with pooled PAMs for 36 h. Thereafter, cells were lysed and phosphorylation of p65 (B, E) and FAK (C, F) were measured colorimetrically by ELISA as described in the Materials and Method Section 2.4.2. (D, G) ROS generation was measured after 36-h exposure to PAMs from ACN-rich juice (J) before (d0) and after 28-d (d28) intervention. Thereafter, cells were washed with PBS and incubated with 5 μmol/L H_2DCFDA for 30 min at 37 °C. Fluorescence intensity was measured (Ex/Em 485/535) as described in Materials and Methods Section 2.4.2. Values are expressed as means with standard deviation. Significant differences were calculated with t-test and values with * * were different with *p-value* < 0.01 compared to corresponding controls (n = 3).

subject had an incomplete urine sample collection (blood n = 35; urine n = 34).

3.1. *Primary and secondary outcome: cancer cell migration, expression of adhesion molecules and mechanism*

As shown in Fig. 1, plasma extracts had different effects on cancer cell migration *in vitro* depending on the cancer cell line. In PANC-1, extracted-plasma metabolites after the ACN-rich juice reduced cell migration significantly in comparison to plasma extracts after placebo (Fig. 1A). On the other hand, no reduction was observed for the migration of AsPC-1 (Fig. 1B). As viability of PANC-1 and AsPC-1 was not affected by incubation with plasma extracts under the experimental conditions (data not shown), one reason for these differences could be the influence of plasma extracts on expression of surface molecules and secretion of cytokines that stimulate endothelial cells (Supplementary data S11 and S12). Briefly, in comparison to AsPC-1, PANC-1 expressed higher levels of α3-, α4-, ß1- and ß2-integrin, E-selectin, ICAM-1 and VEGF-R. However, only ß1-integrin and ICAM-1 expression were significantly reduced on PANC-1 by plasma metabolites extracted after juice intake (Fig. 2A). Furthermore, PANC-1 showed a higher secretion of cytokines, such as TNF-α, IL-1ß, and VEGF compared to AsPC-1, indicating a higher potential for activating CAMs on endothelial cells (Supplementary data S4). Higher expression of CAMs and cytokines secretion may be responsible for higher interaction with endothelial cells and thus migration of PANC-1 across the endothelial layer. To investigate the effect of plasma extracts after juice intake on CAMs of HUVECs, cells were stimulated for 36 h with a so-called ĆytoMIX´ (TNF-α, IL-1ß and VEGF), which were secreted by cancer cells. As shown in Fig. 2B and Fig. 2C, CytoMIX-stimulation resulted in increased expression of ß4-integrin and ICAM-1 in comparison to non-stimulated HUVECs, whereas plasma extracts after juice intake significantly reduced only CytoMIX-stimulated ICAM-1 expression.

Expression of CAMs on tumor cells and the expression of receptors on endothelial cells are important steps in the multistep-cascade of migration and metastasis [17]. It has previously been shown that ACNs were able to reduce cancer cell migration by inhibiting phosphorylation of signalling proteins [18,19]; however, we acknowledge that 311 mg/day of ACNs would be difficult to achieve within a diet. However, compared to other studies we used ACN and their metabolites isolated from plasma samples. Most of the previous studies examined the relation between ACN-rich diet and anti-cancer activities using food frequency questionnaires, or after extracting the ACN-related phenolic metabolites from a prepared stock solution directly used in cancer cells [20–24]. However, this result support studies showing that cancer chemoprevention combined with bioactive phytochemicals could be associated with less toxicity and improved efficacy [25–27].

To investigate the mechanisms behind the observed anti-migratory effects on PANC-1, we pooled the plasma extracts from the volunteers with the highest percentage of migration reduction (n = 10). NF-kB p65 and FAK phosphorylation as well as ROS generation were analyzed after incubation with this pool of extracted plasma samples. The redox-sensitive NF-kB and FAK pathways are associated with the regulation of adhesion molecules. As shown in Fig. 3A, incubation of cells with

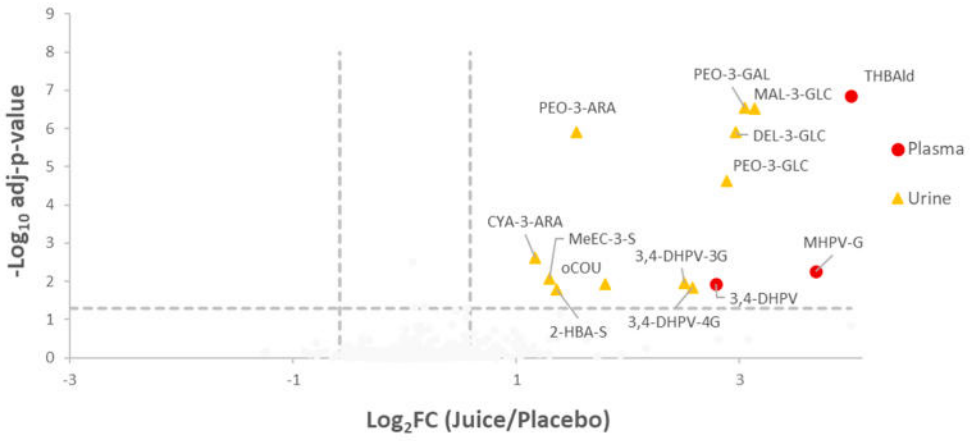

Fig. 4. Volcano plot of log_2FC vs log_{10} FDR-adjusted p-value, showing the metabolites that are significantly associated with ACNs intake in plasma, and urine. The FC value of each metabolite corresponds to the difference between log_2FCpost/pre during ACN-rich juice and log_2FCpost/pre during placebo intervention. To determine the effect of the ACN-rich juice, LMM was used with treatment (juice/placebo), sex and age as fixed factors and subject ID as random factor. *p*-values were calculated and adjusted using FDR (plasma n = 35 and urine n = 34). THBAld: 2,4,6-trihydroxybenzaldehyde; MHPV-G: 4′-hydroxy-3′-methoxyphenyl-γ-valerolactone glucuronide; 3,4-DHPV: 3′,4′-dihydroxyphenyl-γ-valerolactone; oCOU: o-coumaric acid; MeEC-3-S: 3′-methyl(epi)catechin sulphate; 2-HBA-S: 2-hydroxybenzoic acid sulphate; 3,4-DHPV-3 G: 3′,4′-dihydroxyphenyl-γ-valerolactone 3′-glucuronide; 3,4-DHPV-4 G: 3′,4′-dihydroxyphenyl-γ-valerolactone 4′-glucuronide; PEO-3-GAL: peonidin-3-galactoside; PEO-3-GLC: peonidin-3-glucoside; PEO-3-ARA: peonidin-3-arabinoside; CYA-3-ARA: cyanidin-3-arabinoside; MAL-3-GLC: Malvidin-3-glucoside; DEL-3-GLC: delphinidin-3-glucoside; PET-3-GLC: Petunidin-3-glucoside).

pooled plasma extracts after juice intervention over 36 h significantly reduced cell migration. Concomitantly, incubation with plasma extracts after juice intervention significantly blocked phosphorylation of p65 and FAK in PANC-1 and also in CytoMIX-stimulated HUVECs (Fig. 3B-C and E-F) and reduced ROS levels in PANC-1 and stimulated HUVECs (Fig. 3D and G). FAK and NF-kB p65 were associated with increased cancer cell migration and cancer metastasis through higher expression of α- and ß-integrins [28,29]. Therefore, reduction of intracellular cell signalling pathways by plasma ACN metabolites opens a new window concerning cancer preventive strategies.

3.2. *Exploratory outcomes: metabolomics analyses*

From plasma and urine metabolome, 14 out of 902 metabolites (379 in plasma and 523 in urine) were significantly associated with ACN-rich juice intake as shown in Fig. 4. Among these, 3 plasma metabolites resulting from ACN-gut microbiota metabolism were found to be increased: 2,4,6-trihydroxybenzaldehyde (THBAld), 4′-hydroxy-3′-methoxyphenyl-γ-valerolactone glucuronide (MHPV-G) and 3′,4′-dihydroxyphenyl-γ-valerolactone (3,4-DHPV). In urine, 11 metabolites increased after the ACN-rich juice intervention; from these, 6 metabolites were parent ACNs (peonidin-3-galactoside, peonidin-3-glucoside, peonidin-3-arabinoside, cyaniding-3-arabinoside, malvidin-3-glucoside and delphinidin-3-glucoside), while the other 5 metabolites were gut microbial phenolic metabolites (o-coumaric acid (oCOU), 3′-methyl-epicatechin sulphate (MeEC-3-S), 2-hydroxybenzoic acid-sulphate, 3,4-DHPV-3-glucuronide, and 3,4-DHPV-4-glucuronide). In particular, THBAld, 3,4-DHPV and MHPV-G had been shown to have anti-cancer activities, but at supra-physiological doses [22–24,30]. However, we did not observe any association between the increment of plasma THBAld, 3,4-DHPV and MHPV-G and the reduction in PANC-1 migration. Because ACNs can be rapidly absorbed in the stomach, reach the blood and disappear from the circulation within few hours [31,32], it was expected that parent ACNs were only significantly altered in urine and not in plasma. Associations between PANC-1 migration as well as CAM expression of PANC-1 and of stimulated HUVECs with plasma and urine metabolites altered by ACN-rich juice are shown in Supplementary Figure 6. The increment of peonidin and oCOU in urine were inversely associated with PANC-1 migration. Similarly, ICAM-1 expression in PANC-1 was inversely associated with the increase in urinary excretion of MeEC-3-S.

Limitations of our study are the use of extracted plasma from young and healthy volunteers on cancer cell lines *in vitro*. Due to the intense metabolization and fermentation of ACNs, which may vary according to age, sex, and lifestyle, we cannot ascertain that these anti-migratory effects would be observed in patients with cancer or if there would be any interaction with classical chemotherapeutics.

In conclusion, the study showed for the first time that ACN and metabolites isolated from plasma after a long-term ACN-rich juice intervention reduced the migration and expression of CAMs in PANC-1 cancer cells *in vitro* through activation of FAK- and NF-kB-pathways as well as the reduction of ROS. These results are promising and could open a window to investigate interactions of ACNs with classical cancer prevention strategies.

CRediT authorship contribution statement

HM, TM, RGD and CAL: Metabolome analyses. **IB, MF, SR and SK:** conceptualization of the study, migration studies and mechanistic analyses. TM, IB and SK performed the statistical analyses. HM, TM, and IB wrote the first draft of the manuscript. All the authors reviewed and approved the final version of the manuscript.

Conflict of interest statement

The authors declare that they have no known competing financial interests or personal relationships that could have appeared to influence the work reported in this paper.

Data availability

Data will be made available on request.

Acknowledgment

We are deeply grateful to all volunteers who participated in the study. The authors would like to thank Cordula Becker, Katrin Koslowski and Elvira Friedrich for their excellent technical support. The study was funded by the DFG (grant # 1925/5–1) and further supported by CIBERFES, AC19/00096 funded by Instituto de Salud Carlos III and co-funded by European Regional Development Fund "A way to make Europe" and the award of the Generalitat de Catalunya's Agency AGAUR [2017SGR1546] and ICREA Academia 2018. HM would like to thank the scholarship ajuts de personal investigador predoctoral en formació (APIF) from the University of Barcelona.

Appendix A. Supporting information

Supplementary data associated with this article can be found in the online version at doi:10.1016/j.biopha.2022.114076.

References

[1] P.E. Guerrero, L. Miró, B.S. Wong, A. Massaguer, N. Martínez-Bosch, R. de Llorens, P. Navarro, K. Konstantopoulos, E. Llop, R. Peracaula, Knockdown of α2,3-sialyltransferases impairs pancreatic cancer cell migration, invasion and e-selectin-dependent adhesion, Int. J. Mol. Sci. 21 (2020) 1–24, https://doi.org/10.3390/ijms21176239.

[2] N. Makrilia, A. Kollias, L. Manolopoulos, K. Syrigos, Cell adhesion molecules: role and clinical significance in cancer, Cancer Invest 27 (2009) 1023–1037, https://doi.org/10.3109/07357900902769749.

[3] R. Zeeshan, Z. Mutahir, Cancer metastasis - Tricks of the trade, Bosn. J. Basic Med. Sci. 17 (2017) 172–182, https://doi.org/10.17305/bjbms.2017.1908.

[4] J. Cooper, F.G. Giancotti, Integrin signaling in cancer: mechanotransduction, stemness, epithelial plasticity, and therapeutic resistance, Cancer Cell 35 (2019) 347–367, https://doi.org/10.1016/j.ccell.2019.01.007.

[5] J.M. Chan, F. Wang, E.A. Holly, Vegetable and fruit intake and pancreatic cancer in a population-based case-control study in the San Francisco Bay Area, Cancer Epidemiol. Biomark. Prev. 14 (2005) 2093–2097, https://doi.org/10.1158/1055-9965.EPI-05-0226.

[6] N. Lunet, A. Lacerda-Vieira, H. Barros, Fruit and vegetables consumption and gastric cancer: a systematic review and meta-analysis of cohort studies, Nutr. Cancer 53 (2005) 1–10, https://doi.org/10.1207/s15327914nc5301_1.

[7] R.J. Jansen, D.P. Robinson, R.Z. Stolzenberg-Solomon, W.R. Bamlet, M. De Andrade, A.L. Oberg, K.G. Rabe, K.E. Anderson, J.E. Olson, R. Sinha, et al., Nutrients from fruit and vegetable consumption reduce the risk of pancreatic cancer, J. Gastrointest. Cancer 44 (2013) 152–161, https://doi.org/10.1007/s12029-012-9441-y.

[8] K. Maatta, K.-E.A, T.R, Phenolic compounds in berries of black, red, green, and white currants (Ribes sp.), Antioxid. Redox Signal (2001) *3*.

[9] X. Liu, D.A. Martin, J.C. Valdez, S. Sudakaran, F. Rey, B.W. Bolling, Aronia berry polyphenols have matrix-dependent effects on the gut microbiota, Food Chem. 359 (2021), 129831, https://doi.org/10.1016/j.foodchem.2021.129831.

[10] M.C. López De Las Hazas, J.I. Mosele, A. Macià, I.A. Ludwig, M.J. Motilva, Exploring the colonic metabolism of grape and strawberry anthocyanins and their in vitro apoptotic effects in HT-29 colon cancer cells, Antioxid. Redox Signal. 65 (2017) 6477–6487, https://doi.org/10.1021/acs.jafc.6b04096.

[11] J. Jokioja, B. Yang, K.M. Linderborg, Acylated anthocyanins: a review on their bioavailability and effects on postprandial carbohydrate metabolism and inflammation, Compr. Rev. Food Sci. Food Saf. 20 (2021) 5570–5615, https://doi.org/10.1111/1541-4337.12836.

[12] J. Rubert, P. Gatto, M. Pancher, V. Sidarovich, C. Curti, P. Mena, D. Del Rio, A. Quattrone, F. Mattivi, A Screening of Native (Poly)phenols and Gut-Related Metabolites on 3D HCT116 Spheroids Reveals Gut Health Benefits of a Flavan-3-ol Metabolite, Mol. Nutr. Food Res. 2101043 (2022) 1–10, https://doi.org/10.1002/mnfr.202101043.

[13] H. Lamdan, R.S. Garcia-Lazaro, N. Lorenzo, L.G. Caligiuri, D.F. Alonso, H.G. Farina, Anti-proliferative effects of a blueberry extract on a panel of tumor cell lines of different origin, Exp. Oncol. 42 (2020) 101–108, https://doi.org/10.32471/exp-oncology.2312-8852.vol-42-no-2.14766.

[14] S. Kuntz, C. Kunz, S. Rudloff, Inhibition of pancreatic cancer cell migration by plasma anthocyanins isolated from healthy volunteers receiving an anthocyanin-rich berry juice, Eur. J. Nutr. 56 (2017) 203–214, https://doi.org/10.1007/s00394-015-1070-3.

[15] I. Behrendt, I. Röder, F. Will, H. Mostafa, R. Gonzalez-Dominguez, T. Meroño, C. Andres-Lacueva, M. Fasshauer, S. Rudloff, S. Kuntz, Influence of Plasma-Isolated Anthocyanins and Their Metabolites on Cancer Cell Migration (HT-29 and Caco-2) In Vitro: Results of the ATTACH Study, *11*, 1341, Antioxidants 2022 Vol. 11 (2022) *1341*, https://doi.org/10.3390/ANTIOX11071341.

[16] R. González-Domínguez, O. Jáuregui, M.I. Queipo-Ortuño, C. Andrés-Lacueva, Characterization of the Human Exposome by a Comprehensive and Quantitative Large-Scale Multianalyte Metabolomics Platform, Anal. Chem. 92 (2020) 13767–13775, https://doi.org/10.1021/acs.analchem.0c02008.

[17] G. Zhou, D. Chiu, D. Qin, L. Niu, J. Cai, L. He, W. Huang, K. Xu, Detection and clinical significance of cd44v6 and integrin-β1 in pancreatic cancer patients using a triplex real-time RT-PCR assay, Appl. Biochem. Biotechnol. 167 (2012) 2257–2268, https://doi.org/10.1007/s12010-012-9752-2.

[18] W.C. Lim, H. Kim, Y.J. Kim, S.H. Park, J.H. Song, K.H. Lee, I.H. Lee, Y.K. Lee, K. A. So, K.C. Choi, et al., Delphinidin inhibits BDNF-induced migration and invasion in SKOV3 ovarian cancer cells, Bioorg. Med. Chem. Lett. 27 (2017) 5337–5343, https://doi.org/10.1016/j.bmcl.2017.09.024.

[19] C.C. Huang, C.H. Hung, T.W. Hung, Y.C. Lin, C.J. Wang, S.H. Kao, Dietary delphinidin inhibits human colorectal cancer metastasis associating with upregulation of miR-204-3p and suppression of the integrin/FAK axis, Sci. Rep. 9 (2019) 1–11, https://doi.org/10.1038/s41598-019-55505-z.

[20] R. Zamora-Ros, C. Not, E. Guinó, L. Luján-Barroso, R.M. García, S. Biondo, R. Salazar, V. Moreno, Association between habitual dietary flavonoid and lignan intake and colorectal cancer in a Spanish case-control study (the Bellvitge Colorectal Cancer Study), Cancer Causes Control 24 (2013) 549–557, https://doi.org/10.1007/s10552-012-9992-z.

[21] W. Kalt, J.E. McDonald, Y. Liu, S.A.E. Fillmore, Flavonoid metabolites in human urine during blueberry anthocyanin intake, J. Agric. Food Chem. 65 (2017) 1582–1591, https://doi.org/10.1021/acs.jafc.6b05455.

[22] S.C. Forester, Y.Y. Choy, A.L. Waterhouse, P.I. Oteiza, The anthocyanin metabolites gallic acid, 3-O-methylgallic acid, and 2,4,6-trihydroxybenzaldehyde decrease human colon cancer cell viability by regulating pro-oncogenic signals, Mol. Carcinog. 53 (2014) 432–439, https://doi.org/10.1002/mc.21974.

[23] R. Sankaranarayanan, C.K. Valiveti, D.R. Kumar, S. Van Slambrouck, S. S. Kesharwani, T. Seefeldt, J. Scaria, H. Tummala, G.J. Bhat, The flavonoid metabolite 2,4,6-trihydroxybenzoic acid is a CDK inhibitor and an anti-proliferative agent: a potential role in cancer prevention, Cancers (Basel). 11 (2019) 1–18, doi:10.3390/cancers11030427.

[24] P.R. Augusti, A. Quatrin, R. Mello, V.C. Bochi, E. Rodrigues, I.D. Prazeres, A. C. Macedo, S.C. Oliveira-Alves, T. Emanuelli, M.R. Bronze, et al., Antiproliferative effect of colonic fermented phenolic compounds from Jaboticaba (Myrciaria trunciflora) fruit peel in a 3d cell model of colorectal cancer, Molecules (2021) *26*, https://doi.org/10.3390/molecules26154469.

[25] S.K. Abraham, A. Eckhardt, R.G. Oli, H. Stopper, Analysis of in vitro chemoprevention of genotoxic damage by phytochemicals, as single agents or as combinations, Mutat. Res. - Genet. Toxicol. Environ. Mutagen. 744 (2012) 117–124, https://doi.org/10.1016/j.mrgentox.2012.01.011.

[26] J.A. Higgins, M. Zainol, K. Brown, G.D.D. Jones, Anthocyans as tertiary chemopreventive agents in bladder cancer: anti-oxidant mechanisms and interaction with mitomycin C, Mutagenesis 29 (2014) 227–235, https://doi.org/10.1093/mutage/geu009.

[27] X. Li, J. Xu, X. Tang, Y. Liu, X. Yu, Z. Wang, W. Liu, Anthocyanins inhibit trastuzumab-resistant breast cancer in vitro and in vivo, Mol. Med. Rep. 13 (2016) 4007–4013, https://doi.org/10.3892/mmr.2016.4990.

[28] S.K. Mitra, D.D. Schlaepfer, Integrin-regulated FAK-Src signaling in normal and cancer cells, Curr. Opin. Cell Biol. 18 (2006) 516–523, https://doi.org/10.1016/j.ceb.2006.08.011.

[29] M. Shen, Y.Z. Jiang, Y. Wei, B. Ell, X. Sheng, M. Esposito, J. Kang, X. Hang, H. Zheng, M. Rowicki, et al., Tinagl1 Suppresses Triple-Negative Breast Cancer Progression and Metastasis by Simultaneously Inhibiting Integrin/FAK and EGFR Signaling, e7, Cancer Cell 35 (2019) 64–80, https://doi.org/10.1016/j.ccell.2018.11.016.

[30] T. Grimm, A. Schäfer, P. Högger, Antioxidant activity and inhibition of matrix metalloproteinases by metabolites of maritime pine bark extract (Pycnogenol, Free Radic. Biol. Med. 36 (2004) 811–822, https://doi.org/10.1016/j.freeradbiomed.2003.12.017.

[31] I. Krga, D. Milenkovic, Anthocyanins: from sources and bioavailability to cardiovascular- health benefits and molecular mechanisms of action, J. Agric. Food Chem. 67 (2019) 1771–1783, https://doi.org/10.1021/acs.jafc.8b06737.

[32] Y. Wang, Q. Ni, J. Sun, M. Xu, J. Xie, J. Zhang, Y. Fang, G. Ning, Q. Wang, Paraneoplastic β cell dedifferentiation in nondiabetic patients with pancreatic cancer, J. Clin. Endocrinol. Metab. 105 (2020) E1489–E1503, https://doi.org/10.1210/clinem/dgz224.

3.3 Grape/blueberry anthocyanins and their gut-derived metabolites attenuate LPS/nigericin-induced inflammasome activation by inhibiting ASC speck formation in THP-1 monocytes

Behrendt I, Röder I, Will F, Michel G, Friedrich E, Grote D, Martin Z, Dötzer H.P., Fasshauer M, Speckmann M, Kuntz S. *Metabolites* **2024**, 14, 203. doi:10.3390/metabo14040203.

Journal impact factor: 4.1

Abstract: Inflammasomes are multi-protein complexes, which are formed in response to tissue injury, infections, and metabolic stress. However, aberrant inflammasome activation has been linked to several inflammatory diseases. Anthocyanins have been reported to attenuate NLR family pyrin domain-containing 3 (NLRP3) inflammasome activation, but the influence of grape/blueberry anthocyanins and especially their gut-derived metabolites on NLRP3 inflammasome activation in human monocytes remains unclear. Therefore, human leukemic monocytes (THP-1 cells, Tohoku Hospital Pediatrics-1 cells) were preincubated with different concentrations of grape/blueberry anthocyanins, homovanillyl alcohol, or 2,4,6-trihydroxybenzaldehyde (THBA) before the NLRP3 inflammasome was activated by lipopolysaccharide and/or nigericin. Apoptosis-associated speck-like protein containing a CARD (ASC) speck formation, as well as ASC and NLRP3 protein expression, were determined using flow cytometry. Caspase-1 activity was measured in cultured cells, and pro-inflammatory cytokine secretion was determined using enzyme-linked immunosorbent assays. Anthocyanins and their metabolites had no effect on ASC or NLRP3 protein expression. However, THBA significantly inhibited ASC speck formation in primed and unprimed THP-1 monocytes, while caspase-1 activity was significantly declined by grape/blueberry anthocyanins. Furthermore, reduced inflammasome activation resulted in lower pro-inflammatory cytokine secretion. In conclusion, our results show for the first time that grape/blueberry anthocyanins and their gut-derived metabolites exert anti-inflammatory effects by attenuating NLRP3 inflammasome activation in THP-1 monocytes.

Keywords: anthocyanins; gut-derived metabolites; NLRP3 inflammasome; ASC specks; grapes; blueberries

Anhang C: *Supplemental Material*

metabolites

MDPI

Article

Grape/Blueberry Anthocyanins and Their Gut-Derived Metabolites Attenuate LPS/Nigericin-Induced Inflammasome Activation by Inhibiting ASC Speck Formation in THP-1 Monocytes

Inken Behrendt [1,*], Isabella Röder [2], Frank Will [2], Gabriela Michel [3,4], Elvira Friedrich [1], Daniela Grote [1], Zoe Martin [1], Hanna Pauline Dötzer [1], Mathias Fasshauer [1], Martin Speckmann [3,4] and Sabine Kuntz [1]

[1] Institute of Nutritional Science, Justus-Liebig-University Giessen, 35390 Giessen, Germany; elvira.friedrich@ernaehrung.uni-giessen.de (E.F.); grote.d@outlook.de (D.G.); martin.zoe@gmx.de (Z.M.); hanna.doetzer@t-online.de (H.P.D.); mathias.fasshauer@ernaehrung.uni-giessen.de (M.F.); sabine.kuntz@nutr.jlug.de (S.K.)
[2] Department of Beverage Research, Hochschule Geisenheim University, 65366 Geisenheim, Germany; isabella.roeder@googlemail.com (I.R.); frank.will@hs-gm.de (F.W.)
[3] Institute for Clinical Immunology, Transfusion Medicine and Hemostaseology, Justus-Liebig-University Giessen, 35392 Giessen, Germany; gabriela.michel@immunologie.med.uni-giessen.de (G.M.); martin.speckmann@immunologie.med.uni-giessen.de (M.S.)
[4] Flow Cytometry Core Facility, Department of Medicine, Justus-Liebig-University Giessen, 35392 Giessen, Germany
* Correspondence: inken.behrendt@ernaehrung.uni-giessen.de; Tel.: +49-641-9939067

check for updates

Citation: Behrendt, I.; Röder, I.; Will, F.; Michel, G.; Friedrich, E.; Grote, D.; Martin, Z.; Dötzer, H.P.; Fasshauer, M.; Speckmann, M.; et al. Grape/Blueberry Anthocyanins and Their Gut-Derived Metabolites Attenuate LPS/Nigericin-Induced Inflammasome Activation by Inhibiting ASC Speck Formation in THP-1 Monocytes. *Metabolites* **2024**, *14*, 203. https://doi.org/10.3390/metabo14040203

Academic Editors: Christoph Trautwein and Caterina Lonati

Received: 29 February 2024
Revised: 28 March 2024
Accepted: 28 March 2024
Published: 3 April 2024

Abstract: Inflammasomes are multi-protein complexes, which are formed in response to tissue injury, infections, and metabolic stress. However, aberrant inflammasome activation has been linked to several inflammatory diseases. Anthocyanins have been reported to attenuate NLR family pyrin domain-containing 3 (NLRP3) inflammasome activation, but the influence of grape/blueberry anthocyanins and especially their gut-derived metabolites on NLRP3 inflammasome activation in human monocytes remains unclear. Therefore, human leukemic monocytes (THP-1 cells, Tohoku Hospital Pediatrics-1 cells) were preincubated with different concentrations of grape/blueberry anthocyanins, homovanillyl alcohol, or 2,4,6-trihydroxybenzaldehyde (THBA) before the NLRP3 inflammasome was activated by lipopolysaccharide and/or nigericin. Apoptosis-associated speck-like protein containing a CARD (ASC) speck formation, as well as ASC and NLRP3 protein expression, were determined using flow cytometry. Caspase-1 activity was measured in cultured cells, and pro-inflammatory cytokine secretion was determined using enzyme-linked immunosorbent assays. Anthocyanins and their metabolites had no effect on ASC or NLRP3 protein expression. However, THBA significantly inhibited ASC speck formation in primed and unprimed THP-1 monocytes, while caspase-1 activity was significantly declined by grape/blueberry anthocyanins. Furthermore, reduced inflammasome activation resulted in lower pro-inflammatory cytokine secretion. In conclusion, our results show for the first time that grape/blueberry anthocyanins and their gut-derived metabolites exert anti-inflammatory effects by attenuating NLRP3 inflammasome activation in THP-1 monocytes.

Keywords: anthocyanins; gut-derived metabolites; NLRP3 inflammasome; ASC specks; grapes; blueberries

1. Introduction

Anthocyanins are water-soluble secondary plant metabolites, which represent a subclass of flavonoids [1]. They possess a broad range of biological activities and several epidemiological [2–5], as well as experimental [6,7], studies indicate their beneficial health effects especially on cardiovascular diseases. In Europe, mean dietary anthocyanin intake is reported to range from 19 to 65 mg/d, where berries, grapes, and wine are the main dietary

sources [8]. However, in contrast to other flavonoids, absorption of anthocyanins is low [9]. Therefore, most of the ingested anthocyanins reach the colon, where they are extensively metabolized by the gut microbiota into low-molecular-weight metabolites [7,10,11]. These metabolites may be absorbed in the colon by the monocarboxylate transporter-1 [12], thus the gut microbiota plays a crucial role in anthocyanin bioavailability [7,11]. In addition, anthocyanins are unstable at basic pH values and spontaneous degrade into aldehydes and phenolic acids, such as 2,4,6-trihydroxbenzaldehyde (THBA, phloroglucinaldehyde) and 3,4-dihydroxybenzoic acid (protocatechuic acid) in the gastrointestinal tract [7,13]. Hence, gut-derived metabolites can derive from the human gut microbiota or spontaneous anthocyanin degradation. THBA is a degradation product, which results from the A-ring, thus THBA could be formed by each parent anthocyanin independent of B-ring substitution [14]. Therefore, THBA is found at much higher plasma concentrations compared to its parent anthocyanins [15,16]. In this context, using UHPLC–MS/MS analyses, we have recently shown in a randomized, placebo-controlled, crossover trial that THBA was significantly increased in plasma after long-term consumption of an anthocyanin-rich grape/blueberry juice, while plasma concentrations of parent anthocyanins were unaltered [17]. In addition, homovanillyl alcohol (HVA) was significantly increased in feces samples after consumption of the grape/blueberry juice (unpublished data). Furthermore, parent anthocyanins have a short half-life compared to their low-molecular-weight metabolites [10]. Therefore, it is assumed that observed beneficial health effects of dietary anthocyanins are mainly mediated by persistent high metabolite concentrations [18].

Inflammasomes are multi-protein complexes, which can be formed by myeloid cells in response to tissue injury, infections, and metabolic stress as part of the innate immune response [19,20]. However, aberrant inflammasome activation has been linked to several inflammatory diseases such as atherosclerosis, diabetes mellitus type 2, and neurodegenerative diseases [21]. Canonical NLR family pyrin domain-containing 3 (NLRP3) inflammasome activation leads to the formation of a large multimeric ASC speck, comprising NLRP3, the adaptor molecule apoptosis-associated speck-like protein containing a CARD (ASC), and pro-caspase-1. Upon inflammasome assembly, auto-catalytic activation of caspase-1 takes place, resulting in the maturation and release of the inflammatory cytokines IL-1β and IL-18. Furthermore, activation of caspase-1 causes pyroptosis, an inflammatory form of programmed cell death [22]. Thus, inhibition of the NLRP3 inflammasome may exert beneficial health effects in the prevention and treatment of inflammatory diseases. Therefore, searching for new approaches to prevent NLRP3 inflammasome activation is crucial. Anthocyanins and their gut-derived metabolites are known for their anti-inflammatory and anti-oxidative properties [23–25]. In addition, anthocyanins have been reported to attenuate NRLP3 inflammasome activation in several in vitro and in vivo studies. For instance, malvidin supplementation diminished NLRP3 inflammasome activation in mice with LPS-induced acute liver injury [26]. Similarly, malvidin inhibited activation of the NLRP3 inflammasome in mice with acute kidney injury and human renal tubular epithelial cells [27]. However, the influence of grape/blueberry anthocyanins and especially their gut-derived metabolites on NLRP3 inflammasome activation in human monocytes remains unclear. Therefore, the present study aimed to determine the potential of grape/blueberry anthocyanins and their gut-derived metabolites homovanillyl alcohol (HVA) and THBA to attenuate NLRP3 inflammasome activation. In summary, to the best of our knowledge, our results show for the first time that grape/blueberry anthocyanins and their gut-derived metabolites exert anti-inflammatory effects by attenuating NLRP3 inflammasome activation in THP-1 monocytes.

2. Materials and Methods

2.1. Preparation and Characterization of the Powdered Anthocyanin-Rich Grape/Blueberry Extract

The anthocyanin-rich grape/blueberry extract (GBE) was produced at Geisenheim University (Department of Beverage Research, Geisenheim, Germany) from an anthocyanin-rich grape/blueberry juice. Briefly, the juice was made from 80% red grape juice (grape

variety Accent (Hochschule Geisenheim University, Geisenheim, Germany)) blended with 20% bilberry juice (Heidelbeersaft blank BIO; Bayernwald KG, Hengersberg, Germany). The juice was loaded onto a pilot column (Kronalab Chromatographie und Labortechnik GmbH, Sinsheim, Germany) filled with SP70 Sepabeads® absorber resin (Resindion S.r.l., Binasco, Italy), and water-soluble juice constituents like sugars, organic acids, and minerals were washed out with distilled water. Afterwards anthocyanins and colorless polyphenols were eluted with ethanol (Merck GmbH, Darmstadt, Germany). The ethanolic fraction was concentrated using rotary evaporation (Hei-Vap Industrial 0.1.6; Heidolph Instruments GmbH & Co. KG, Schwabach, Germany), and the resulting anthocyanin-rich extract was spray dried (B-290 mini Spray Dryer; Büchi Labortechnik GmbH, Essen, Germany) with maltodextrin (DE17-19; Applichem GmbH, Darmstadt, Germany) as the carrier agent. The powdered extract was analyzed after membrane filtration (0.45 µM) for total phenolics, and anthocyanins were analyzed using HPLC–PDA/ESI–MS as previously described [28]. A representative LC–MS chromatogram of the powdered anthocyanin-rich grape/blueberry extract is shown in Figure S1. Quantitation was carried out in duplicate using peak areas detected at 520 nm and based on external calibration via the reference substance cyanidin-3-glucoside (0.1–100 mg/L; linearity of calibration, $r^2 = 0.9999$). For cyanidin-3-glucoside, the limit of detection was 0.01 mg/L and the limit of quantitation was 0.04 mg/L. Anthocyanins were identified using mass spectra and literature data.

2.2. THP-1 Cell Culture

THP-1 cells are derived from a 1-year-old patient with acute monocytic leukemia and are reported to be a reliable model for NLRP3 inflammasome activation [22,29]. The THP-1 cell line was obtained from Leibniz Institute DSMZ-German Collection of Microorganisms and Cell Cultures (Braunschweig, Germany). Monocytic THP-1 cells were cultured in complete media RPMI-1640 GlutaMAX™ (Invitrogen GmbH, Darmstadt, Germany) supplemented with 7.5% fetal bovine serum (Invitrogen GmbH) and 10 mM Hepes (Invitrogen GmbH). Cells were kept at 37 °C in a humidified incubator at 5% CO_2, and cell density was maintained between 2×10^5 and 1×10^6 cells/mL. THP-1 cells can be cultured up to 3 months without a change in cell behavior [30] and were used between passage 9 and 18.

2.3. Cell Viability and Cytotoxicity

THP-1 cells (8×10^5 cells/mL) were seeded in 48-well plates and subjected to various concentrations of grape/blueberry anthocyanins or their gut-derived metabolites [17]. The molecular structures of the gut-derived metabolites HVA and THBA are shown in Figure S2. The GBE was freshly prepared each time at a concentration of 1 mg/mL. For HVA (purity 99%, CAS No.: 2380-78-1; Sigma-Aldrich, Taufkirchen, Germany) and THBA (purity $\geq$ 97%; CAS No.: 487-70-7; Sigma-Aldrich), stock solutions of 10 mM were prepared. Treatment solutions were sterile-filtered, and THP-1 cells were incubated with the indicated concentrations for 24 h. The cytotoxic effects of each treatment solution were assessed using flow cytometry. Therefore, THP-1 cells were stained with Guava® ViaCount™ Reagent (Merck GmbH) and incubated for 10 min at room temperature in the dark. A total of 1000 events were acquired on a Guava® Muse® Cell Analyzer (Merck GmbH), and cell viability was determined. The representative gating strategy is shown in Figure S3.

2.4. NLRP3 Inflammasome Activation

To examine the influence of grape/blueberry anthocyanins and their gut-derived metabolites on the NLRP3 inflammasome, TPH-1 monocytes were preincubated with different concentrations of the GBE, HVA, or THBA for 24 h before the NLRP3 inflammasome was activated. After preincubation with grape/blueberry anthocyanins or their gut-derived metabolites, the medium was replaced and THP-1 monocytes were either left untreated or primed with 10 ng/mL LPS (*Escherichia coli* 0111: B4, Sigma-Aldrich) in serum-free media for 4 h before the inflammasome was activated by adding 10 µM nigericin (Sigma-Aldrich) for further 40 min.

2.5. Flow Cytometry

Intracellular ASC speck formation, as well as ASC and NLRP3 protein expression, were determined using flow cytometry. THP-1 monocytes were fixed and permeabilized (Biolegend, Amsterdam, The Netherlands) according to the manufacturer's instructions. Fixed cells were stored in sodium azide-containing buffer at 4 °C until the next day. Then, cells were intracellularly stained with fluorescence-labeled monoclonal antibodies [anti-ASC-PE (Biolegend) and anti-NLRP3-APC (Miltenyi, Bergisch Gladbach, Germany)] or the corresponding isotype controls [mouse IgG1κ (Biolegend) and IgG1-REAfinity™ (Miltenyi)] in the dark at room temperature for 10 or 20 min, respectively. In total, 10,000 cells were acquired on a BD FACSCanto™ II Flow Cytometer (BD Bioscience, Heidelberg, Germany), and flow cytometric data were analyzed with FlowJo software version 10.8.1 (BD Bioscience, Heidelberg, Germany). To exclude debris, cells were first gated using forward light scatter area (FSC-A) versus side scatter area (SSC-A). Next, FSC-A versus FSC-height (FSC-H) was used to perform doublet exclusion. Single cells were then gated for ASC and NLRP3 expression compared to the matching isotype control, and median fluorescence intensity (MFI) was assessed (Figure S4). High ASC-expressing cells were further gated using ASC fluorescence pulse area (ASC-A) and ASC fluorescence pulse width (ASC-W). ASC speck forming cells were selected via the observed reduction in ASC-W due to ASC condensation and the percentage of ASC speck-positive cells was quantified (Figure S5).

2.6. Caspase-Glo® 1 Inflammasome Assay

Caspase-1 activity in cultured cells was measured using the Caspase-Glo® 1 Inflammasome Assay (Promega, Walldorf, Germany). Briefly, THP-1 monocytes (5×10^4 cells) were seeded in a white opaque 96-well plate. Cells were either left untreated or the NLRP3 inflammasome was activated as indicated. For the measurement of caspase-1 activity, 100 µL of Caspase-Glo® Reagent was added to each well and luminescence was measured after 60 min on a BioTek Synergy H1 microplate reader (Biotek GmbH, Karlsruhe, Germany).

2.7. Enzyme-Linked Immunosorbent Assays (ELISA)

Secretion of the pro-inflammatory cytokines IL-1β and IL-18 into the cell culture supernatant was determined using commercial ELISA kits (Invitrogen) according to the manufacturer's instructions. Absorbance was measured at 450 nm using a BioTek Synergy H1 microplate reader (Biotek GmbH).

2.8. Statistical Analyses

GraphPad Prism version 10.0.3 (GraphPad Software, San Diego, CA, USA) was used for statistical analyses. All experiments were run in duplicate, and results are expressed as means ± SD (standard deviation). Significant differences between treatments were calculated with one-way analysis of variance (ANOVA) followed by Dunnett's multiple comparisons test. Adjusted *p*-values of <0.05 were considered statistically significant, and adjusted *p*-values are given in all figures.

3. Results

3.1. Composition of the Powdered Anthocyanin-Rich Grape/Blueberry Extract

In total, the anthocyanin content of the powdered grape/blueberry extract was 61.4 mg/g. Due to the high grape content of the juice that the extract originated from, almost half of the identified anthocyanins were peonidin derivates (about 47%). Peonidin-3,5-diglucoside was the most abundant anthocyanin, followed by malvidin-3,5-diglucoside and delphinidin-3-arabinoside (Table 1). The total phenol content of the powdered grape/blueberry extract was 185 mg/g, with 18 mg/g colorless phenolics.

Table 1. Anthocyanin composition of the powdered anthocyanin-rich grape/blueberry extract.

Anthocyanins [1]	Rt [min]	$[M+H]^+$	λmax [nm]	mg/g	[%]
Delphinidin-3,5-diglucoside	7.10	627, 465, 303	520	0.3	0.4
Cyanidin-3,5-diglucoside	8.65	611, 449, 287	514	1.3	2.0
Delphinidin-3-galactoside	9.57	465, 303	522	3.2	5.2
Delphinidin-3-glucoside	10.41	465, 303	522	3.7	6.0
Peonidin-3,5-diglucoside	11.13	625, 463, 301	513	23.4	38.1
Delphinidin-3-arabinoside	11.84	435, 303	522	6.7	10.9
Malvidin-3,5-diglucoside	12.06	655, 493, 331	521	6.7	10.9
Petunidin-3-galactoside	12.72	479, 317	524	0.8	1.3
Cyanidin-3-arabinoside	13.03	419, 287	517	1.5	2.5
Petunidin-3-glucoside	13.52	479, 317	521	2.6	4.3
Peonidin-3-galactoside	14.10	463, 301	515	0.2	0.4
Petunidin-3-arabinoside	14.59	449, 317	524	0.5	0.9
Peonidin-3-glucoside	15.00	463, 301	516	5.1	8.3
Malvidin-3-glucoside	15.95	493, 331	524	3.9	6.4
Malvidin-3-arabinoside	16.99	463, 331	526	0.3	0.5
Malvidin-3-(6″-coumaryl)-5-diglucoside	21.69	801, 639, 493, 331	524	1.2	1.9
∑				61.4	100

[1] The powdered grape/blueberry extract was analyzed using HPLC–PDA/ESI–MS (n = 2), and the data were expressed as mean ± SD mg cyanidin-3-glucoside equivalents per g. Rt, retention time; $[M+H]^+$, photoionization mass; λmax (lambda max), wavelength maxima.

3.2. Effect of Grape/Blueberry Anthocyanins and Their Gut-Derived Metabolites on THP-1 Cell Viability

To determine the potential cytotoxic effects of grape/blueberry anthocyanins and their gut-derived metabolites on THP-1 cells, THP-1 monocytes were treated with increasing concentrations of the GBE, HVA, or THBA for 24 h before cell viability was measured using flow cytometry. As shown in Figure 1a, incubation with 0 to 500 µg/mL of the GBE for 24 h had no effect on cell viability. In addition, HVA concentrations up to 125 µM were nontoxic to THP-1 monocytes (Figure 1b). In contrast, cell viability was slightly affected by the highest THBA concentration and decreased from 95.5 ± 1.0% for control cells to 90.0 ± 3.8% for THBA-treated cells ($p < 0.01$; Figure 1c). Based on these results, non-cytotoxic GBE concentrations of 15 and 50 µg/mL were used for all subsequent experiments. For gut-derived anthocyanin metabolites, non-cytotoxic concentrations of 1 and 50 µM were selected to represent physiological, as well as pharmacological, doses.

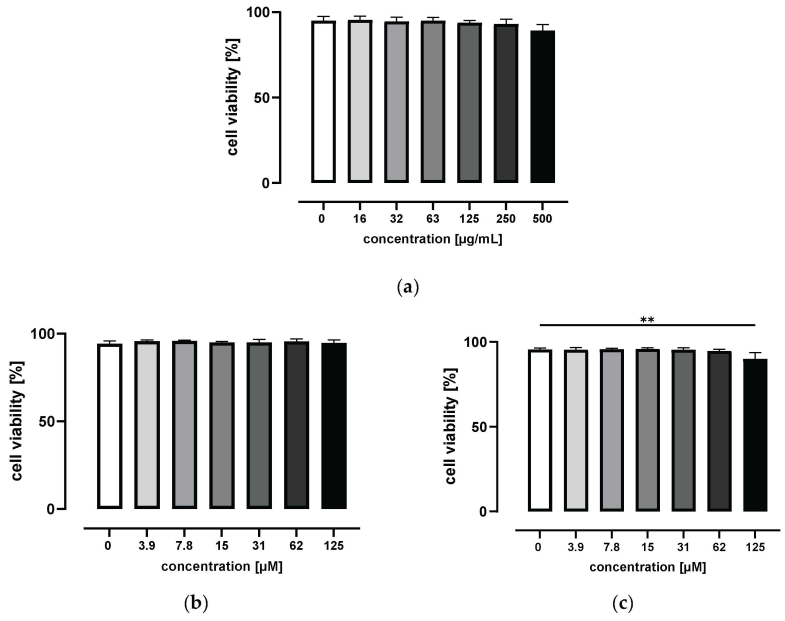

Figure 1. Effect of grape/blueberry anthocyanins and their gut-derived metabolites on THP-1 cell viability. THP-1 monocytes were incubated with the indicated concentrations of (**a**) the GBE, (**b**) HVA,

or (**c**) THBA for 24 h before cell viability was measured by flow cytometry. Data are presented as mean ± SD (n = 3). Significant differences compared to the untreated control were calculated using one-way ANOVA followed by Dunnett's multiple comparisons test. ** $p < 0.01$.

3.3. Grape/Blueberry Anthocyanins and Their Gut-Derived Metabolites Have No Effect on ASC and NLRP3 Protein Expression in THP-1 Monocytes

LPS is a toll like-receptor 4 agonist, and priming THP-1 cells with LPS for several hours is reported to result in transcriptional upregulation of several inflammasome components [22]. To investigate the influence of grape/blueberry anthocyanins and their gut-derived metabolites on ASC and NLRP3 protein expression, THP-1 monocytes were preincubated with different concentrations of the GBE, HVA, or THBA before the NLRP3 inflammasome was primed with LPS. ASC and NLRP3 protein expression were determined using flow cytometry, whereas high basal protein expression rates were observed in THP-1 monocytes. However, neither ASC nor NLRP3 protein expression was induced through LPS priming in the present study. In addition, preincubation with grape/blueberry anthocyanins and their gut-derived metabolites had no effect on ASC or NLRP3 protein expression in THP-1 monocytes (Figure S6).

3.4. Grape/Blueberry Anthocyanins and Their Gut-Derived Metabolites Attenuate ASC Speck Formation in THP-1 Monocytes

ASC speck formation is a hallmark of NLRP3 inflammasome activation. While under resting conditions ASC molecules are diffuse distributed in the cytoplasm, NLRP3 inflammasome activation leads to the formation of a single supramolecular ASC speck. This condensation of ASC molecules could be observed using flow cytometry as a decline in ASC pulse width (ASC-W) [31]. Therefore, the quantification of ASC speck-positive cells using flow cytometry is a sensitive method to determine NLRP3 inflammasome activation on a cellular level [22]. To validate this method, THP-1 monocytes were either left untreated or primed with LPS followed by activation of the inflammasome with the pore-forming toxin nigericin [32]. As expected, no formation of ASC specks could be observed in untreated and LPS-treated THP-1 monocytes. In contrast, nigericin treatment with and without prior LPS priming resulted in a significant increase of ASC speck-positive cells compared to the untreated control ($p < 0.0001$; Figure 2).

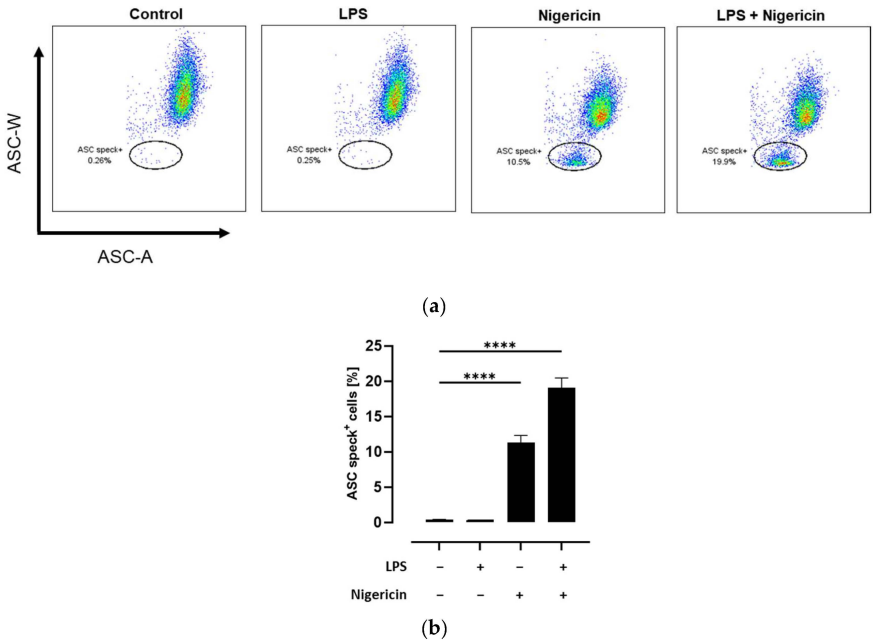

Figure 2. Detection of ASC speck formation in THP-1 cells using flow cytometry. THP-1 monocytes were either left untreated or primed with LPS followed by activation of the NLRP3 inflammasome

with nigericin as mentioned in the methods section. Flow analysis was performed and the percentage of ASC speck-positive cells was quantified. Data are presented as (**a**) representative dot plots and (**b**) column bars with mean ± SD (n = 3). Significant differences compared to the untreated control were calculated using one-way ANOVA followed by Dunnett's multiple comparisons test. **** $p < 0.0001$.

After validating this method, we next investigated potential inhibitory effects of grape/blueberry anthocyanins and their gut-derived metabolites towards NLRP3 inflammasome activation. Therefore, THP-1 monocytes were preincubated with different concentrations of the GBE, HVA, or THBA before the NLRP3 inflammasome was activated with LPS and/or nigericin. There was a decline in the percentage of ASC speck-positive cells after preincubation with the GBE (15 µg/mL) in LPS- and nigericin-treated cells. However, after correction for multiple comparisons this effect was no longer statistically significant (Figure 3a). In contrast, no impact of GBE treatment on ASC speck formation in unprimed nigericin-treated cells was observed (Figure 3b). Interestingly, THBA (50 µM) significantly inhibited ASC speck formation in LPS- and nigericin-treated THP-1 monocytes ($p < 0.01$), while HVA had no effect (Figure 3c). However, the percentage of ASC speck-positive cells was decreased by low and high HVA, as well as THBA, doses in unprimed, nigericin-treated THP-1 monocytes, whereas the effects of THBA were still significant after correction for multiple testing ($p < 0.05$; Figure 3d). Taken together, these results indicate that grape/blueberry anthocyanins and their gut-derived metabolites attenuate ASC speck formation in primed and unprimed THP-1 monocytes.

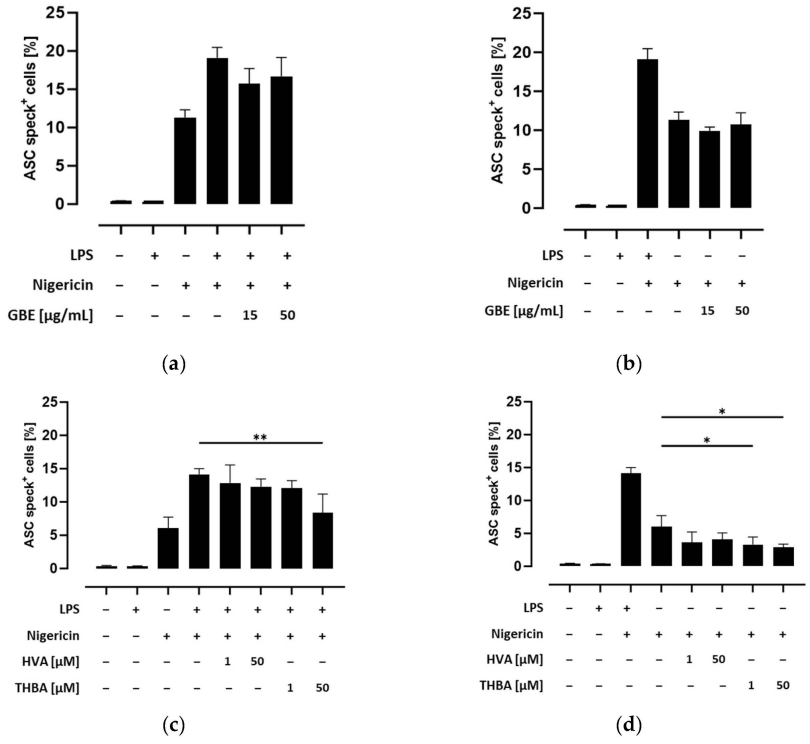

Figure 3. Effect of grape/blueberry anthocyanins and their gut-derived metabolites on ASC speck formation in THP-1 cells. THP-1 monocytes were preincubated with the indicated concentrations of grape/blueberry anthocyanins and their gut-derived metabolites before the NLRP3 inflammasome was activated as mentioned in the methods section. Cells were flow cytometrically analyzed and the percentage of ASC speck-positive cells was quantified. Data are presented as mean ± SD (n = 3). Significant differences compared to (**a**,**c**) LPS- and nigericin-stimulated cells or (**b**,**d**) cells treated only with nigericin were calculated using one-way ANOVA followed by Dunnett's multiple comparisons test. * $p < 0.05$ and ** $p < 0.01$.

3.5. Effect of Grape/Blueberry Anthocyanins and Their Gut-Derived Metabolites on Caspase-1 Activity in THP-1 Monocytes

Upon NLRP3 inflammasome activation, ASC and pro-caspase-1 molecules interact via their respective caspase recruitment domains, leading to the auto-proteolytic activation of caspase-1 [33]. This activation of caspase-1 is usually monitored through western blot analysis of cleaved caspase-1. However, this method does not directly reflect caspase-1 activity. For this reason, in the present study, a bioluminescent, coupled-enzyme assay utilizing a Z-WEHD-aminoluciferin substrate for caspase-1 was used to determine caspase-1 activity. Active caspase-1 cleaves the Z-WEHD-aminoluciferin substrate, leading to the release of aminoluciferin, resulting in a luciferase reaction and light production, which can be measured with a luminescence microplate reader [34].

As shown in Figure S7a, inflammasome activation led to a significant increase in caspase-1 activity in nigericin-stimulated THP-1 monocytes. Nevertheless, this response was significantly enhanced by priming with LPS. To confirm the specific determination of caspase-1 activity, the caspase-1 inhibitor Ac-YVAD-CHO was used for testing in parallel wells in preliminary tests. We further assessed whether caspase-1 activity was influenced by grape/blueberry anthocyanins and their gut-derived metabolites in THP-1 cells. Therefore, THP-1 monocytes were preincubated with different concentrations of the GBE, HVA, or THBA before the NLRP3 inflammasome was activated by LPS and/or nigericin. We found that caspase-1 activity was significantly inhibited by preincubation with the GBE both in LPS and nigericin, as well as in cells treated only with nigericin ($p < 0.0001$; Figure 4a,b). Surprisingly, caspase-1 activity slightly but not significantly increased in LPS-primed cells preincubated with the gut-derived anthocyanin metabolites HVA and THBA (Figure 4c). Similarly, after inflammasome activation, caspase-1 activity was enhanced in unprimed HVA or THBA-treated THP-1 monocytes ($p < 0.05$; Figure 4d). In conclusion, these results indicate that grape/blueberry anthocyanins inhibit inflammasome activation by inhibiting caspase-1 activity, while gut-derived metabolites may exert contrary effects on caspase-1-activity in THP-1 monocytes.

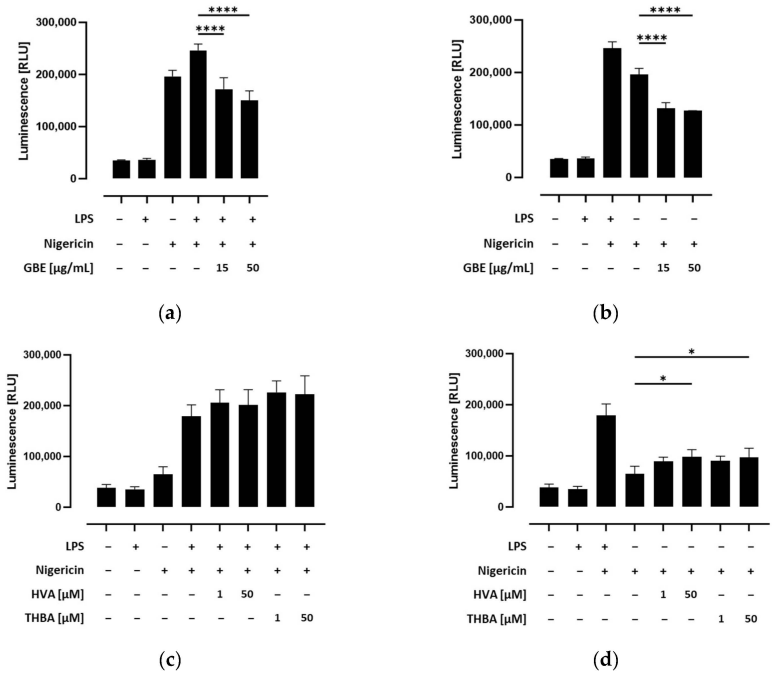

Figure 4. Effect of grape/blueberry anthocyanins and their gut-derived metabolites on caspase-1 activity in THP-cells. THP-1 monocytes were preincubated with the indicated concentrations of grape/blueberry anthocyanins and their gut-derived metabolites before the NLRP3 inflammasome was activated as mentioned in the methods section. Caspase-1 activity was measured by using the Caspase-Glo® 1 Inflammasome Assay and luminescence was measured. Data are

presented as mean ± SD (n = 3). Significant differences compared to (**a**,**c**) LPS- and nigericin-stimulated cells or (**b**,**d**) cells treated only with nigericin were calculated using one-way ANOVA followed by Dunnett's multiple comparisons test. * $p < 0.05$, **** $p < 0.0001$. RLU, relative light unit.

3.6. Grape/Blueberry Anthocyanins and Their Gut-Derived Metabolites Ameliorate Inflammatory Cytokine Secretion after NLRP3 Inflammasome Activation in THP-1 Monocytes

Secretion of the inflammatory cytokines IL-1β and IL-18 requires the cleavage of their pro-forms into their bioactive forms by active caspase-1 [21]. Thus, we next investigated the efficacy of grape/blueberry anthocyanins and their gut-derived metabolites to attenuate pro-inflammatory cytokine release. Therefore, THP-1 monocytes were preincubated with different concentrations of the GBE, HVA, or THBA before the NLRP3 inflammasome was activated by LPS and/or nigericin, and IL-1β and IL-18 concentrations in the cell-culture supernatants were measured using ELISAs. Our results show that NLRP3 inflammasome activation significantly induced IL-1β and IL-18 secretion in primed and unprimed THP-1 monocytes (Figure S7b,c), albeit that inflammatory cytokine release was significantly enhanced by LPS priming. However, preincubation with the GBE (15 and 50 µg/mL) decreased IL-1β concentrations in the cell-culture supernatants of LPS- and nigericin-treated cells, whereas the effect of the higher concentration was still significant after correction for multiple testing ($p < 0.01$; Figure 5a). In addition, preincubation with THBA (50 µM) drastically declined IL-1β secretion after LPS/nigericin-induced inflammasome activation ($p < 0.01$), whereas preincubation with HVA showed only modest effects (Figure 5c). In addition, the efficacy of grape/blueberry anthocyanins and their gut-derived metabolites to attenuate IL-18 secretion was less pronounced even at high concentrations (Figure 5b,d). After inflammasome activation, IL-18 release by THP-1 monocytes was decreased by preincubation with the GBE (15 µg/mL) and THBA (50 µM). However, after correction for multiple testing these effects were no longer statistically significant. Consequently, these results indicate that grape/blueberry anthocyanins and their gut-derived metabolites ameliorate inflammatory cytokine secretion after inflammasome activation in THP-1 monocytes, whereas the efficacy of grape/blueberry anthocyanins and their metabolites to attenuate IL-18 secretion is less pronounced.

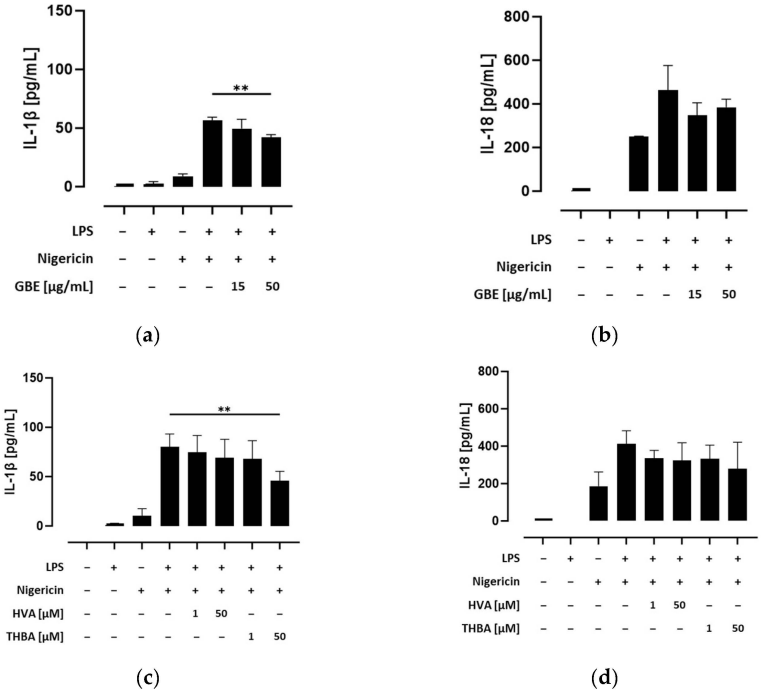

Figure 5. Effect of grape/blueberry anthocyanins and their gut-derived metabolites on inflammatory cytokine secretion in THP-1 cells. THP-1 monocytes were preincubated with the indicated concentrations

of grape/blueberry anthocyanins and their gut-derived metabolites before the NLRP3 inflammasome was activated as mentioned in the methods section. The release of (**a**,**c**) IL-1β and (**b**,**d**) IL-18 into the cell-culture supernatant was measured using ELISA. Data are presented as mean ± SD of at least three replicated experiments. Significant differences compared to LPS- and nigericin-stimulated cells were calculated using one-way ANOVA followed by Dunnett's multiple comparisons test. ** $p < 0.01$.

4. Discussion

In the last years, growing evidence indicates a link between excessive NLRP3 inflammasome activation and inflammatory diseases [21]. Therefore, searching for new approaches to preventing NLRP3 inflammasome activation is crucial. Anthocyanins and their gut-derived metabolites are known for their anti-inflammatory and anti-oxidative properties [23–25]. Therefore, the present study aimed to determine the potential of grape/blueberry anthocyanins, and especially their gut-derived metabolites, to attenuate NLRP3 inflammasome activation.

Canonical inflammasome activation is a two-step process comprising priming and activation. During the priming step, damage-associated molecular patterns and pathogen-associated molecular patterns such as LPS induce the nuclear factor (NF)-κB mediated expression of different NLRP3 inflammasome components [35]. For this reason, we primed THP-1 monocytes with LPS for several hours before ASC and NLRP3 protein expression was assessed using flow cytometry. We noted a high basal NLRP3 protein expression, which was also observed by Gritsenko et al. [19]. However, neither ASC nor NLRP3 protein expression was induced by LPS in the present study. In another study, ASC protein expression was not significantly altered by LPS priming in primary human monocytes, whereas NLRP3 protein expression was significantly upregulated [36]. In addition, LPS priming of primary human monocytes and THP-1 cells also resulted in higher NLRP3 protein expression rates in a further study [19]. However, in these studies, 10- to 100-fold higher LPS concentrations were used, and protein expression was assessed through western blot analyses [19,36]. In contrast, protein expression was determined using flow cytometry on a single cell level in the present study. Therefore, discrepancies in study results may be due to experimental and methodological differences.

Several studies reveal that anthocyanins exert anti-inflammatory properties by inhibiting NF-κB signaling pathway activation [37]. Therefore, we next examined the influence of grape/blueberry anthocyanins and their gut-derived metabolites on ASC and NLRP3 protein expression in THP-1 monocytes. A recent study reported that ASC and NLRP3 mRNA levels were significantly decreased by different blueberry extracts in LPS-treated murine RAW264.7 macrophages [38]. Moreover, NLRP3 protein expression was also significantly inhibited to varying extents depending on the respective blueberry variety [38]. In other studies, malvidin, which is the predominating anthocyanin in blueberries [39], inhibited LPS-induced NLRP3 protein expression in various mouse tissues [26,27,40,41]. In contrast, the observed effects of malvidin on ASC protein expression are more inconsistent. While LPS-induced ASC protein expression has been found to be significantly decreased by malvidin treatment in liver and kidney tissues of mice, ASC expression in mice cerebrum was not affected [26,27,40]. Similarly, in a randomized placebo-controlled clinical trial, mRNA levels of ASC and NLRP3 were not significantly lower in peripheral blood mononuclear cells (PBMCs) from patients with nonalcoholic fatty liver disease (NAFLD), compared to the control group, after 12 weeks of anthocyanin supplementation [42]. In addition, no inhibitory effects of grape/blueberry anthocyanins and their gut-derived metabolites on ASC or NLRP3 protein expression in THP-1 monocytes were observed in the present study. Therefore, we next investigated whether grape/blueberry anthocyanins and their gut-derived metabolites inhibit NLRP3 inflammasome assembly rather than ASC or NLRP3 expression.

ASC speck formation is a unique hallmark of inflammasome activation that can be observed using fluorescence microscopy. In addition, western blot analyses can be used to discriminate between ASC monomers and ASC oligomers [22]. However, these techniques

are either non-quantitative or time consuming. Therefore, ASC speck formation was determined using intracellular flow cytometry in the present study. This powerful approach was recently introduced by Sester et al. and allows researchers to assess the formation of ASC specks on a single cell level [22,31]. Although neither ASC nor NLRP3 protein expression was induced by LPS priming in the present study, inflammasome activation was significantly higher in LPS-primed cells compared to unprimed cells, as shown by a significantly higher percentage of ASC speck-positive THP-1 monocytes. Therefore, our results illustrate that priming regulates NLRP3 inflammasome activation beyond the transcriptional upregulation of inflammasome components. Indeed, growing evidence indicates that priming of the NLRP3 inflammasome induces complex post-translational modifications such as ubiquitination and phosphorylation, which influence NLRP3 inflammasome activation [21,43]. To the best of our knowledge, our results show for the first time that ASC speck formation is attenuated by grape/blueberry anthocyanins and their gut-derived metabolites in primed, as well as unprimed, THP-1 monocytes. The fact, that ASC speck formation was also diminished in unprimed monocytes indicates that anthocyanins and their gut-derived metabolites may possibly prevent NLRP3 oligomerization and/or ASC-NLRP3 interaction. In this context, Erianin, a low-molecular-weight molecule with two phenyl rings, has been reported to prevent NLRP3 inflammasome assembly by direct binding to the NLRP3 protein [44]. On the other hand, nigericin treatment causes mitochondrial dysfunction, resulting in increased reactive oxygen species (ROS) generation and oxidative stress, which are known to induce NLRP3 inflammasome activation [32]. Cellular redox homeostasis is maintained by the nuclear factor erythroid 2-like factor 2 (Nrf2) signaling pathway [45]. A recent study reported that malvidin significantly increased Nrf2 protein expression in the colon tissue of mice with LPS-induced septic intestinal injury [41]. Furthermore, another study found that pretreatment with malvidin decreased LPS/ATP-induced ASC oligomerization, as well as ASC speck formation, in human renal tubular epithelial cells (HK-2 cells) by activating the Nrf2 pathway, and decreased ROS generation [27]. In addition, malvidin has been found to alleviate LPS/ATP-induced mitochondrial dysfunction and ROS generation in BV-2 microglia cells [40]. Similarly, anthocyanins from *Hibiscus syriacus* L. inhibited LPS/ATP-induced NLRP3 inflammasome activation in BV-2 microglia cells by alleviating mitochondrial ROS production in a further study [46]. Therefore, grape/blueberry anthocyanins and their gut-derived metabolites may inhibit ASC speck formation in THP-1 monocytes by ameliorating oxidative stress and preventing the interactions of inflammasome components.

Upon NLRP3 inflammasome activation, ASC and pro-caspase-1 molecules interact via their respective caspase recruitment domains, leading to the auto-proteolytic activation of caspase-1, which is an inflammatory caspase that catalyzes the maturation and release of IL-1β and IL-18 [32]. Hence, inhibition of caspase-1 activity may diminish the inflammatory response. Therefore, we next investigated whether the observed reduction in ASC speck formation by grape/blueberry anthocyanins and their gut-derived metabolites was accompanied by a decrease in capase-1 activity. Our results show that caspase-1 activity was significantly inhibited by grape/blueberry anthocyanins in primed and unprimed THP-1 monocytes, indicating that grape/blueberry anthocyanins may inhibit the recruitment and/or the auto-catalytic activation of caspase-1. However, anthocyanins may also inhibit caspase-1 expression. A recent study reported that treatment with different blueberry extracts reduced the levels of mRNA and protein expression of caspase-1 in RAW264.7 macrophages [38]. In addition, studies have found LPS-induced protein expression of cleaved caspase-1 to be significantly decreased by malvidin treatment in several mouse tissues [26,27,40]. Similarly, malvidin reduced the protein levels of cleaved caspase-1 in LPS/ATP-treated HK-2 cells [27]. Therefore, grape/blueberry anthocyanins may decrease caspase-1 activity by inhibiting the expression and activation of its inactive pro-form.

The maturation and release of the inflammatory cytokines IL-1β and IL-18 require active caspase-1 [21]. Therefore, we finally examined the influence of grape/blueberry anthocyanins and their gut-derived metabolites on IL-1β and IL-18 secretion into the cell-

culture supernatant of LPS- and nigericin-treated THP-1 monocytes. As recently reported, IL-1β is not basally expressed in human monocytes, whereas IL-18 is constitutively expressed [19]. However, in the present study NLRP3 inflammasome activation by nigericin treatment significantly induced IL-1β and IL-18 release in primed and unprimed THP-1 monocytes. These results indicate that at least low levels of IL-1β are basally expressed in THP-1 monocytes. In addition, preincubation with grape/blueberry anthocyanins and their gut-derived metabolites significantly decreased IL-1β concentrations in the cell-culture supernatants of LPS- and nigericin-treated THP-1 monocytes, whereas the effects on IL-18 concentrations were only modest and less pronounced even at high concentrations. Therefore, grape/blueberry anthocyanins and their gut-derived metabolites may not only attenuate ASC speck formation and caspase-1 activity but also pro-inflammatory cytokine expression. Indeed, gene expression of IL-1β has been found to be significantly inhibited by blueberry extracts in murine RAW264.7 macrophages [38], and red raspberry supplementation has been found to prevent high-fat-diet-induced IL-1β, as well as IL-18, mRNA and protein expression in the liver tissue of mice [47]. Similarly, in other studies, malvidin alleviated LPS-induced IL-1β expression in several mouse tissues [26,27,41]. In addition, after supplementation of anthocyanins for 12 weeks, IL-1β and IL-18 mRNA expression rates have been found to be significantly lower in PBMCs from NAFLD patients compared to the placebo group [42], and IL-1β and IL-18 plasma levels also significantly decreased in the anthocyanin group [42]. Taken together, this evidence indicates that grape/blueberry anthocyanins and their gut-derived metabolites attenuate pro-inflammatory cytokine release upon NLRP3 inflammasome activation and therefore may exert beneficial health effects in the prevention and treatment of inflammatory diseases.

To the best of our knowledge, our results show for the first time that grape/blueberry anthocyanins and their gut-derived metabolites exert anti-inflammatory effects by attenuating NLRP3 inflammasome activation in primed and unprimed human monocytes. In particular, THBA exhibited a strong potential to inhibit NLRP3 inflammasome activation, while the dampening impact of THBA on NLRP3 inflammasome activation was more pronounced at the high, supraphysiological concentration. In contrast, maximal systemic THBA concentrations between 103 and 582 nM were observed after single doses of 500 mg ^{13}C-labeled cyanidin-3-glucoside or elderberry anthocyanins, respectively [15,16]. Therefore, the physiological relevance of the current results has to be considered. However, potential additive and synergistic effects of anthocyanin metabolites may exert in vivo [48], amplifying the efficiency of physiologically attainable anthocyanin and metabolite concentrations to inhibit inflammasome activation. One strength of the current study is that several events of the NLRP3 inflammasome activation cascade were monitored through the evaluation of multiple read-outs. In addition, ASC speck formation was determined using intracellular flow cytometry, which is a sensitive and powerful approach to assess inflammasome activation. However, the underlying molecular mechanisms by which grape/blueberry anthocyanins and their gut-derived metabolites attenuate NLRP3 inflammasome activation remain to be shown and should be addressed in future studies, since understanding the precise molecular pathways involved would provide deeper insights into the observed outcomes. One limitation of the present study is that cancerogenic cells, like THP-1 monocytes, may not completely reflect the behavior of primary cells. However, THP-1 cells display similar features of NLRP3 inflammasome activation compared to primary human monocytes. In addition, THP-1 cells have been confirmed as a sufficient model to assess NLRP3 inflammasome activation in prior studies [19,29]. Nevertheless, most of our knowledge about the influence of anthocyanins and their metabolites on NLRP3 inflammasome activation comes from preclinical in vitro studies and animal models. Translating findings from those models to humans requires careful consideration of interspecies differences in metabolism and physiology. Therefore, further clinical studies confirming these findings in primary human monocytes are necessary to provide conclusions that are even more definitive.

5. Conclusions

In conclusion, our results show that grape/blueberry anthocyanins and their metabolites exert anti-inflammatory effects by attenuating NLRP3 inflammasome activation. Therefore, grape/blueberry anthocyanins and especially their physiological relevant metabolite THBA might be useful for the prevention and treatment of several inflammatory diseases.

Supplementary Materials: The following supporting information can be downloaded at: https://www.mdpi.com/article/10.3390/metabo14040203/s1, Figure S1: Representative HPLC-MS chromatogram of the powdered anthocyanin-rich grape/blueberry extract; Figure S2: Molecular structures of gut-derived anthocyanin metabolites; Figure S3: Gating strategy to assess cell viability; Figure S4: Gating strategy to assess ASC and NLRP3 protein expression; Figure S5: Gating strategy to assess ASC speck formation; Figure S6: Effect of grape/blueberry anthocyanins and their gut-derived metabolites on ASC and NLRP3 protein expression in THP-1 cells; Figure S7: NLRP3 inflammasome activation in THP-1 cells.

Author Contributions: Conceptualization, I.B. and S.K.; methodology, I.B., G.M., M.S. and S.K.; formal analysis, I.B.; investigation, I.B., E.F., D.G., Z.M. and H.P.D.; grape/blueberry extract preparation and characterization, I.R. and F.W.; writing—original draft preparation, I.B.; writing—review and editing, G.M., M.S., M.F. and S.K.; visualization, I.B.; supervision, S.K. All authors have read and agreed to the published version of the manuscript.

Funding: This research received no external funding.

Institutional Review Board Statement: Not applicable.

Informed Consent Statement: Not applicable.

Data Availability Statement: Data is contained within the article or Supplementary Materials.

Acknowledgments: The authors would like to thank the Flow Cytometry Core Facility (Justus-Liebig-University Giessen) for using BD Canto II and for technical assistance. We would also like to thank Nico Wittmann (University of Greifswald, Department Pediatric and Adolescent Medicine, Section of Pediatric Rheumatology) for his valuable support during the establishment of inflammasome activation.

Conflicts of Interest: The authors declare no conflicts of interest.

References

1. Liu, J.; Zhou, H.; Song, L.; Yang, Z.; Qiu, M.; Wang, J.; Shi, S. Anthocyanins: Promising Natural Products with Diverse Pharmacological Activities. *Molecules* **2021**, *26*, 3807. [CrossRef] [PubMed]
2. Mink, P.J.; Scrafford, C.G.; Barraj, L.M.; Harnack, L.; Hong, C.-P.; Nettleton, J.A.; Jacobs, D.R. Flavonoid intake and cardiovascular disease mortality: A prospective study in postmenopausal women. *Am. J. Clin. Nutr.* **2007**, *85*, 895–909. [CrossRef] [PubMed]
3. McCullough, M.L.; Peterson, J.J.; Patel, R.; Jacques, P.F.; Shah, R.; Dwyer, J.T. Flavonoid intake and cardiovascular disease mortality in a prospective cohort of US adults. *Am. J. Clin. Nutr.* **2012**, *95*, 454–464. [CrossRef] [PubMed]
4. Cassidy, A.; Mukamal, K.J.; Liu, L.; Franz, M.; Eliassen, A.H.; Rimm, E.B. High anthocyanin intake is associated with a reduced risk of myocardial infarction in young and middle-aged women. *Circulation* **2013**, *127*, 188–196. [CrossRef] [PubMed]
5. Jennings, A.; Welch, A.A.; Fairweather-Tait, S.J.; Kay, C.; minihane, A.-M.; Chowienczyk, P.; Jiang, B.; Cecelja, M.; Spector, T.; Macgregor, A.; et al. Higher anthocyanin intake is associated with lower arterial stiffness and central blood pressure in women. *Am. J. Clin. Nutr.* **2012**, *96*, 781–788. [CrossRef] [PubMed]
6. Krga, I.; Milenkovic, D. Anthocyanins: From Sources and Bioavailability to Cardiovascular-Health Benefits and Molecular Mechanisms of Action. *J. Agric. Food Chem.* **2019**, *67*, 1771–1783. [CrossRef] [PubMed]
7. Mattioli, R.; Francioso, A.; Mosca, L.; Silva, P. Anthocyanins: A Comprehensive Review of Their Chemical Properties and Health Effects on Cardiovascular and Neurodegenerative Diseases. *Molecules* **2020**, *25*, 3809. [CrossRef] [PubMed]
8. Zamora-Ros, R.; Knaze, V.; Luján-Barroso, L.; Slimani, N.; Romieu, I.; Touillaud, M.; Kaaks, R.; Teucher, B.; Mattiello, A.; Grioni, S.; et al. Estimation of the intake of anthocyanidins and their food sources in the European Prospective Investigation into Cancer and Nutrition (EPIC) study. *Br. J. Nutr.* **2011**, *106*, 1090–1099. [CrossRef] [PubMed]
9. Prior, R.L.; Wu, X. Anthocyanins: Structural characteristics that result in unique metabolic patterns and biological activities. *Free Radic. Res.* **2006**, *40*, 1014–1028. [CrossRef] [PubMed]
10. Kay, C.D.; Pereira-Caro, G.; Ludwig, I.A.; Clifford, M.N.; Crozier, A. Anthocyanins and Flavanones Are More Bioavailable than Previously Perceived: A Review of Recent Evidence. *Annu. Rev. Food Sci. Technol.* **2017**, *8*, 155–180. [CrossRef] [PubMed]

11. Eker, M.E.; Aaby, K.; Budic-Leto, I.; Brnčić, S.R.; El, S.N.; Karakaya, S.; Simsek, S.; Manach, C.; Wiczkowski, W.; Pascual-Teresa, S.d. A Review of Factors Affecting Anthocyanin Bioavailability: Possible Implications for the Inter-Individual Variability. *Foods* **2019**, *9*, 2. [CrossRef] [PubMed]
12. Jokioja, J.; Yang, B.; Linderborg, K.M. Acylated anthocyanins: A review on their bioavailability and effects on postprandial carbohydrate metabolism and inflammation. *Compr. Rev. Food Sci. Food Saf.* **2021**, *20*, 5570–5615. [CrossRef] [PubMed]
13. Kay, C.D.; Kroon, P.A.; Cassidy, A. The bioactivity of dietary anthocyanins is likely to be mediated by their degradation products. *Mol. Nutr. Food Res.* **2009**, *53* (Suppl. S1), S92–S101. [CrossRef] [PubMed]
14. Mueller, D.; Jung, K.; Winter, M.; Rogoll, D.; Melcher, R.; Richling, E. Human intervention study to investigate the intestinal accessibility and bioavailability of anthocyanins from bilberries. *Food Chem.* **2017**, *231*, 275–286. [CrossRef] [PubMed]
15. de Ferrars, R.M.; Czank, C.; Zhang, Q.; Botting, N.P.; Kroon, P.A.; Cassidy, A.; Kay, C.D. The pharmacokinetics of anthocyanins and their metabolites in humans. *Br. J. Pharmacol.* **2014**, *171*, 3268–3282. [CrossRef] [PubMed]
16. de Ferrars, R.M.; Cassidy, A.; Curtis, P.; Kay, C.D. Phenolic metabolites of anthocyanins following a dietary intervention study in post-menopausal women. *Mol. Nutr. Food Res.* **2014**, *58*, 490–502. [CrossRef] [PubMed]
17. Mostafa, H.; Behrendt, I.; Meroño, T.; González-Domínguez, R.; Fasshauer, M.; Rudloff, S.; Andres-Lacueva, C.; Kuntz, S. Plasma anthocyanins and their metabolites reduce in vitro migration of pancreatic cancer cells, PANC-1, in a FAK- and NF-kB dependent manner: Results from the ATTACH-study a randomized, controlled, crossover trial in healthy subjects. *Biomed. Pharmacother.* **2023**, *158*, 114076. [CrossRef] [PubMed]
18. Cassidy, A. Berry anthocyanin intake and cardiovascular health. *Mol. Aspects Med.* **2018**, *61*, 76–82. [CrossRef] [PubMed]
19. Gritsenko, A.; Yu, S.; Martin-Sanchez, F.; Diaz-Del-Olmo, I.; Nichols, E.-M.; Davis, D.M.; Brough, D.; Lopez-Castejon, G. Priming Is Dispensable for NLRP3 Inflammasome Activation in Human Monocytes In Vitro. *Front. Immunol.* **2020**, *11*, 565924. [CrossRef] [PubMed]
20. Groslambert, M.; Py, B.F. Spotlight on the NLRP3 inflammasome pathway. *J. Inflamm. Res.* **2018**, *11*, 359–374. [CrossRef] [PubMed]
21. Guo, H.; Callaway, J.B.; Ting, J.P.-Y. Inflammasomes: Mechanism of action, role in disease, and therapeutics. *Nat. Med.* **2015**, *21*, 677–687. [CrossRef] [PubMed]
22. Zito, G.; Buscetta, M.; Cimino, M.; Dino, P.; Bucchieri, F.; Cipollina, C. Cellular Models and Assays to Study NLRP3 Inflammasome Biology. *Int. J. Mol. Sci.* **2020**, *21*, 4294. [CrossRef] [PubMed]
23. Zhu, C.-W.; Lü, H.; Du, L.-L.; Li, J.; Chen, H.; Zhao, H.-F.; Wu, W.-L.; Chen, J.; Li, W.-L. Five blueberry anthocyanins and their antioxidant, hypoglycemic, and hypolipidemic effects in vitro. *Front. Nutr.* **2023**, *10*, 1172982. [CrossRef] [PubMed]
24. Gonçalves, A.C.; Nunes, A.R.; Falcão, A.; Alves, G.; Silva, L.R. Dietary Effects of Anthocyanins in Human Health: A Comprehensive Review. *Pharmaceuticals* **2021**, *14*, 690. [CrossRef] [PubMed]
25. Wang, B.; Tang, X.; Mao, B.; Zhang, Q.; Tian, F.; Zhao, J.; Chen, W.; Cui, S. Effects of in vitro fecal fermentation on the metabolism and antioxidant properties of cyanidin-3-O-glucoside. *Food Chem.* **2024**, *431*, 137132. [CrossRef] [PubMed]
26. Fan, H.; Cui, J.; Liu, F.; Zhang, W.; Yang, H.; He, N.; Dong, Z.; Dong, J. Malvidin protects against lipopolysaccharide-induced acute liver injury in mice via regulating Nrf2 and NLRP3 pathways and suppressing apoptosis and autophagy. *Eur. J. Pharmacol.* **2022**, *933*, 175252. [CrossRef] [PubMed]
27. Fan, H.; Sun, Y.; Zhang, X.; Xu, Y.; ming, Y.; Zhang, L.; Zhao, P. Malvidin promotes PGC-1α/Nrf2 signaling to attenuate the inflammatory response and restore mitochondrial activity in septic acute kidney injury. *Chem. Biol. Interact.* **2024**, *388*, 110850. [CrossRef] [PubMed]
28. Behrendt, I.; Röder, I.; Will, F.; Mostafa, H.; Gonzalez-Dominguez, R.; Meroño, T.; Andres-Lacueva, C.; Fasshauer, M.; Rudloff, S.; Kuntz, S. Influence of Plasma-Isolated Anthocyanins and Their Metabolites on Cancer Cell Migration (HT-29 and Caco-2) In Vitro: Results of the ATTACH Study. *Antioxidants* **2022**, *11*, 1341. [CrossRef]
29. Wittmann, N.; Behrendt, A.-K.; Mishra, N.; Bossaller, L.; Meyer-Bahlburg, A. Instructions for Flow Cytometric Detection of ASC Specks as a Readout of Inflammasome Activation in Human Blood. *Cells* **2021**, *10*, 2880. [CrossRef] [PubMed]
30. Chanput, W.; Mes, J.J.; Wichers, H.J. THP-1 cell line: An in vitro cell model for immune modulation approach. *Int. Immunopharmacol.* **2014**, *23*, 37–45. [CrossRef] [PubMed]
31. Sester, D.P.; Thygesen, S.J.; Sagulenko, V.; Vajjhala, P.R.; Cridland, J.A.; Vitak, N.; Chen, K.W.; Osborne, G.W.; Schroder, K.; Stacey, K.J. A novel flow cytometric method to assess inflammasome formation. *J. Immunol.* **2015**, *194*, 455–462. [CrossRef] [PubMed]
32. Jo, E.-K.; Kim, J.K.; Shin, D.-M.; Sasakawa, C. Molecular mechanisms regulating NLRP3 inflammasome activation. *Cell. Mol. Immunol.* **2016**, *13*, 148–159. [CrossRef] [PubMed]
33. Hamilton, C.; Anand, P.K. Right place, right time: Localisation and assembly of the NLRP3 inflammasome. *F1000Research* **2019**, *8*, 676. [CrossRef] [PubMed]
34. O'Brien, M.; Moehring, D.; Muñoz-Planillo, R.; Núñez, G.; Callaway, J.; Ting, J.; Scurria, M.; Ugo, T.; Bernad, L.; Cali, J.; et al. A bioluminescent caspase-1 activity assay rapidly monitors inflammasome activation in cells. *J. Immunol. Methods* **2017**, *447*, 1–13. [CrossRef] [PubMed]
35. Zheng, D.; Liwinski, T.; Elinav, E. Inflammasome activation and regulation: Toward a better understanding of complex mechanisms. *Cell Discov.* **2020**, *6*, 36. [CrossRef] [PubMed]
36. Awad, F.; Assrawi, E.; Jumeau, C.; Georgin-Lavialle, S.; Cobret, L.; Duquesnoy, P.; Piterboth, W.; Thomas, L.; Stankovic-Stojanovic, K.; Louvrier, C.; et al. Impact of human monocyte and macrophage polarization on NLR expression and NLRP3 inflammasome activation. *PLoS ONE* **2017**, *12*, e0175336. [CrossRef] [PubMed]

37. Deepa, P.; Hong, M.; Sowndhararajan, K.; Kim, S. A Review of the Role of an Anthocyanin, Cyanidin-3-O-β-glucoside in Obesity-Related Complications. *Plants* **2023**, *12*, 3889. [CrossRef] [PubMed]
38. Wang, H.; Guo, X.; Liu, J.; Li, T.; Fu, X.; Liu, R.H. Comparative suppression of NLRP3 inflammasome activation with LPS-induced inflammation by blueberry extracts (*Vaccinium* spp.). *RSC Adv.* **2017**, *7*, 28931–28939. [CrossRef]
39. Stevenson, D.; Scalzo, J. Anthocyanin composition and content of blueberries from around the world. *J. Berry Res.* **2012**, *2*, 179–189. [CrossRef]
40. Zhao, P.; Li, X.; Yang, Q.; Lu, Y.; Wang, G.; Yang, H.; Dong, J.; Zhang, H. Malvidin alleviates mitochondrial dysfunction and ROS accumulation through activating AMPK-α/UCP2 axis, thereby resisting inflammation and apoptosis in SAE mice. *Front. Pharmacol.* **2022**, *13*, 1038802. [CrossRef] [PubMed]
41. Wang, G.; Ma, F.; Zhang, W.; Xin, Y.; Ping, K.; Wang, Y.; Dong, J. Malvidin alleviates LPS-induced septic intestinal injury through the nuclear factor erythroid 2-related factor 2/reactive oxygen species/NLRP3 inflammasome pathway. *Inflammopharmacology* **2023**, *32*, 893–901. [CrossRef] [PubMed]
42. Zhu, X.; Lin, X.; Zhang, P.; Liu, Y.; Ling, W.; Guo, H. Upregulated NLRP3 inflammasome activation is attenuated by anthocyanins in patients with nonalcoholic fatty liver disease: A case-control and an intervention study. *Clin. Res. Hepatol. Gastroenterol.* **2022**, *46*, 101843. [CrossRef] [PubMed]
43. Grebe, A.; Hoss, F.; Latz, E. NLRP3 Inflammasome and the IL-1 Pathway in Atherosclerosis. *Circ. Res.* **2018**, *122*, 1722–1740. [CrossRef] [PubMed]
44. Zhang, X.; Hu, L.; Xu, S.; Ye, C.; Chen, A. Erianin: A Direct NLRP3 Inhibitor With Remarkable Anti-Inflammatory Activity. *Front. Immunol.* **2021**, *12*, 739953. [CrossRef] [PubMed]
45. Shi, Y.-S.; Li, X.-X.; Li, H.-T.; Zhang, Y. Pelargonidin ameliorates CCl4-induced liver fibrosis by suppressing the ROS-NLRP3-IL-1β axis via activating the Nrf2 pathway. *Food Funct.* **2020**, *11*, 5156–5165. [CrossRef] [PubMed]
46. Molagoda, I.M.N.; Lee, K.T.; Choi, Y.H.; Jayasingha, J.A.C.C.; Kim, G.-Y. Anthocyanins from Hibiscus syriacus L. Inhibit NLRP3 Inflammasome in BV2 Microglia Cells by Alleviating NF-κB- and ER Stress-Induced Ca^{2+} Accumulation and Mitochondrial ROS Production. *Oxid. Med. Cell. Longev.* **2021**, *2021*, 1246491. [CrossRef] [PubMed]
47. Zhu, M.-J.; Kang, Y.; Xue, Y.; Liang, X.; García, M.P.G.; Rodgers, D.; Kagel, D.R.; Du, M. Red raspberries suppress NLRP3 inflammasome and attenuate metabolic abnormalities in diet-induced obese mice. *J. Nutr. Biochem.* **2018**, *53*, 96–103. [CrossRef] [PubMed]
48. Di Gesso, J.L.; Kerr, J.S.; Zhang, Q.; Raheem, S.; Yalamanchili, S.K.; O'Hagan, D.; Kay, C.D.; O'Connell, M.A. Flavonoid metabolites reduce tumor necrosis factor-α secretion to a greater extent than their precursor compounds in human THP-1 monocytes. *Mol. Nutr. Food Res.* **2015**, *59*, 1143–1154. [CrossRef] [PubMed]

4. Diskussion

4.1 Einfluss von Anthocyanen und ihrer Metabolite auf die Migration kanzerogener Zellen

Laut statistischem Bundesamt stellen Tumorerkrankungen die zweithäufigste Todesursache in Deutschland dar (Statistisches Bundesamt 2024). Vor dem Hintergrund, dass mehr als 90 % aller tumorbedingten Sterbefälle auf Metastasen zurückzuführen sind, stellt die Inhibierung der Metastasierung einen wichtigen therapeutischen Ansatzpunkt dar. Daher wurde, im **ersten Teil** der vorliegenden Dissertation, der Einfluss physiologischer Anthocyan- und Metabolit-Konzentrationen auf das Migrationspotenzial kanzerogener Zellen untersucht.

Um zu untersuchen, inwiefern Anthocyane und ihre Metabolite die Migration kanzerogener Zellen beeinflussen, wurde im Vorfeld, am Institut für Ernährungswissenschaft der Justus-Liebig-Universität Gießen, eine randomisierte, Placebo-kontrollierte *Cross-over*-Interventionsstudie durchgeführt, im Rahmen derer 35 junge, gesunde Probanden (Alter: 24,4 ± 2,3 Jahre; BMI: 21,7 ± 2,6 kg/m²), über einen Zeitraum von 4 Wochen, täglich 330 mL eines Anthocyan-reichen Trauben-/Heidelbeersafts (942 mg/L als Cyanidin-3-Glukosid-Äquivalente, 2622 mg/L Gesamtphenole) bzw. 330 mL eines Anthocyan-reduzierten Placebosafts (6 mg/L als Cyanidin-3-Glukosid-Äquivalente, 115 mg/L Gesamtphenole) zu sich nahmen. Sowohl vor als auch nach der jeweiligen Intervention wurden Blutproben genommen und die Anthocyane sowie deren Metabolite mittels Festphasenextraktion aus dem Plasma isoliert, um deren Einfluss auf die Migration kanzerogener Zellen *in vitro* zu untersuchen. Dies ermöglichte es, die *in vivo* stattfindende Absorption, Verteilung, Metabolisierung und Ausscheidung (Bioverfügbarkeit) der Anthocyane in den *in vitro*-Funktionsstudien zu berücksichtigen. Eine detaillierte Beschreibung des Studiendesigns ist in Behrendt et al. (2022) dargestellt. Die Ergebnisse der ATTACH-Studie (Anthocyanins Target Tumor cell Adhesion - Cancer vs. Endothelial Cell (HUVEC) interactions) zeigen, dass die nach 4-wöchiger Intervention mit einem Anthocyan-reichen Trauben-/Heidelbeersaft aus dem Plasma gesunder Probanden isolierten Anthocyane sowie deren Metabolite, in physiologischen Konzentrationen, *in vitro* die Migration von Kolonkarzinom- und Pankreaskarzinomzellen (HT-29 und PANC-1) hemmen (Behrendt et al. 2022; Mostafa et al. 2023). Dabei gingen die für PANC-1 beobachteten, anti-migratorischen Effekten mit einer verminderten ICAM-1 sowie Integrin-β1 Expression auf den Pankreaskarzinomzellen einher (Mostafa et al. 2023). In diesem Zusammenhang konnte bereits gezeigt werden, dass Veränderungen der Integrin Expression das invasive und migratorische Potenzial der Tumorzellen beeinflussen (Cooper und Giancotti

2019). Insbesondere Integrin-β1 scheint sowohl *in vitro* als auch *in vivo* eine wichtige Rolle für die Progression und Metastasierung von Tumoren zu spielen. So konnte bereits für verschiedene Tumorarten gezeigt werden, dass die Expression von Integrin-β1 mit der Bildung von Metastasen sowie einer schlechteren klinischen Prognose assoziiert ist (Pan et al. 2018). Zudem kann *in vitro* die Adhäsion und Migration von Pankreaskarzinomzellen durch *Knockdown* von Integrin-β1 gehemmt werden. Darüber hinaus konnte im Tiermodell gezeigt werden, dass durch *Knockdown* von Integrin-β1 sowohl das Wachstum des Primärtumors um 50 % reduziert als auch die spontane Metastasierung der Pankreaskarzinomzellen vollständig gehemmt wird (Grzesiak et al. 2011). Allerdings muss an dieser Stelle offenbleiben, ob die Expression von Zelladhäsionsmolekülen auf Kolonkarzinomzellen in ähnlicher Weise durch aus dem Plasma isolierte Anthocyane sowie deren Metabolite beeinflusst wird. In diesem Zusammenhang konnten Yun et al. (2010) jedoch bereits zeigen, dass das invasive Potenzial von Kolonkarzinomzellen (HT-29) durch Applikation eines, aus Trauben (*Vitis coignetiae Pulliat*) hergestellten, Anthocyan-haltigen Extrakts gehemmt wird, was mit einer verminderten ICAM-1 Expression einherging. Zudem konnte beobachtet werden, dass Delphinidin die Invasion und Migration von Kolonkarzinomzellen hemmt, indem es die Expression von Integrin-αV/β3 sowie die Aktivierung des FAK-SFK-Signalwegs inhibiert (Huang et al. 2019).

Neben der Integrin-Liganden-Interaktion wird die Tumorzelladhäsion und -migration auch durch Zytokine (IL-1β, TNF-α) und Wachstumsfaktoren (VEGF, *vascular endothelial growth factor*), die von den Tumorzellen sekretiert werden, beeinflusst. Diese können sowohl autokrin auf die Tumorzellen selbst wie auch parakrin auf die Endothelzellen wirken. So zeigen die Ergebnisse der vorliegenden Arbeit, dass die basale Expression von Integrin-β4 und ICAM-1 auf humanen Endothelzellen durch Inkubation mit einem CytoMix aus TNF-α, IL-1β und VEGF stimuliert wird. Dabei wurde die Zytokin- und Wachstumsfaktor-induzierte ICAM-1 Expression auf den Endothelzellen durch aus dem Plasma isolierte Anthocyane sowie deren Metabolite signifikant gehemmt (Mostafa et al. 2023). Dies könnte wiederum die Adhäsion der Tumorzellen an das Endothel wie auch die transendotheliale **Migration** beeinflussen. Zudem zeigen die Ergebnisse der vorliegenden Arbeit, dass aus dem Plasma isolierte Anthocyane sowie deren Metabolite die Aktivierung des NFκB- sowie die Aktivierung des FAK-SFK-Signalwegs, sowohl in PANC-1 als auch in CytoMix-stimulierten HUVECs, hemmen (Mostafa et al. 2023). In diesem Zusammenhang konnte bereits gezeigt werden, dass durch Applikation eines FAK Inhibitors die Integrin-β1 Expression auf Kolonkarzinomzellen (HCT116 und SW480) gehemmt wird (Buhrmann et al. 2017). Zudem wird durch die Aktivierung des FAK-SFK-Signalwegs die Stabilität endothelialer Zell-Zell-Kontakte herabgesetzt, wodurch die

transendotheliale Migration der Tumorzellen erleichtert wird (Reymond et al. 2013; Sulzmaier et al. 2014). Somit könnte die Inhibierung dieser Signalwege für die verminderte Expression der Zelladhäsionsmoleküle auf den Endothel- und Tumorzellen sowie die beobachteten anti-migratorischen Effekte verantwortlich sein.

Die Behandlung mit Chemotherapeutika stellt eine wichtige Säule der Tumortherapie dar. Insbesondere 5-FU ist eines der am häufigsten eingesetzten und effektivsten Chemotherapeutika bei der Behandlung des kolorektalen Karzinoms (Wang et al. 2021). Zudem wird 5-FU auch im Rahmen konventioneller Behandlungsregime bei Pankreaskarzinomen eingesetzt (Leitlinienprogramm Onkologie 2021). Präklinische *in vitro*- und *in vivo*-Studien zeigen, dass Polyphenole die Wirksamkeit von Chemotherapeutika steigern können, wobei hierbei vor allem der Einfluss auf wachstumsassoziierte Parameter untersucht wurde (Fantini et al. 2015). Allerdings gibt es bisher nur wenige Studien, in denen potenzielle Wechselwirkungen zwischen Anthocyanen und klassischen Chemotherapeutika untersucht wurden. Li et al. (2021a) konnten in diesem Zusammenhang zeigen, dass die anti-proliferativen sowie anti-migratorischen Effekte von 5-FU und Celecoxib durch Brombeer-Anthocyane gesteigert werden. Zudem zeigen die Ergebnisse der vorliegenden Arbeit, dass durch die Behandlung mit 5-FU die Migration von HT-29 Zellen dosisabhängig gehemmt wird. Darüber hinaus führte die Koinkubation mit 5-FU und aus dem Plasma isolierter Anthocyane sowie deren Metabolite zu einer stärkeren Hemmung der Migration von HT-29 Zellen als die alleinige Behandlung mit 5-FU (Behrendt et al. 2022). Dabei sind die beobachteten anti-migratorischen Effekte möglicherweise auf eine Hemmung des FAK-SFK-Signalwegs zurückzuführen. In diesem Zusammenhang konnte bereits gezeigt werden, dass das Camptothecin-Analogon Irinotecan die Migration von LM-8 Zellen hemmt, indem es die Autophosphorylierung der FAK an Y397 reduziert (Yui et al. 2010). Somit könnten aus dem Plasma isolierte Anthocyane sowie deren Metabolite möglicherweise die anti-migratorische Wirkung von 5-FU potenzieren, indem sie – wie im Rahmen dieser Arbeit bereits für PANC-1 Zellen gezeigt werden konnte – die Phosphorylierung der FAK inhibieren. Allerdings muss an dieser Stelle offenbleiben über welche molekularen Mechanismen Anthocyane und ihre Metabolite die anti-migratorische Wirkung von 5-FU beeinflussen. Zudem ist unklar, inwiefern aus dem Plasma isolierte Anthocyane und deren Metabolite die Wirkung anderer Chemotherapeutika, sowie Kombinationen dieser, ebenfalls beeinflussen.

Obwohl 5-FU eines der effektivsten Chemotherapeutika bei der Behandlung des kolorektalen Karzinoms darstellt (Wang et al. 2021), wird dessen Wirksamkeit häufig durch die Entwicklung

von Chemoresistenzen beeinträchtigt (Vodenkova et al. 2020). In diesem Zusammenhang scheint die gesteigerte Aktivierung des NFκB-Signalwegs, insbesondere die Aktivierung der p65 Untereinheit, eine wichtige Rolle zu spielen (Fantini et al. 2015; Vodenkova et al. 2020). So wirkt die Inhibierung des NFκB-Signalwegs der Entwicklung von Chemoresistenzen effektiv entgegen (Vodenkova et al. 2020). Interessanterweise konnte ebenfalls gezeigt werden, dass durch die Hemmung von VCAM-1 und Integrin-β1 die Chemosensitivität von Tumorzellen gesteigert wird (Läubli und Borsig 2019). Die Ergebnisse der vorliegenden Arbeit zeigen, dass aus dem Plasma isolierte Anthocyane sowie deren Metabolite, sowohl die Aktivierung des NFκB-Signalwegs als auch die Integrin-β1 Expression der Pankreaskarzinomzellen hemmen (Mostafa et al. 2023). Somit könnten Anthocyane und ihre Metabolite möglicherweise nicht nur die Migration von Tumorzellen hemmen, sondern auch deren Chemosensitivität steigern.

Um zu untersuchen, welche Anthocyane und Metabolite für die beobachteten anti-migratorischen Effekte verantwortlich sind, wurde in der Arbeitsgruppe von Prof. Dr. Cristina Andrés-Lacueva (Biomarkers & Nutrimetabolomic Research Group, Nutrition & Food Science Department, University of Barcelona, Spanien) eine Metabolom-Analyse der Plasma- und Urinproben durchgeführt. Insgesamt konnten 902 Metabolite nachgewiesen werden, von denen 14 signifikant mit der Aufnahme des Anthocyan-reichen Trauben-/Heidelbeersafts assoziiert waren. Interessanterweise nahm dabei im Plasma die Konzentration mikrobieller Metabolite wie **2,4,6-Trihydroxybenzaldehyd**, Methoxyphenyl-γ-Valerolacton-Glucuronid und 3′,4′-Dihydroxyphenyl-γ-Valerolacton signifikant zu, nicht aber die Konzentration nativer Anthocyane (Mostafa et al. 2023). Ein Grund hierfür könnte sein, dass Anthocyane schnell aus dem systemischen Kreislauf eliminiert werden und eine deutlich kürzere Plasmahalbwertszeit aufweisen als ihre niedermolekularen, phenolischen Metabolite (Kay et al. 2017). Interventionsstudien zeigen, dass bereits 0,5 bis 2 Stunden nach der oralen Aufnahme von Anthocyanen maximale Plasmakonzentrationen dieser erreicht werden (Prior und Wu 2006). Hierbei ist jedoch anzumerken, dass die im Rahmen der ATTACH-Studie gewonnen Blutproben durchschnittlich 6 Stunden nach der letzten Saftaufnahme gewonnen wurden, so dass möglicherweise – aufgrund der beschriebenen Pharmakokinetik – zu diesem Zeitpunkt bereits kaum noch native Anthocyane im Plasma nachweisbar waren.

Sowohl für 2,4,6-Trihydroxybenzaldehyd als auch für γ-Valerolactone konnten bereits anti-kanzerogene Effekte gezeigt werden (Forester und Waterhouse 2010; Rubert et al. 2022; Grimm et al. 2004). Zudem ist 3′,4′-Dihydroxyphenyl-γ-Valerolacton in der Lage die Adhäsion

von THP-1 Zellen an TNF-α stimulierte humane Endothelzellen (*human umbilical vein endothelial cells*, HUVECs) zu reduzieren, indem es die VCAM-1 Expression auf den Endothelzellen hemmt (Lee et al. 2017). Im Gegensatz dazu war in der vorliegenden Arbeit keiner der Plasmametabolite mit den beobachteten anti-migratorischen Effekten assoziiert. Allerdings stellt die Bestimmung von Anthocyanen und ihrer Metabolite im Plasma nur eine Momentaufnahme dar, während die Bestimmung im 24-h Urin die Absorption der Anthocyane quantitativ besser widerspiegelt (Kalt et al. 2020). Dies könnte erklären, warum die in den *in vitro*-Studien beobachteten anti-migratorischen Effekte zwar mit der Ausscheidung von Anthocyanen und ihrer Metabolite im Urin, nicht aber mit den im Plasma zirkulierenden Metaboliten assoziiert waren (Mostafa et al. 2023).

Die für die Herstellung des Interventionssafts verwendete Rebsorte *Accent* weist im Vergleich zu anderen Rebsorten einen besonders hohen Anthocyan-Gehalt auf (Fröhling et al. 2012). Zudem machen Anthocyane bis zu 60 % der in reifen Heidelbeeren enthaltenen Polyphenole aus (Kalt et al. 2020). Allerdings kann trotz des randomisierten, Placebo-kontrollierten Studiendesigns, nicht vollständig ausgeschlossen werden, dass die in der vorliegenden Arbeit beobachteten Effekte, zumindest teilweise, auch auf andere im Trauben-/Heidelbeersaft enthaltende phenolische Verbindungen zurückzuführen sein könnten.

Darüber hinaus konnten wir in den *in vitro*-Funktionsstudien Probanden-abhängige Effekte beobachten, die sowohl auf Unterschiede in der Absorption, Verteilung, Metabolisierung und Ausscheidung (Bioverfügbarkeit) der Anthocyane als auch auf Unterschiede in der Zusammensetzung der intestinalen Mikrobiota zurückzuführen sein könnten (Eker et al. 2019). In diesem Zusammenhang ist anzumerken, dass die in den Funktionsstudien verwendeten Anthocyane sowie deren Metabolite aus dem Plasma gesunder Probanden isoliert wurden. Allerdings kann bei Patienten mit kolorektalen Karzinom häufig eine Zunahme pathogener Bakterienspezies im Gastrointestinaltrakt beobachtet werden (Dysbiose). Zudem scheint diese Dysbiose zur Pathogenese und Progression des kolorektalen Karzinoms beizutragen (Wong und Yu 2023). Des Weiteren wirkt sich die Einnahme von Chemotherapeutika ebenfalls stark auf die Zusammensetzung der intestinalen Mikrobiota (Roggiani et al. 2023) und somit auch auf die Metabolisierung der Anthocyane aus. Daher sollte in zukünftigen Studien untersucht werden, inwiefern die Metabolisierung sowie die Bioverfügbarkeit von Anthocyanen durch die Einnahme von Chemotherapeutika beeinflusst wird.

4.2 Einfluss von Anthocyanen und ihrer Metabolite auf die Aktivierung des NLRP3 Inflammasoms

Vor dem Hintergrund, dass die übermäßige Aktivierung des NLRP3 Inflammasoms zur Entstehung der LGI beiträgt, stellt die Inhibierung dieses inflammatorischen Prozesses einen wichtigen präventiven Ansatzpunkt dar, um der LGI und somit der Entstehung inflammatorischer Erkrankungen – insbesondere kardiovaskulärer Erkrankungen – in einem sehr frühen *sub*-klinischen Stadium präventiv entgegenzuwirken. Daher wurde, im **zweiten Teil** der vorliegenden Dissertation, der Einfluss von Anthocyanen und ihrer Metabolite auf die Aktivierung des NLRP3 Inflammasoms in humanen Monozyten untersucht.

Zu diesem Zweck wurde zunächst ein *in vitro*-Modell etabliert, um die Formierung des NLRP3 Inflammasoms in THP-1 Monozyten zu induzieren. Hierzu wurden die Zellen mit LPS stimuliert (*Priming*) und/oder die Aktivierung des NLRP3 Inflammasoms mit Nigericin induziert. Während unter basalen Bedingungen das Adaptormolekül ASC diffus im Zytosol verteilt ist, kommt es nach Aktivierung des NLRP3 Inflammasoms zur Formierung eines einzelnen, makromolekularen ASC Specks. Die Kondensation der ASC-Proteine führt zur Abnahme der ASC Fluoreszenz Pulsweite, so dass sich ASC Speck-positive und -negative Zellen mittels **TOFIE** (*time of flight inflammasome evaluation*) durchflusszytometrisch als zwei getrennte Populationen darstellen lassen (Sester et al. 2015). Daher wurde diese leistungsstarke Methode in der vorliegenden Arbeit genutzt, um die Aktivierung des NLRP3 Inflammasoms auf Einzelzellniveau nachzuweisen. Dabei konnte die Bildung von ASC Specks nach Aktivierung des NLRP3 Inflammasoms, sowohl mit als auch ohne vorheriges *Priming*, in THP-1 Monozyten **durchflusszytometrisch** nachgewiesen werden. Zudem konnte ein signifikanter Anstieg der Caspase-1-Aktivität sowie eine gesteigerte Sekretion inflammatorischer Zytokine (IL-1β und IL-18) in den Zellkulturüberstand beobachtet werden (Behrendt et al. 2024).

Nach erfolgreicher Validierung dieses *in vitro*-Modells, wurde zunächst der Einfluss nativer Anthocyane auf die Aktivierung des NLRP3 Inflammasoms untersucht. Dazu wurden monozytäre THP-1 Zellen mit verschiedenen Konzentrationen eines Anthocyan-reichen Trauben-/Heidelbeerextrakts, welcher aus dem Interventionssaft der ATTACH-Studie hergestellt wurde, präinkubiert, bevor das NLRP3 Inflammasom mit LPS und/oder Nigericin *in vitro* aktiviert wurde. Hierbei zeigte sich, dass die Aktivierung des NLRP3 Inflammasoms in THP-1 Monozyten durch Präinkubation mit dem Anthocyan-reichen Trauben-/Heidelbeerextrakt gehemmt wird. Dabei war die verminderte IL-1β und IL-18 Sekretion vor

allem auf die signifikante Hemmung der Caspase-1-Aktivität zurückzuführen (Behrendt et al. 2024). Allerdings ist anzumerken, dass der in den *in vitro*-Studien eingesetzte Anthocyan-reiche Trauben-/Heidelbeerextrakt nicht nur Anthocyane, sondern auch weitere phenolische Verbindungen enthielt. Zudem sind Anthocyane bei den in der Zellkultur herrschenden Bedingungen sehr instabil (Zhang et al. 2019), so dass die beobachteten anti-inflammatorischen Effekte möglicherweise nicht nur auf die in dem Extrakt enthaltenen Anthocyane, sondern zumindest teilweise auch auf andere phenolische Verbindungen sowie Degradationsprodukte zurückzuführen sein könnten. Außerdem ist bekannt, dass nur etwa 1-2 % der über die Nahrung aufgenommenen Anthocyane unverändert in den systemischen Kreislauf gelangen, da diese sowohl durch körpereigene als auch durch Enzyme der intestinalen Mikrobiota intensiv metabolisiert werden (Eker et al. 2019). Dabei entstehen zahlreiche phenolische Metabolite, die wahrscheinlich in einem höheren Ausmaß zur biologischen Wirksamkeit der Anthocyane beitragen als die nativen Verbindungen selbst (Kay et al. 2017). Daher sollte in der vorliegenden Arbeit ebenfalls der Einfluss von 2,4,6-Trihydroxybenzaldehyd und Homovanillinalkohol auf das NLRP3 Inflammasom untersucht werden, da der Anstieg dieser phenolischen Metabolite im Plasma bzw. Fäzes, im Rahmen der ATTACH-Studie, signifikant mit der Aufnahme des Anthocyan-reichen Trauben-/Heidelbeersafts assoziiert war (Mostafa et al. 2023, nicht publizierte Daten der ATTACH-Studie). Dabei zeigte sich, dass insbesondere durch Präinkubation mit dem Plasmametaboliten 2,4,6-Trihydroxybenzaldehyd die Aktivierung des NLRP3 Inflammasoms und somit die Sekretion der pro-inflammatorischen Zytokine IL-1β und Il-18 signifikant gehemmt wird (Behrendt et al. 2024). Allerdings ist anzumerken, dass in den *in vitro*-Studien zum Teil hohe pharmakologische Konzentrationen von bis zu 50 µM eingesetzt wurden (Behrendt et al. 2024). Im Gegensatz dazu wurden in humanen Interventionsstudien, nach Bolusgabe von 500 mg ^{13}C-markiertem Cyanidin-3-Glukosid bzw. 10 g Heidelbeerextrakt (entspricht 2,4 g Anthocyanen), für 2,4,6-Trihydroxybenzaldehyd maximale Plasmakonzentrationen von 103 bis 582 nM beobachtet (Ferrars et al. 2014a; Ferrars et al. 2014b). Allerdings scheinen *in vivo* potenzielle additive und/oder synergistische Effekte die Wirksamkeit physiologischer Anthocyan- und Metabolit-Konzentrationen zu verstärken. In diesem Zusammenhang konnte bereits gezeigt werden, dass verschiedene Flavonoid-Metabolite, sowohl einzeln als auch in Kombination, eine höhere biologische Wirksamkeit aufweisen, als die nativen Verbindungen (Di Gesso et al. 2015).

THP-1-Zellen stellen ein weit verbreitetes *in vitro*-Modell dar, um die Aktivierung des NLRP3-Inflammasoms zu untersuchen. Allerdings wurden in den bisherigen Studien hauptsächlich differenzierte THP-1 Makrophagen untersucht (Zito et al. 2020). Während die Aktivierung des

NLRP3 Inflammasoms in Makrophagen einen zweistufigen Prozess darstellt, konnte kürzlich gezeigt werden, dass der *Priming*-Schritt für die Aktivierung des NLRP3 Inflammasoms in humanen Monozyten ($CD14^{++}$, THP-1 Monozyten) nicht zwingend erforderlich ist (Gritsenko et al. 2020; Wittmann et al. 2021). Diese Ergebnisse konnten in der vorliegenden Arbeit für THP-1 Monozyten bestätigt werden. Somit scheinen THP-1 Monozyten ein geeignetes *in vitro*-Modell darzustellen, um die Aktivierung des NLRP3 Inflammasoms in humanen Monozyten zu untersuchen. Jedoch ist anzumerken, dass es sich bei THP-1 Monozyten um kanzerogene Zellen handelt, so dass die Ergebnisse der vorliegenden Arbeit möglicherweise nicht vollständig auf primäre, humane Monozyten übertragbar sind. So wird durch die Bindung von LPS an den TLR-4 die Aktivierung des NFκB-Signalwegs induziert, infolge dessen die Transkription von NLRP3 Inflammasom-Komponenten gesteigert wird (Zito et al. 2020; Zheng et al. 2020). Allerdings ist bekannt, dass primäre Monozyten im Vergleich zu THP-1 Monozyten stärker auf die Stimulation mit LPS reagieren. Dies ist vor allem auf die höhere CD14 (*cluster of differentiation*) Expression primärer Monozyten zurückzuführen. Dabei fungiert CD14 als Co-Rezeptor, der zusammen mit dem TLR-4 das LPS Signal ins Zytosol der Zelle weiterleitet (Bosshart und Heinzelmann 2016). Dies könnte auch erklären, warum in der vorliegenden Arbeit weder die Expression von ASC noch von NLRP3 durch *Priming* der THP-1 Monozyten mit LPS gesteigert wurde (Behrendt et al. 2024). Allerdings induziert der *Priming*-Schritt nicht nur die Transkription von Inflammasom-Komponenten, sondern auch komplexe posttranslationale Modifikationen dieser, wie (De)-Ubiquitinierungs- und (De)-Phosphorylierungsreaktionen, welche ebenfalls an der Regulation der Inflammasom Aktivierung beteiligt sind (Grebe et al. 2018; Guo et al. 2015). Dies könnte erklären, warum in der vorliegenden Arbeit nach *Priming* mit LPS eine stärkere Aktivierung des NLRP3 Inflammasoms beobachtet wurde als ohne vorheriges *Priming* (Behrendt et al. 2024). Zudem zeigen die Ergebnisse der vorliegenden Arbeit, dass Anthocyane sowie deren Metabolite die Nigericin-induzierte Aktivierung des NLRP3 Inflammasoms hemmen (Behrendt et al. 2024). Bei Nigericin handelt es sich um ein bakterielles, porenformendes Toxin, dass häufig verwendet wird, um die Aktivierung des NLRP3 Inflammasoms *in vitro* zu induzieren (Jo et al. 2016). Allerdings kann das NLRP3 Inflammasom *in vivo* durch zahlreiche weitere, chemisch und strukturell sehr unterschiedliche Stimuli, wie z.B. ATP und Cholesterol-Kristalle, aktiviert werden, wobei die genauen molekularen Mechanismen die zur Aktivierung des NLPR3 Inflammasoms führen bisher nicht eindeutig geklärt wurden (Jo et al. 2016). Daher sollte zukünftig untersucht werden, ob Anthocyane und ihre Metabolite ebenfalls in der Lage sind

z.B. die ATP- oder Cholesterol-Kristall-induzierte Aktivierung des NLRP3 Inflammasoms in humanen Monozyten zu hemmen.

Zusammenfassend zeigen die Ergebnisse der vorliegenden Arbeit, dass Anthocyane sowie deren Metabolite die Aktivierung des NLRP3 Inflammasoms in THP-1 Monozyten hemmen. Dies könnte sich positiv auf das inflammatorische Geschehen auswirken und somit der Entstehung inflammatorischer Erkrankungen – insbesondere kardiovaskulären Erkrankungen – präventiv entgegenwirken. Allerdings muss an dieser Stelle offenbleiben über welche molekularen Mechanismen Anthocyane und ihre Metabolite die Hemmung des NLRP3 Inflammasoms in THP-1 Monozyten induzieren. Zudem ist anzumerken, dass die meisten Erkenntnisse zum Einfluss von Anthocyanen und ihrer Metabolite auf die Aktivierung des NLRP3 Inflammasoms aus präklinischen Tier- und *in vitro*-Studien stammen. Daher sollte die physiologische Relevanz der Ergebnisse zukünftig sowohl in primären humanen Monozyten als auch in klinische Studien bestätigt werden.

5. Zusammenfassung

Anthocyanen wird ein hohes gesundheitsförderndes Potenzial zugeschrieben. Allerdings ist die Bioverfügbarkeit nativer Anthocyane relativ gering. Nur etwa 1-2 % der über die Nahrung aufgenommenen Anthocyane gelangen unverändert in den systemischen Kreislauf, da sie sowohl im Gastrointestinaltrakt als auch in der Leber intensiv metabolisiert werden. Dabei entsteht eine Vielzahl an phenolischen Metaboliten, die vermutlich in einem höheren Ausmaß zur biologischen Wirksamkeit der Anthocyane beitragen als die nativen Verbindungen selbst. Ziel dieser Dissertation war es daher, das anti-migratorische und anti-inflammatorische Potenzial von **Anthocyanen sowie deren Metaboliten** in kanzerogenen Zellen zu untersuchen.

Da Tumorerkrankungen die zweithäufigste Todesursache in Deutschland darstellen und mehr als 90 % aller tumorbedingten Sterbefälle auf Metastasen zurückzuführen sind, stellt die Inhibierung der Metastasierung einen wichtigen therapeutischen Ansatzpunkt dar. Daher wurde, im **ersten Teil** dieser Dissertation, mithilfe von *in vitro*-Migrationsmodellen (Boyden Kammer), der Einfluss physiologischer Anthocyan- und Metabolit-Konzentrationen auf das **Migrationspotenzial** kanzerogener Zellen untersucht. Da Zelladhäsionsmoleküle eine wichtige Rolle für die Tumoradhäsion und -migration spielen, wurde ebenfalls untersucht, inwiefern die Expression dieser durch Anthocyane sowie deren Metabolite beeinflusst wird. Dazu wurde die Expression der Zelladhäsionsmoleküle auf den Tumor- und Endothelzellen durchflusszytometrisch analysiert. Dabei zeigte sich, dass die nach 4-wöchiger Intervention mit einem Anthocyan-reichen Trauben-/Heidelbeersaft aus dem Plasma gesunder Probanden isolierten Anthocyane sowie deren Metabolite, in physiologischen Konzentrationen, *in vitro* die Migration von Kolonkarzinom- und Pankreaskarzinomzellen (HT-29 und PANC-1) hemmen. Dabei gingen die für PANC-1 beobachteten anti-migratorischen Effekten mit einer verminderten ICAM-1 sowie Integrin-β1 Expression auf den Pankreaskarzinomzellen einher. Da die Tumorzelladhäsion neben der Integrin-Liganden-Interaktion auch durch Wachstumsfaktoren und Zytokine, die von den Tumorzellen sekretiert werden, beeinflusst wird, wurde zudem der Einfluss von Anthocyanen und ihrer Metabolite auf die CytoMix (TNF-α, IL-1β und VEGF)-stimulierte Expression der Zelladhäsionsmoleküle auf den Endothelzellen untersucht. Dabei konnte die CytoMix-induzierte ICAM-1 Expression durch aus dem Plasma isolierte Anthocyane sowie deren Metabolite signifikant gehemmt werden. Zudem waren die aus dem Plasma isolierten Anthocyane sowie deren Metabolite in der Lage die Aktivierung des NFκB- und FAK-SFK-Signalwegs, sowohl in PANC-1 als auch in CytoMix-stimulierten HUVECs, zu hemmen und so wiederum die Adhäsion der Tumorzellen an das Endothel wie

auch die transendotheliale Migration zu beeinflussen. Zudem wurde die Migration von HT-29 Zellen durch Koinkubation mit dem Chemotherapeutikum 5-FU und aus dem Plasma isolierter Anthocyane sowie deren Metabolite stärker gehemmt als durch 5-FU allein. Allerdings ist die klinische Relevanz dieser *in vitro*-Ergebnisse unklar.

Kardiovaskuläre Erkrankungen stellen die häufigste Todesursache in Deutschland dar. Charakteristisch für diese vaskulären Erkrankungen ist eine chronische, niedrig-gradige Inflammation, die häufig mit Übergewicht und Adipositas assoziiert ist. Dabei scheint, auf mechanistischer Ebene, eine übermäßige Aktivierung des **NLRP3 Inflammasoms** zur Entstehung der LGI beizutragen. Die kanonische Aktivierung des NLRP3 Inflammasoms erfolgt typischerweise in zwei Schritten. Während der erste Schritt (*Priming*) eine gesteigerte Transkription der Inflammasom-Komponenten NLRP3 und pro-IL-1β bewirkt, induziert die Aktivierung des NLRP3 Inflammasoms die autoproteolytische Aktivierung der pro-Caspase-1, welche die Reifung der pro-inflammatorischen Zytokine IL-1β und IL-18 katalysiert. Die Freisetzung dieser Zytokine führt zur Aktivierung weiterer Immunzellen und so zu einer sich potenzierenden inflammatorischen Antwort. Somit stellt die Inhibierung dieses inflammatorischen Geschehens einen wichtigen präventiven Ansatzpunkt dar, um der LGI und der Entstehung kardiovaskulärer Erkrankungen in einem sehr frühen *sub*-klinischen Stadium präventiv entgegenzuwirken. Daher wurde, im **zweiten Teil** dieser Dissertation, der Einfluss von Anthocyanen und ihrer Metabolite auf die Aktivierung des NLRP3 Inflammasoms in humanen Monozyten untersucht. Dazu wurden monozytäre THP-1 Zellen zunächst mit LPS stimuliert (*Priming*) und/oder die Aktivierung des NLRP3 Inflammasoms mit Nigericin induziert. Hierbei zeigte sich, dass die Aktivierung des NLRP3 Inflammasoms in THP-1 Monozyten durch Präinkubation mit dem Anthocyan-reichen Trauben-/Heidelbeerextrakt gehemmt wird. Dabei war die verminderte IL-1β und IL-18 Sekretion vor allem auf die signifikante Hemmung der Caspase-1-Aktivität zurückzuführen. Zudem wurde die Aktivierung des NLRP3 Inflammasoms und somit die Sekretion von IL-1β und Il-18 durch Präinkubation mit dem Plasmametaboliten 2,4,6-Trihydroxybenzaldehyd signifikant gehemmt. Zusammenfassend zeigen die Ergebnisse der vorliegenden Arbeit, dass Anthocyane als auch deren Metabolite in der Lage sind die Aktivierung des NLRP3 Inflammasoms in THP-1 Monozyten zu hemmen. Dies könnte sich positiv auf das inflammatorische Geschehen auswirken und somit der Entstehung inflammatorischer Erkrankungen, insbesondere kardiovaskulären Erkrankungen, präventiv entgegenwirken. Allerdings sollte die physiologische Relevanz der Ergebnisse zukünftig durch klinische Studien bestätigt werden.

6. Abstract

Anthocyanins are attributed with a high health-promoting potential. However, bioavailability of native anthocyanins is reported to be low. Only about 1–2% of dietary anthocyanins enter the systemic circulation as native compounds, as they are extensively metabolized both in the gastrointestinal tract and in the liver. This results in the formation of a wide range of phenolic metabolites, which are presumed to contribute more substantially to the biological activity of anthocyanins than the native compounds themselves. Therefore, the aim of this dissertation was to investigate the anti-migratory and anti-inflammatory potential of anthocyanins and their metabolites in different cancer cell lines.

Since cancer represents the second leading cause of death in Germany and more than 90% of all cancer-related deaths are attributable to metastases, the inhibition of metastasis represents an important therapeutic strategy. Therefore, in the first part of this dissertation, the influence of physiological concentration of anthocyanins and their metabolites on the migratory potential of carcinogenic cells was investigated using *in vitro* migration models (Boyden chamber assay). As cell adhesion molecules play an important role in tumor cell adhesion and migration, the extent to which their expression is influenced by anthocyanins and their metabolites was also examined. For this purpose, the expression of cell adhesion molecules on tumor and endothelial cells was analyzed by flow cytometry. The results demonstrated that physiological concentrations of anthocyanins and their metabolites, isolated from the plasma of healthy subjects following a four-week intervention with an anthocyanin-rich grape/blueberry juice, inhibited the migration of colon and pancreatic cancer cells (HT-29 and PANC-1) *in vitro*. The anti-migratory effects observed in PANC-1 cells were associated with reduced ICAM-1 and integrin-β1 expression on the pancreatic cancer cells. Since tumor cell adhesion is influenced not only by integrin-ligand interactions but also by growth factors and cytokines secreted by tumor cells, the effects of anthocyanins and their metabolites on CytoMix (TNF-α, IL-1β, and VEGF)-stimulated expression of cell adhesion molecules on endothelial cells were also investigated. It was shown that CytoMix-induced ICAM-1 expression was significantly inhibited by plasma-isolated anthocyanins and their metabolites. Furthermore, plasma-isolated anthocyanins and their metabolites inhibited activation of the NFκB and FAK-SFK signaling pathways in both PANC-1 and CytoMix-stimulated HUVECs, thereby influencing tumor cell adhesion to the endothelium, as well as transendothelial migration. In addition, HT-29 colon cancer cell migration was inhibited more strongly by co-incubation with the chemotherapeutic

agent 5-FU plus plasma-isolated anthocyanins and their metabolites than by 5-FU alone. However, the clinical relevance of these *in vitro* findings remains unclear.

Cardiovascular diseases represent the leading cause of death in Germany. These vascular diseases are characterized by a chronic low-grade inflammation (LGI), which is frequently associated with overweight and obesity. Mechanistically, excessive activation of the NLRP3 inflammasome may contribute to the development of the LGI. Canonical activation of the NLRP3 inflammasome is a two-step process. While the first step (priming) induces increased transcription of the inflammasome components NLRP3 and pro-IL-1β, activation of the NLRP3 inflammasome subsequently induces the autoproteolytic activation of pro-caspase-1, which catalyzes the maturation of the pro-inflammatory cytokines IL-1β and IL-18. The release of these cytokines leads to the activation of additional immune cells and thus to a self-amplifying inflammatory response. Consequently, inhibition of this inflammatory process represents an important preventive strategy to counteract LGI and the development of cardiovascular diseases at a very early subclinical stage. Therefore, in the second part of this dissertation, the influence of anthocyanins and their metabolites on NLRP3 inflammasome activation was investigated in human monocytes. For this purpose, monocytic THP-1 cells were first stimulated with LPS (priming) and/or NLRP3 inflammasome activation was induced with nigericin. The results demonstrated that activation of the NLRP3 inflammasome in THP-1 monocytes was inhibited by preincubation with an anthocyanin-rich grape/blueberry extract. The reduced secretion of IL-1β and IL-18 was mainly attributable to significant inhibition of caspase-1 activity. Moreover, activation of the NLRP3 inflammasome and thus secretion of IL-1β and IL-18 were significantly inhibited by preincubation with the plasma metabolite 2,4,6-trihydroxybenzaldehyde.

In summary, the results of the present work demonstrate that both anthocyanins and their metabolites are capable of inhibiting NLRP3 inflammasome activation in THP-1 monocytes. This may positively influence inflammatory processes and thereby contribute to the prevention of inflammatory diseases, particularly cardiovascular diseases. However, the physiological relevance of these findings should be confirmed in future clinical studies.

7. Literaturverzeichnis

Alappat, B.; Alappat, J. Anthocyanin Pigments: Beyond Aesthetics. *Molecules* **2020**, *25*, doi:10.3390/molecules25235500.

Alday-Parejo, B.; Stupp, R.; Rüegg, C. Are Integrins Still Practicable Targets for Anti-Cancer Therapy? *Cancers (Basel)* **2019**, *11*, doi:10.3390/cancers11070978.

Algarra, M.; Fernandes, A.; Mateus, N.; Freitas, V. de; Esteves da Silva, J.C.G.; Casado, J. Anthocyanin profile and antioxidant capacity of black carrots (Daucus carota L. ssp. sativus var. atrorubens Alef.) from Cuevas Bajas, Spain. *Journal of Food Composition and Analysis* **2014**, *33*, 71–76, doi:10.1016/j.jfca.2013.11.005.

Baldrighi, M.; Mallat, Z.; Li, X. NLRP3 inflammasome pathways in atherosclerosis. *Atherosclerosis* **2017**, *267*, 127–138, doi:10.1016/j.atherosclerosis.2017.10.027.

Behrendt, I.; Röder, I.; Will, F.; Michel, G.; Friedrich, E.; Grote, D.; Martin, Z.; Dötzer, H.P.; Fasshauer, M.; Speckmann, M.; et al. Grape/Blueberry Anthocyanins and Their Gut-Derived Metabolites Attenuate LPS/Nigericin-Induced Inflammasome Activation by Inhibiting ASC Speck Formation in THP-1 Monocytes. *Metabolites* **2024**, *14*, doi:10.3390/metabo14040203.

Behrendt, I.; Röder, I.; Will, F.; Mostafa, H.; Gonzalez-Dominguez, R.; Meroño, T.; Andres-Lacueva, C.; Fasshauer, M.; Rudloff, S.; Kuntz, S. Influence of Plasma-Isolated Anthocyanins and Their Metabolites on Cancer Cell Migration (HT-29 and Caco-2) In Vitro: Results of the ATTACH Study. *Antioxidants (Basel)* **2022**, *11*, doi:10.3390/antiox11071341.

Blankenberg, S.; Barbaux, S.; Tiret, L. Adhesion molecules and atherosclerosis. *Atherosclerosis* **2003**, *170*, 191–203, doi:10.1016/s0021-9150(03)00097-2.

Bosshart, H.; Heinzelmann, M. THP-1 cells as a model for human monocytes. *Ann. Transl. Med.* **2016**, *4*, 438, doi:10.21037/atm.2016.08.53.

Buhrmann, C.; Shayan, P.; Goel, A.; Shakibaei, M. Resveratrol Regulates Colorectal Cancer Cell Invasion by Modulation of Focal Adhesion Molecules. *Nutrients* **2017**, *9*, doi:10.3390/nu9101073.

Cassidy, A.; Bertoia, M.; Chiuve, S.; Flint, A.; Forman, J.; Rimm, E.B. Habitual intake of anthocyanins and flavanones and risk of cardiovascular disease in men. *Am. J. Clin. Nutr.* **2016**, *104*, 587–594, doi:10.3945/ajcn.116.133132.

Cooper, J.; Giancotti, F.G. Integrin Signaling in Cancer: Mechanotransduction, Stemness, Epithelial Plasticity, and Therapeutic Resistance. *Cancer Cell* **2019**, *35*, 347–367, doi:10.1016/j.ccell.2019.01.007.

Czank, C.; Cassidy, A.; Zhang, Q.; Morrison, D.J.; Preston, T.; Kroon, P.A.; Botting, N.P.; Kay, C.D. Human metabolism and elimination of the anthocyanin, cyanidin-3-glucoside: a (13)C-tracer study. *Am. J. Clin. Nutr.* **2013**, *97*, 995–1003, doi:10.3945/ajcn.112.049247.

Dawson, J.C.; Serrels, A.; Stupack, D.G.; Schlaepfer, D.D.; Frame, M.C. Targeting FAK in anticancer combination therapies. *Nat. Rev. Cancer* **2021**, *21*, 313–324, doi:10.1038/s41568-021-00340-6.

Devêvre, E.F.; Renovato-Martins, M.; Clément, K.; Sautès-Fridman, C.; Cremer, I.; Poitou, C. Profiling of the three circulating monocyte subpopulations in human obesity. *J. Immunol.* **2015**, *194*, 3917–3923, doi:10.4049/jimmunol.1402655.

Di Gesso, J.L.; Kerr, J.S.; Zhang, Q.; Raheem, S.; Yalamanchili, S.K.; O'Hagan, D.; Kay, C.D.; O'Connell, M.A. Flavonoid metabolites reduce tumor necrosis factor-α secretion to a greater extent than their precursor compounds in human THP-1 monocytes. *Mol. Nutr. Food Res.* **2015**, *59*, 1143–1154, doi:10.1002/mnfr.201400799.

Di Lorenzo, C.; Colombo, F.; Biella, S.; Stockley, C.; Restani, P. Polyphenols and Human Health: The Role of Bioavailability. *Nutrients* **2021**, *13*, doi:10.3390/nu13010273.

Eker, M.E.; Aaby, K.; Budic-Leto, I.; Brnčić, S.R.; El, S.N.; Karakaya, S.; Simsek, S.; Manach, C.; Wiczkowski, W.; Pascual-Teresa, S.d. A Review of Factors Affecting Anthocyanin Bioavailability: Possible Implications for the Inter-Individual Variability. *Foods* **2019**, *9*, doi:10.3390/foods9010002.

Fang, J. Bioavailability of anthocyanins. *Drug Metab. Rev.* **2014**, *46*, 508–520, doi:10.3109/03602532.2014.978080.

Fantini, M.; Benvenuto, M.; Masuelli, L.; Frajese, G.V.; Tresoldi, I.; Modesti, A.; Bei, R. In vitro and in vivo antitumoral effects of combinations of polyphenols, or polyphenols and anticancer drugs: perspectives on cancer treatment. *Int. J. Mol. Sci.* **2015**, *16*, 9236–9282, doi:10.3390/ijms16059236.

Fares, J.; Fares, M.Y.; Khachfe, H.H.; Salhab, H.A.; Fares, Y. Molecular principles of metastasis: a hallmark of cancer revisited. *Signal Transduct. Target. Ther.* **2020**, *5*, 28, doi:10.1038/s41392-020-0134-x.

Ferrars, R.M. de; Czank, C.; Zhang, Q.; Botting, N.P.; Kroon, P.A.; Cassidy, A.; Kay, C.D. The pharmacokinetics of anthocyanins and their metabolites in humans. *Br. J. Pharmacol.* **2014a**, *171*, 3268–3282, doi:10.1111/bph.12676.

Ferrars, R.M. de; Cassidy, A.; Curtis, P.; Kay, C.D. Phenolic metabolites of anthocyanins following a dietary intervention study in post-menopausal women. *Mol. Nutr. Food Res.* **2014b**, *58*, 490–502, doi:10.1002/mnfr.201300322.

Forester, S.C.; Waterhouse, A.L. Gut metabolites of anthocyanins, gallic acid, 3-O-methylgallic acid, and 2,4,6-trihydroxybenzaldehyde, inhibit cell proliferation of Caco-2 cells. *J. Agric. Food Chem.* **2010**, *58*, 5320–5327, doi:10.1021/jf9040172.

Fröhling, B.; Patz, C.-D.; Dietrich, H.; Will, F. Anthocyanins, total phenolics and antioxidant capacities of commercial red grape juices, black currant and sour cherry nectars. *Fruit Processing* **2012**, 100–104.

Garcia-Larsen, V.; Thawer, N.; Charles, D.; Cassidy, A.; van Zele, T.; Thilsing, T.; Ahlström, M.; Haahtela, T.; Keil, T.; Matricardi, P.M.; et al. Dietary Intake of Flavonoids and Ventilatory Function in European Adults: A GA²LEN Study. *Nutrients* **2018**, *10*, doi:10.3390/nu10010095.

Ghanim, H.; Aljada, A.; Hofmeyer, D.; Syed, T.; Mohanty, P.; Dandona, P. Circulating Mononuclear Cells in the Obese Are in a Proinflammatory State. *Circulation* **2004**, *110*, 1564–1571, doi:10.1161/01.CIR.0000142055.53122.FA.

Gonçalves, A.C.; Nunes, A.R.; Falcão, A.; Alves, G.; Silva, L.R. Dietary Effects of Anthocyanins in Human Health: A Comprehensive Review. *Pharmaceuticals (Basel)* **2021**, *14*, doi:10.3390/ph14070690.

Grebe, A.; Hoss, F.; Latz, E. NLRP3 Inflammasome and the IL-1 Pathway in Atherosclerosis. *Circ. Res.* **2018**, *122*, 1722–1740, doi:10.1161/CIRCRESAHA.118.311362.

Grimm, T.; Schäfer, A.; Högger, P. Antioxidant activity and inhibition of matrix metalloproteinases by metabolites of maritime pine bark extract (pycnogenol). *Free Radic. Biol. Med.* **2004**, *36*, 811–822, doi:10.1016/j.freeradbiomed.2003.12.017.

Gritsenko, A.; Yu, S.; Martin-Sanchez, F.; Diaz-Del-Olmo, I.; Nichols, E.-M.; Davis, D.M.; Brough, D.; Lopez-Castejon, G. Priming Is Dispensable for NLRP3 Inflammasome Activation in Human Monocytes In Vitro. *Front. Immunol.* **2020**, *11*, 565924, doi:10.3389/fimmu.2020.565924.

Groslambert, M.; Py, B.F. Spotlight on the NLRP3 inflammasome pathway. *J. Inflamm. Res.* **2018**, *11*, 359–374, doi:10.2147/JIR.S141220.

Grzesiak, J.J.; Tran Cao, H.S.; Burton, D.W.; Kaushal, S.; Vargas, F.; Clopton, P.; Snyder, C.S.; Deftos, L.J.; Hoffman, R.M.; Bouvet, M. Knockdown of the β(1) integrin subunit reduces primary tumor growth and inhibits pancreatic cancer metastasis. *Int. J. Cancer* **2011**, *129*, 2905–2915, doi:10.1002/ijc.25942.

Guerrero, P.E.; Miró, L.; Wong, B.S.; Massaguer, A.; Martínez-Bosch, N.; Llorens, R.d.; Navarro, P.; Konstantopoulos, K.; Llop, E.; Peracaula, R. Knockdown of α2,3-Sialyltransferases Impairs Pancreatic Cancer Cell Migration, Invasion and E-selectin-Dependent Adhesion. *Int. J. Mol. Sci.* **2020**, *21*, doi:10.3390/ijms21176239.

Guo, H.; Callaway, J.B.; Ting, J.P.-Y. Inflammasomes: mechanism of action, role in disease, and therapeutics. *Nat. Med.* **2015**, *21*, 677–687, doi:10.1038/nm.3893.

Guyot, F.; Faivre, J.; Manfredi, S.; Meny, B.; Bonithon-Kopp, C.; Bouvier, A.M. Time trends in the treatment and survival of recurrences from colorectal cancer. *Ann. Oncol.* **2005**, *16*, 756–761, doi:10.1093/annonc/mdi151.

Henein, M.Y.; Vancheri, S.; Longo, G.; Vancheri, F. The Role of Inflammation in Cardiovascular Disease. *Int. J. Mol. Sci.* **2022**, *23*, doi:10.3390/ijms232112906.

Hoss, F.; Rodriguez-Alcazar, J.F.; Latz, E. Assembly and regulation of ASC specks. *Cell. Mol. Life Sci.* **2017**, *74*, 1211–1229, doi:10.1007/s00018-016-2396-6.

Huang, C.-C.; Hung, C.-H.; Hung, T.-W.; Lin, Y.-C.; Wang, C.-J.; Kao, S.-H. Dietary delphinidin inhibits human colorectal cancer metastasis associating with upregulation of miR-204-3p and suppression of the integrin/FAK axis. *Sci. Rep.* **2019**, *9*, 18954, doi:10.1038/s41598-019-55505-z.

Jo, E.-K.; Kim, J.K.; Shin, D.-M.; Sasakawa, C. Molecular mechanisms regulating NLRP3 inflammasome activation. *Cell. Mol. Immunol.* **2016**, *13*, 148–159, doi:10.1038/cmi.2015.95.

Kalt, W.; Cassidy, A.; Howard, L.R.; Krikorian, R.; Stull, A.J.; Tremblay, F.; Zamora-Ros, R. Recent Research on the Health Benefits of Blueberries and Their Anthocyanins. *Adv. Nutr.* **2020**, *11*, 224–236, doi:10.1093/advances/nmz065.

Kay, C.D.; Kroon, P.A.; Cassidy, A. The bioactivity of dietary anthocyanins is likely to be mediated by their degradation products. *Mol. Nutr. Food Res.* **2009**, *53 Suppl 1*, S92-101, doi:10.1002/mnfr.200800461.

Kay, C.D.; Pereira-Caro, G.; Ludwig, I.A.; Clifford, M.N.; Crozier, A. Anthocyanins and Flavanones Are More Bioavailable than Previously Perceived: A Review of Recent Evidence. *Annu. Rev. Food Sci. Technol.* **2017**, *8*, 155–180, doi:10.1146/annurev-food-030216-025636.

Kluge, H.H.P. WHO European regional obesity report 2022. *World Health Organization*: Copenhagen, **2022**, ISBN 9789289057738. Online verfügbar unter: https://www.who.int/europe/publications/i/item/9789289057738, zuletzt geprüft am 14.06.2024.

Krga, I.; Milenkovic, D. Anthocyanins: From Sources and Bioavailability to Cardiovascular-Health Benefits and Molecular Mechanisms of Action. *J. Agric. Food Chem.* **2019**, *67*, 1771–1783, doi:10.1021/acs.jafc.8b06737.

Kuntz, S.; Kunz, C.; Rudloff, S. Inhibition of pancreatic cancer cell migration by plasma anthocyanins isolated from healthy volunteers receiving an anthocyanin-rich berry juice. *Eur. J. Nutr.* **2017**, *56*, 203–214, doi:10.1007/s00394-015-1070-3.

Läubli, H.; Borsig, L. Altered Cell Adhesion and Glycosylation Promote Cancer Immune Suppression and Metastasis. *Front. Immunol.* **2019**, *10*, 2120, doi:10.3389/fimmu.2019.02120.

Lee, C.C.; Kim, J.H.; Kim, J.S.; Oh, Y.S.; Han, S.M.; Park, J.H.Y.; Lee, K.W.; Lee, C.Y. 5-(3',4'-Dihydroxyphenyl-γ-valerolactone), a Major Microbial Metabolite of Proanthocyanidin, Attenuates THP-1 Monocyte-Endothelial Adhesion. *Int. J. Mol. Sci.* **2017**, *18*, doi:10.3390/ijms18071363.

Lee, H.-M.; Kim, J.-J.; Kim, H.J.; Shong, M.; Ku, B.J.; Jo, E.-K. Upregulated NLRP3 inflammasome activation in patients with type 2 diabetes. *Diabetes* **2013**, *62*, 194–204, doi:10.2337/db12-0420.

Leitlinienprogramm Onkologie. S3-Leitlinie Exokrines Pankreaskarzinom. Langversion 2.0 **2021**, Registernummer: 032-010OL. Online verfügbar unter https://www.leitlinienprogramm-onkologie.de/leitlinien/pankreaskarzinom/, zuletzt geprüft am 30.04.2024.

Li, X.; Chen, L.; Gao, Y.; Zhang, Q.; Chang, A.K.; Yang, Z.; Bi, X. Black raspberry anthocyanins increased the antiproliferative effects of 5-Fluorouracil and Celecoxib in colorectal cancer cells and mouse model. *Journal of Functional Foods* **2021a**, *87*, 104801, doi:10.1016/j.jff.2021.104801.

Li, Y.; Huang, H.; Liu, B.; Zhang, Y.; Pan, X.; Yu, X.-Y.; Shen, Z.; Song, Y.-H. Inflammasomes as therapeutic targets in human diseases. *Signal Transduct. Target. Ther.* **2021b**, *6*, 247, doi:10.1038/s41392-021-00650-z.

Liu, T.; Zhang, L.; Joo, D.; Sun, S.-C. NF-κB signaling in inflammation. *Signal Transduct. Target. Ther.* **2017**, *2*, 17023-, doi:10.1038/sigtrans.2017.23.

Makrilia, N.; Kollias, A.; Manolopoulos, L.; Syrigos, K. Cell adhesion molecules: role and clinical significance in cancer. *Cancer Invest.* **2009**, *27*, 1023–1037, doi:10.3109/07357900902769749.

Mattos, R.T.; Medeiros, N.I.; Menezes, C.A.; Fares, R.C.G.; Franco, E.P.; Dutra, W.O.; Rios-Santos, F.; Correa-Oliveira, R.; Gomes, J.A.S. Chronic Low-Grade Inflammation in Childhood Obesity Is Associated with Decreased IL-10 Expression by Monocyte Subsets. *PLoS One* **2016**, *11*, e0168610, doi:10.1371/journal.pone.0168610.

Molla, M.D.; Akalu, Y.; Geto, Z.; Dagnew, B.; Ayelign, B.; Shibabaw, T. Role of Caspase-1 in the Pathogenesis of Inflammatory-Associated Chronic Noncommunicable Diseases. *J. Inflamm. Res.* **2020**, *13*, 749–764, doi:10.2147/JIR.S277457.

Mostafa, H.; Behrendt, I.; Meroño, T.; González-Domínguez, R.; Fasshauer, M.; Rudloff, S.; Andres-Lacueva, C.; Kuntz, S. Plasma anthocyanins and their metabolites reduce in vitro migration of pancreatic cancer cells, PANC-1, in a FAK- and NF-kB dependent manner: Results from the ATTACH-study a randomized, controlled, crossover trial in healthy subjects. *Biomed. Pharmacother.* **2023**, *158*, 114076, doi:10.1016/j.biopha.2022.114076.

Mueller, D.; Jung, K.; Winter, M.; Rogoll, D.; Melcher, R.; Richling, E. Human intervention study to investigate the intestinal accessibility and bioavailability of anthocyanins from bilberries. *Food Chem.* **2017**, *231*, 275–286, doi:10.1016/j.foodchem.2017.03.130.

Ngamsamer, C.; Sirivarasai, J.; Sutjarit, N. The Benefits of Anthocyanins against Obesity-Induced Inflammation. *Biomolecules* **2022**, *12*, doi:10.3390/biom12060852.

Pan, B.; Guo, J.; Liao, Q.; Zhao, Y. β1 and β3 integrins in breast, prostate and pancreatic cancer: A novel implication. *Oncol. Lett.* **2018**, *15*, 5412–5416, doi:10.3892/ol.2018.8076.

Parmenter, B.H.; Dalgaard, F.; Murray, K.; Cassidy, A.; Bondonno, C.P.; Lewis, J.R.; Croft, K.D.; Kyrø, C.; Gislason, G.; Scalbert, A.; et al. Habitual flavonoid intake and ischemic stroke incidence in the Danish Diet, Cancer, and Health Cohort. *Am. J. Clin. Nutr.* **2021**, *114*, 348–357, doi:10.1093/ajcn/nqab138.

Pretre, V.; Papadopoulos, D.; Regard, J.; Pelletier, M.; Woo, J. Interleukin-1 (IL-1) and the inflammasome in cancer. *Cytokine* **2022**, *153*, 155850, doi:10.1016/j.cyto.2022.155850.

Prior, R.L.; Wu, X. Anthocyanins: structural characteristics that result in unique metabolic patterns and biological activities. *Free Radic. Res.* **2006**, *40*, 1014–1028, doi:10.1080/10715760600758522.

Ralston, J.C.; Lyons, C.L.; Kennedy, E.B.; Kirwan, A.M.; Roche, H.M. Fatty Acids and NLRP3 Inflammasome-Mediated Inflammation in Metabolic Tissues. *Annu. Rev. Nutr.* **2017**, *37*, 77–102, doi:10.1146/annurev-nutr-071816-064836.

Reymond, N.; d'Água, B.B.; Ridley, A.J. Crossing the endothelial barrier during metastasis. *Nat. Rev. Cancer* **2013**, *13*, 858–870, doi:10.1038/nrc3628.

RKI. *Krebs in Deutschland für 2019/2020*, 14. Auflage. Robert Koch-Institut und die Gesellschaft der epidemiologischen Krebsregister in Deutschland e.V.: Berlin, **2023**, ISBN 978-3-89606-323-6. Online verfügbar unter: https://edoc.rki.de/handle/176904/11438, zuletzt geprüft am 14.06.2024.

Roggiani, S.; Mengoli, M.; Conti, G.; Fabbrini, M.; Brigidi, P.; Barone, M.; D'Amico, F.; Turroni, S. Gut microbiota resilience and recovery after anticancer chemotherapy. *Microbiome Res. Rep.* **2023**, *2*, 16, doi:10.20517/mrr.2022.23.

Rubert, J.; Gatto, P.; Pancher, M.; Sidarovich, V.; Curti, C.; Mena, P.; Del Rio, D.; Quattrone, A.; Mattivi, F. A Screening of Native (Poly)phenols and Gut-Related Metabolites on 3D HCT116 Spheroids Reveals Gut Health Benefits of a Flavan-3-ol Metabolite. *Mol. Nutr. Food Res.* **2022**, *66*, e2101043, doi:10.1002/mnfr.202101043.

Sester, D.P.; Thygesen, S.J.; Sagulenko, V.; Vajjhala, P.R.; Cridland, J.A.; Vitak, N.; Chen, K.W.; Osborne, G.W.; Schroder, K.; Stacey, K.J. A novel flow cytometric method to assess inflammasome formation. *J. Immunol.* **2015**, *194*, 455–462, doi:10.4049/jimmunol.1401110.

Sharma, B.R.; Kanneganti, T.-D. NLRP3 inflammasome in cancer and metabolic diseases. *Nat. Immunol.* **2021**, *22*, 550–559, doi:10.1038/s41590-021-00886-5.

Shi, N.; Chen, X.; Chen, T. Anthocyanins in Colorectal Cancer Prevention Review. *Antioxidants (Basel)* **2021**, *10*, doi:10.3390/antiox10101600.

Statistisches Bundesamt. Todesursachenstatistik Deutschland. **2024,** Online verfügbar unter: https://www-genesis.destatis.de/genesis/online?sequenz=tabelleErgebnis&selectionname=23211-0002#abreadcrumb, zuletzt geprüft am 14.06.2024.

Sulzmaier, F.J.; Jean, C.; Schlaepfer, D.D. FAK in cancer: mechanistic findings and clinical applications. *Nat. Rev. Cancer* **2014**, *14*, 598–610, doi:10.1038/nrc3792.

Tsutsumi, A.; Horikoshi, Y.; Fushimi, T.; Saito, A.; Koizumi, R.; Fujii, Y.; Hu, Q.Q.; Hirota, Y.; Aizawa, K.; Osakabe, N. Acylated anthocyanins derived from purple carrot (Daucus carota L.) induce elevation of blood flow in rat cremaster arteriole. *Food Funct.* **2019**, *10*, 1726–1735, doi:10.1039/c8fo02125b.

Vetrani, C.; Di Nisio, A.; Paschou, S.A.; Barrea, L.; Muscogiuri, G.; Graziadio, C.; Savastano, S.; Colao, A.; On, B.O.T.O.P.O.N.E.R.A.A.O.G. From Gut Microbiota through Low-Grade Inflammation to Obesity: Key Players and Potential Targets. *Nutrients* **2022**, *14*, doi:10.3390/nu14102103.

Vodenkova, S.; Buchler, T.; Cervena, K.; Veskrnova, V.; Vodicka, P.; Vymetalkova, V. 5-fluorouracil and other fluoropyrimidines in colorectal cancer: Past, present and future. *Pharmacol. Ther.* **2020**, *206*, 107447, doi:10.1016/j.pharmthera.2019.107447.

Vogiatzoglou, A.; Mulligan, A.A.; Lentjes, M.A.H.; Luben, R.N.; Spencer, J.P.E.; Schroeter, H.; Khaw, K.-T.; Kuhnle, G.G.C. Flavonoid intake in European adults (18 to 64 years). *PLoS One* **2015**, *10*, e0128132, doi:10.1371/journal.pone.0128132.

Wang, N.; Yang, L.; Dai, J.; Wu, Y.; Zhang, R.; Jia, X.; Liu, C. 5-FU inhibits migration and invasion of CRC cells through PI3K/AKT pathway regulated by MARCH1. *Cell Biol. Int.* **2021**, *45*, 368–381, doi:10.1002/cbin.11493.

Wang, X.; Yang, D.-Y.; Yang, L.-Q.; Zhao, W.-Z.; Cai, L.-Y.; Shi, H.-P. Anthocyanin Consumption and Risk of Colorectal Cancer: A Meta-Analysis of Observational Studies. *J. Am. Coll. Nutr.* **2019**, *38*, 470–477, doi:10.1080/07315724.2018.1531084.

Wang, X.; Zhang, Z.-F.; Zheng, G.-H.; Wang, A.-M.; Sun, C.-H.; Qin, S.-P.; Zhuang, J.; Lu, J.; Ma, D.-F.; Zheng, Y.-L. The Inhibitory Effects of Purple Sweet Potato Color on Hepatic Inflammation Is Associated with Restoration of NAD^+ Levels and Attenuation of NLRP3 Inflammasome Activation in High-Fat-Diet-Treated Mice. *Molecules* **2017**, *22*, doi:10.3390/molecules22081315.

Wittmann, N.; Behrendt, A.-K.; Mishra, N.; Bossaller, L.; Meyer-Bahlburg, A. Instructions for Flow Cytometric Detection of ASC Specks as a Readout of Inflammasome Activation in Human Blood. *Cells* **2021**, *10*, doi:10.3390/cells10112880.

Wong, C.C.; Yu, J. Gut microbiota in colorectal cancer development and therapy. *Nat. Rev. Clin. Oncol.* **2023**, *20*, 429–452, doi:10.1038/s41571-023-00766-x.

Wu, X.; Beecher, G.R.; Holden, J.M.; Haytowitz, D.B.; Gebhardt, S.E.; Prior, R.L. Concentrations of anthocyanins in common foods in the United States and estimation of normal consumption. *J. Agric. Food Chem.* **2006**, *54*, 4069–4075, doi:10.1021/jf060300l.

Yu, G.; Xu, M.; Zhou, L.; Zheng, K.; Zhu, X.; Sui, J.; Xin, C.; Chang, W.; Zhang, W.; Cao, F. High expression of phosphorylated focal adhesion kinase predicts a poor prognosis in human colorectal cancer. *Front. Pharmacol.* **2022**, *13*, 989999, doi:10.3389/fphar.2022.989999.

Yui, Y.; Itoh, K.; Yoshioka, K.; Naka, N.; Watanabe, M.; Hiraumi, Y.; Matsubara, H.; Watanabe, K.-i.; Sano, K.; Nakahata, T.; et al. Mesenchymal mode of migration participates in pulmonary metastasis of mouse osteosarcoma LM8. *Clin. Exp. Metastasis* **2010**, *27*, 619–630, doi:10.1007/s10585-010-9352-x.

Yun, J.W.; Lee, W.S.; Kim, M.J.; Lu, J.N.; Kang, M.H.; Kim, H.G.; Kim, D.C.; Choi, E.J.; Choi, J.Y.; Kim, H.G.; et al. Characterization of a profile of the anthocyanins isolated from Vitis coignetiae Pulliat and their anti-invasive activity on HT-29 human colon cancer cells. *Food Chem. Toxicol.* **2010**, *48*, 903–909, doi:10.1016/j.fct.2009.12.031.

Zamora-Ros, R.; Knaze, V.; Luján-Barroso, L.; Slimani, N.; Romieu, I.; Touillaud, M.; Kaaks, R.; Teucher, B.; Mattiello, A.; Grioni, S.; et al. Estimation of the intake of anthocyanidins and their food sources in the European Prospective Investigation into Cancer and Nutrition (EPIC) study. *Br. J. Nutr.* **2011**, *106*, 1090–1099, doi:10.1017/S0007114511001437.

Zhang, J.; Giampieri, F.; Afrin, S.; Battino, M.; Zheng, X.; Reboredo-Rodriguez, P. Structure-stability relationship of anthocyanins under cell culture condition. *Int. J. Food Sci. Nutr.* **2019**, *70*, 285–293, doi:10.1080/09637486.2018.1506753.

Zhao, X.; Guan, J.-L. Focal adhesion kinase and its signaling pathways in cell migration and angiogenesis. *Adv. Drug Deliv. Rev.* **2011**, *63*, 610–615, doi:10.1016/j.addr.2010.11.001.

Zheng, D.; Liwinski, T.; Elinav, E. Inflammasome activation and regulation: toward a better understanding of complex mechanisms. *Cell Discov.* **2020**, *6*, 36, doi:10.1038/s41421-020-0167-x.

Zhou, J.; Zhu, Y.-F.; Chen, X.-Y.; Han, B.; Li, F.; Chen, J.-Y.; Peng, X.-L.; Luo, L.-P.; Chen, W.; Yu, X.-P. Black rice-derived anthocyanins inhibit HER-2-positive breast cancer epithelial-mesenchymal transition-mediated metastasis in vitro by suppressing FAK signaling. *Int. J. Mol. Med.* **2017**, *40*, 1649–1656, doi:10.3892/ijmm.2017.3183.

Zhu, Y.; Sun, H.; He, S.; Lou, Q.; Yu, M.; Tang, M.; Tu, L. Metabolism and prebiotics activity of anthocyanins from black rice (Oryza sativa L.) in vitro. *PLoS One* **2018**, *13*, e0195754, doi:10.1371/journal.pone.0195754.

Zito, G.; Buscetta, M.; Cimino, M.; Dino, P.; Bucchieri, F.; Cipollina, C. Cellular Models and Assays to Study NLRP3 Inflammasome Biology. *Int. J. Mol. Sci.* **2020**, *21*, doi:10.3390/ijms21124294.

8. Weitere Publikationen

1. Berehndt I, Eichner G, Fasshauer M. Association of antioxidants use with all-cause and cause-specific mortality: A prospective study of the UK Biobank. *Antioxidants* (Basel) **2020**, 9, 1287. doi: 10.3390/antiox9121287. *Journal impact factor*: 7.0
2. Behrendt I, Fasshauer M, Eichner. Gluten intake and metabolic health: conflicting findings from the UK Biobank. *Eur J Nutr.* **2021**, 60, 1547-1559. doi:10.1007/s00394-020-02351-9. *Journal impact factor*: 5.0
3. Behrendt I, Fasshauer M, Eichner G. Gluten intake and all-cause and cause-specific mortality: Prospective findings from the UK Biobank. *J Nutr.* **2021,** 151, 591-597. doi: 10.1093/jn/nxaa387. *Journal impact factor*: 4.2
4. Schaefer S.M., Kaiser A, Behrendt I, Eichner G, Fasshauer M. Association of alcohol types, coffee and tea intake with risk of dementia: Prospective cohort study of UK Biobank Participants. *Brain Sci.* **2022**, 12, 360. doi: 10.3390/brainsci12030360. *Journal impact factor*: 3.3
5. Schaefer S.M., Kaiser A, Behrendt I, Eichner G, Fasshauer M. Association of alcohol types, coffee and tea intake with mortality: prospective cohort study of UK Biobank participants. *Br J Nutr.* **2022**, 129 1-11. doi: 10.1017/S000711452200040X. *Journal impact factor*: 3.6
6. Kaiser A, Schaefer S.M., Behrendt I, Eichner G, Fasshauer M. Assocation of all-cause mortality with sugar intake from different sources in the prospective cohort of UK Biobank participants. *Br J Nutr.* **2022**, 1-107:1-10. doi: 10.1017/S0007114522003233. *Journal impact factor*: 3.6
7. Kaiser A, Schaefer S.M., Behrendt I, Eichner G, Fasshauer M. Association of sugar intake from different sources with incident depresseion in the prospective cohort of UK Biobank participants. *Eur J Nutr.* **2023**, 62, 727-738. doi: 10.1007/s00394-022-03022-7. *Journal impact factor*: 5.0

9. Erklärung

Erklärung gemäß der Promotionsordnung des Fachbereichs 09 vom 07. Juli 2004 § 17(2)

„Ich erkläre: Ich habe die vorgelegte Dissertation selbständig und ohne unerlaubte fremde Hilfe und nur mit den Hilfen angefertigt, die ich in der Dissertation angegeben habe. Alle Textstellen, die wörtlich oder sinngemäß aus veröffentlichten Schriften entnommen sind, und alle Angaben, die auf mündlichen Auskünften beruhen, sind als solche kenntlich gemacht.

Bei den von mir durchgeführten und in der Dissertation erwähnten Untersuchungen habe ich die Grundsätze guter wissenschaftlicher Praxis, wie sie in der „Satzung der Justus-Liebig-Universität Gießen zur Sicherung guter wissenschaftlicher Praxis“ niedergelegt sind, eingehalten.“

Gießen, den 18.06.2024

Inken Behrendt

Anhang

Anhang A

***Supplemental Material*:**

Influence of Plasma-Isolated Anthocyanins and Their Metabolites on Cancer Cell Migration (HT-29 and Caco-2) In Vitro: Results of the ATTACH Study.

Behrendt I, Röder I, Will F, Mostafa H, Gonzalez-Dominguez R, Meroño T, Andres-Lacueva C, Fasshauer M, Rudloff S, Kuntz S. *Antioxidants* **2022**, 11, 1341. doi:10.3390/antiox11071341.

Journal impact factor: 7.0

Anhang B

***Supplemental Material*:**

Plasma anthocyanins and their metabolites prevent in-vitro migration of pancreatic cancer cells, PANC-1 in a FAK- and NF-kB dependent manner: results from the ATTACH-study a randomized, controlled, crossover trial in healthy subjects.

Mostafa H[1], Behrendt I[1], Meroño T, González-Domínguez R, Fasshauer M, Rudloff S, Andres-Lacueva C, Kuntz S. *Biomed. Pharmacother.* **2023**, 158, 114076. doi:10.1016/j.biopha.2022.114076.

Journal impact factor: 7.5 [1]Co-first authorship

Anhang C

***Supplemental Material*:**

Grape/blueberry anthocyanins and their gut-derived metabolites attenuate LPS/nigericin-induced inflammasome activation by inhibiting ASC speck formation in THP-1 monocytes.

Behrendt I, Röder I, Will F, Michel G, Friedrich E, Grote D, Martin Z, Dötzer H.P., Fasshauer M, Speckmann M, Kuntz S. *Metabolites* **2024**, 14, 203. doi:10.3390/metabo14040203.

Journal impact factor: 4.1

Anhang A

Supplemental Material:

Influence of Plasma-Isolated Anthocyanins and Their Metabolites on Cancer Cell Migration (HT-29 and Caco-2) In Vitro: Results of the ATTACH Study.

Behrendt I, Röder I, Will F, Mostafa H, Gonzalez-Dominguez R, Meroño T, Andres-Lacueva C, Fasshauer M, Rudloff S, Kuntz S. *Antioxidants* **2022**, 11, 1341. doi:10.3390/antiox11071341.

Journal impact factor: 7.0

Supplementary Material

Influence of plasma isolated anthocyanins and their metabolites on cancer cell migration (HT-29 and Caco-2): Results of the ATTACH study

Authors:

Inken Behrendt [1]*, Isabella Röder [2], Frank Will [2], Hamza Mostafa [3,4], Raúl Gonzalez-Dominguez [3,4], Tomás Meroño [3,4], Cristina Andres-Lacueva [3,4], Mathias Fasshauer [1], Silvia Rudloff [5] and Sabine Kuntz [1]

[1] Department of Nutritional Science, Human Nutrition, Justus-Liebig-University, Giessen (Germany)
[2] Department of Beverage Research, Hochschule Geisenheim University (Germany)
[3] Biomarkers and Nutrimetabolomics Laboratory, Department of Nutrition, Food Sciences and Gastronomy, Food Innovation Network (XIA), Nutrition and Food Safety Research Institute (INSA), Facultat de Farmàcia i Ciències de l'Alimentació , Universitat de Barcelona (UB), Barcelona (Spain)
[4] Centro de Investigación Biomédica en Red de Fragilidad y Envejecimiento Saludable (CIBERFES), Instituto de Salud Carlos III, Madrid, 28029 (Spain).
[5] Department of Nutritional Science and Department of Pediatrics, Justus-Liebig-University, Giessen (Germany)
* Correspondence: inken.behrendt@ernaehrung.uni-giessen.de

Table S1. Foodstuffs that were restricted or not allowed during the run-in and 28-day intervention period.

Foodstuffs allowed with **minor restrictions**[1]	Foodstuffs **not allowed**
Milk and milk products: milk, yoghurt and other milk products with fruit, nuts (no red fruit). **Vegetables**: yellow and green paprika, leek, spinach, cauliflower, broccoli, onions (no red onions). **Fruit**: bananas, pears, white grapes, apples (max. 1 piece/day), peaches, apricots (max. 1 piece/day), kiwis, pineapple. **Breakfast cereals**: cereals (no wholemeal/ without red fruits/ dark chocolate/ bran). **Fat, spices**: vegetable fat and oil, paprika spice, chili spice, cayenne pepper, curry spice. **Sweets**: ice cream with fruits, nuts (without red fruit / dark chocolate), marmalade/ jam/ jelly (without red fruit). **Allowed (per day):** 1 cup of tea, 1 cup of coffee, 1 glass of ale or glass of white wine (no red wine). Please note: fruit and vegetable, if possible, have to be peeled before consumption, especially, if consumed more portions a day, forgo red fruits, no consume external leaves of salad, no consume cereal products, listed spice and mixed spices use sparing.	**Fruit**: blueberries, blackberries, cranberries, strawberries, bilberries, raspberries, currants, lingonberries, cherries, red grapes, pomegranate, plums, watermelon. **Fruit containing foodstuffs**: red marmalade/ jellies, cake with red fruits, yoghurt with red fruits, ice cream with red fruits, desserts, muesli, muesli bars, cereals with wholemeal, dark chocolate, cocoa powder, gumdrop with fruit. **Vegetables**: purple potatoes, purple carrots, tomatoes, red and orange peppers, red cabbage, beetroot, radicchio, red radish, rhubarb, red and black pulses (kidney beans, red lentils), eggplant, pumpkin, red onions. **Other**: tomato sauce, puree, or paste, ketchup, red pesto. **Avoid** red wine, fruit and vegetable juice, fruit spritzer, smoothies, fruit tea, green tea, coffee, rooibos tea, alcoholic drinks (bear, wine, schnapps, and liqueur). Please note: anthocyanins may be food additives listed as number E 163.

[1]Foodstuffs were categorized according to their anthocyanin content based on data using the USDA database for the Flavonoid Content of Selected Foods (Release 3.3 (2018); http://www.ars.usda.gov/) or the database on polyphenol contents in food (Polyphenol-Explorer, Release 3.0 (http://www.phenol-explorer.eu/compounds)

Table S2. Baseline characteristics and mean dietary intake of the study population during the two intervention periods (n=34).

Dietary intake per day[1]	Intervention period 1	Intervention period 2
Age, *years*	24.4 ± 2.3	
Weight, *kg*	64.3 ± 11.7	63.2 ± 12.07
BMI, kg/m^2	21.7 ± 2.6	21.3 ± 2.2
Dietary intake (3-day protocol)		
Energy, *kcal/d*	1698 ± 552	1855 ± 578
Fat, *g/d*	63.4 ± 17.9	64.4 ± 18.7
Carbohydrates, *g/d*	250.9 ± 63.2	245.8 ± 48.1
Dietary fibre, *g/d*	20.3 ± 5.3	19.4 ± 6.0
Protein, *g/d*	60.6 ± 16.4	54.7 ± 13.7
Retinol equivalents, *µg/d*	714 ± 263	682 ± 207
ß-carotene, *µg/d*	1,698 ± 1,520	1,387 ± 1,147
Vitamin E, *µg/d*	6,925 ± 6,630	7,201 ± 6,921
Vitamin C, *mg/d*	57.14 ± 34.2	63.88 ± 40.4

[1]Participants recorded their dietary intake over 3 days during each intervention period. Dietary records were analyzed using the DGE-PC professional software (Version 1.10.0.0) and values are expressed as means ± SD .

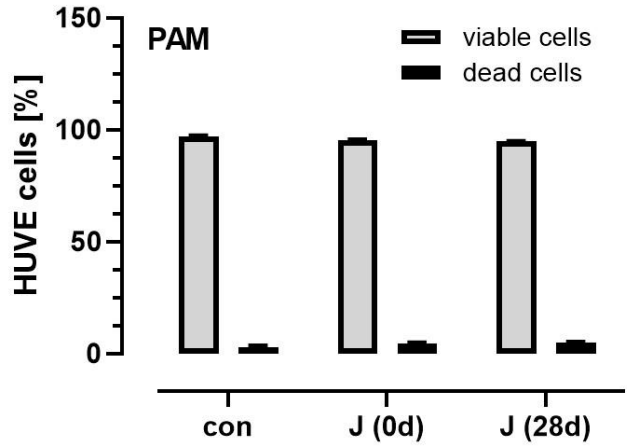

Figure S1. Effects of PAM on HUVE cell viability. Cells were seeded at a density of $1x10^5$ cells/mL in 24-well plates in complete medium with or without PAM from the anthocyanin-rich juice, which were isolated before (J (0d)) or after 28-days intervention (J (28d)) or with medium alone (con). After 36 h incubation, cells were washed twice with PBS, trypsinized and cell viability was measured using a Guava® Muse® Cell Analyzer. Data are expressed as bars [%] with standard deviation. Significant differences were calculated with ANOVA with multiple comparison test (n=2).

Anhang B

Supplemental Material:

Plasma anthocyanins and their metabolites prevent in-vitro migration of pancreatic cancer cells, PANC-1 in a FAK- and NF-kB dependent manner: results from the ATTACH-study a randomized, controlled, crossover trial in healthy subjects.

Mostafa H[1], Behrendt I[1], Meroño T, González-Domínguez R, Fasshauer M, Rudloff S, Andres-Lacueva C, Kuntz S. *Biomed. Pharmacother.* **2023**, 158, 114076. doi:10.1016/j.biopha.2022.114076.

Journal impact factor: 7.5 [1]Co-first authorship

Supplementary methods

S1. Solid phase extraction (SPE) of plasma samples for cell culture assays. Plasma extraction of anthocyanins and their metabolites was based on the method described recently [Behrendt et al 2022, Kuntz S et al 2017]. Briefly, each aliquot (5 mL of plasma acidified with 150 µl of 50% aqueous formic acid (LGC Promochem, Wesel, Germany)) was loaded onto an Oasis-HLB (5 mL/200 mg) SPE cartridge (Waters, Inc., Eschborn, Germany), preconditioned with 5 mL of methanol (Thermo Fischer Scientific, Langenselbold, Germany) and 1% formic acid, followed by 5 mL of acidified water (1% formic acid). The cartridge was then washed with 5 mL of acidified water, after which anthocyanins and their metabolites were eluted with 5 mL of acidified methanol. Afterwards, N_2 gas was applied for 2h to dry the extract which was then stored at -80ºC until further analysis. For cell culture studies, SPE-isolated metabolites from 1 mL plasma were diluted in 1 mL DMEM (Dulbecco's modified Eagle's medium), 1 mL RPMI 1640 (Roswell Park Memorial Institute) media or 1 ml Endothelial growth medium II (Promocell GmbH, Germany), adjusted to pH 7.4, sterile filtered (Micro-Spin Eppendorf filter, pore size 0.2 µm; Eppendorf, Eugendorf, Germany) and immediately used for cell culture studies.

S2. Plasma and urine sample preparation. Plasma and urine sample preparation including all chemicals and standards used in this study have been described previously [González-Domínguez R et al 2020]. Plasma samples were prepared based on the protein precipitation approach. Briefly, the precipitation solution was made of cold acetonitrile containing 1.5 M formic acid and 10 mM ammonium formate. The reconstitution solution was water:acetonitrile (80:20, v/v) containing 0.1% formic acid and 100 µg/L of a mixture of 13 internal standards (ISs). Using a Sirocco protein precipitation plate, 100 µl of plasma were added and mixed with 400 µl of the protein precipitation solution. The plate was then kept in a -20ºC freezer for 10 min to promote the protein precipitation. N_2 pressure was applied and the extract was collected in a 96-well collection plate and transferred to the speed vacuum concentrator until dryness. Finally, the samples were reconstituted with 100 µl of the reconstitution solution containing the ISs mix and transferred to Agilent well plates for further analysis. Urine samples were treated in two different procedures. Urine samples were taken from the -80ºC freezer and kept to be thawed and centrifuged for 10 min at 4ºC at 10,000xg. The 13 ISs mix mentioned above was used as ISs at a concentration of 100 µg/L. The first treatment was urine dilution, i.e., a 50 µl aliquot of the centrifuged urine was diluted with 200 µl of ultrapure water containing 0.1% formic acid (1:4 v/v) and the ISs- solution, and then transferred to 96-well plates for further analysis. The second treatment was a reversed solid phase extraction (SPE) using Oasis HLB plates. Conditioning of the plates was done by adding 1 ml of methanol and 1 ml of the equilibration solution consisting of water with 0.1% formic acid and 10 mM of ammonium formate. Then, 1 ml of urine containing 20 µl of 2% orthophosphoric acid and the set of the 13 ISs mix was loaded, followed by 1 ml of the equilibration solution. Then, 1.5 ml of the elution solution were added consisting of

methanol with 0.1% formic acid and 10 mM ammonium formate. Finally, a speed vacuum concentrator (Gyrozen®, scanspeed 32) was used to dry the extracts which were then reconstituted with 100 µl of the previously mentioned reconstitution solution and transferred to Agilent well plates for further analysis.

S3. Cancer Cell lines. The two human pancreatic carcinoma cell lines, PANC-1 and AsPC-1 were purchased from American Type Culture Collection (ATCC) and cultured following the recommendations of ATCC (http://www.lgcstandards-atcc.org/). PANC-1 is an epithelioid carcinoma cell line derived from ductal cell origin of the human pancreas from a 56-year-old Caucasian male (3). PANC-1 cells were sub-cultured twice a week in DMEM and supplemented with 5 mmol/L L-glutamine, 1 mmol/L sodium pyruvate and 10% fetal bovine serum (FBS) at 37°C in a humidified atmosphere containing 5% CO_2. AsPC-1, a human pancreatic adenocarcinoma cell line derived from metastatic sites (ascites) of a 62-year-old Caucasian female were grown in RPMI 1640 medium and supplemented as described above for PANC-1. After reaching 60% confluence, cells were passaged in a 1:4 split ratio with TrypLE™ Express solution and passages between P12-P28 were used. Both cell lines showed characteristics of tumorigenicity and differ in their pheno- and genotype [Wang Y et al 2020, Deer EL et al 2010].

S4. Endothelial cells. HUVECs (Human umbilical vein endothelial cells) were obtained from pooled donors (from up to four different umbilical cords). These cells were cultured on 75-cm^2 flasks at 37°C, 5% CO_2 in Endothelial growth medium II supplemented with 10 ml ready-to-use growth supplement. After reaching 80-90% confluence, cells were passaged in a 1:3 split ratio with accutase-solution (0.15 ml/cm^2) and were used at passages between P2-P6. Detached cells were seeded on 0.1% fibronectin-coated wells and allowed to growth until they reached 100% confluence (mechanistic studies) or on 0.1% fibronectin-coated 24-well-transwell inserts of 24-well-plates (migration studies).

S5. Analysis of cell surface proteins (CAM) by flow cytometry analysis. 100 µL of cell suspension were used for staining with fluorochrome labelled monoclonal anti-human **REAfinity™ antibodies** in V1-channel (CD104 (ß4-integrin)-Vioblue, CD 49d (Viobright V423)), B1-channel (CD106 (VCAM-1)-FITC, CD49f (a6-integrin)-VioBright FITC), B2-channel (CD62E (E-selectin)-PE, VEGFR-PE), B4-channel (CD18 (ß2-integrin)-PE-Vio770), R1-channel (CD29 (ß1-integrin), CD54 (ICAM-1)-APC) and R2-channel (CD49c (α3-integrin)-APC-Vio770) and B3-channel for live-dead exclusion with propidium iodide solution (PI). Fluorochrome labelled IgG1-REAfinity™ antibodies were used as isotype controls. Compensation matrix for multicolour-measurement to avoid spillover was presented in Supplemental Table 3. Briefly, 100 µl cell suspension was stained for 10 min at 4°C under dark conditions with anti-human **REAfinity™ or** IgG1-REAfinity™ **Isotype control or left unstained.** Reaction was stopped by adding 1000 µL cold MACS Running Buffer. Prior the flow cytometry measurements, 10 µl of PI was used for exclusion of dead cells. Thereafter, 100 µl cells

suspension was measured automatically by flow cytometry with MACS Quant 10 (MQ10) and the quantification was performed using the MACSQuantify Version 2.13.2 software (Miltenyi, Bergisch-Gladbach, Germany) by comparing the mean fluorescence intensity (MFI). MFI was expressed as median with interquartile range (25^{th}–75^{th}). Representative Gating strategy and MFI quantification was given in Supplemental Figure 2.

S6. Cytokine determination. The secretion of tumor necrosis factor-α (TNF-α), interleukin-1ß (IL-1ß), IL-8 and VEGF present in the supernatant of pancreatic cancer cells and unstimulated HUVECs was measured colorimetrically using sandwich ELISAs with HRP-conjugate in the Digicsan Reader (Asys, Austria) according to the manufacturer's instructions. After the cultivation, the particulates were removed from the cell culture supernatant immediately by centrifugation (1,500xg, 5 min, RT) and samples were aliquoted and stored at -20°C with avoiding repeated freeze-thaw cycles. Quantification of secreted proteins from cells was performed using the Microwin software Version 2.15 and concentrations were given as pg/mL. The minimum detectable dose (MDD) of human TNF-α was 11.3 pg/mL, of IL-8 was 14.7 pg/mL, of human VEGF was 10.6 pg/mL, and of IL-1ß was 6.9 pg/mL. The optical density (OD) of each well was measured within 30 min after stopping the HRP-enzymatic reaction using the microplate reader at 450 nm. Concentrations were determined based on a calibration curve using standards for all cytokines. Protein secretion was expressed as are expressed as median with interquartile range (25^{th}–75^{th}).

S7. p65 and FAK activation measured by ELISA. Commercially available immunosorbent assays for FAK and NF-kB were used to determine phosphorylated levels of FAK at tyrosine residue 397(FAK [pY397]) in prepared cell lysates and the InstantOne™ ELISA for measurement of phosphorylated human NF-kB p65 in cell lysates. Cells were lysed using the recommended cell extraction buffer after incubation with plasma extracts and lysates were collected and stored at −80°C. The standard protocol of the manufacturer was followed thereafter. OD was measured at 450 nm and the expression of pFAK and p65 protein was calculated using a four-parameter algorithm providing the best standard curve fit. The background absorbance was subtracted from all data points, including standards, unknowns and controls prior to plotting. The results are expressed as mean ± SD.

S8. Determination of ROS with carboxy-H_2-DCFDA (5-(and-6)-carboxy-2′,7′-dichlorodihydrofluorescein di-acetate). ROS determination and sample preparation have been described previously (5). Cellular ROS generation was determined by incubating cells in medium with 5-(and-6)-carboxy-2′,7′-dichlorodihydrofluorescein diacetate (carboxy-H_2-DCFDA). As noted by the manufacturer, an increase in carboxy-H_2-DCFDA fluorescence is primarily due to the reaction with intracellular ROS. The cell-permeable carboxy-H_2-DCFDA diffuses into cells and was retained in the intracellular level after cleavage by intracellular esterases. Upon oxidation by ROS, the non-fluorescent carboxy-H_2-DCFDA is converted to the highly fluorophore DCF (Ex 485 nm/Em 518

nm). Therefore, cells were grown in media with supplements and allowed to adhere for 24h on 24-well plates. After replacing the media, cells were exposed to medium containing extracted plasma samples (pH 7.4) and allowed to grow for another 5h. Cells were washed twice with HBSS and were incubated at 37^{O}C with 5 µmol/L carboxy-H_2-DCFDA for 30 min. Fluorescence increment was monitored over time using the Ascent microplate fluorescence reader. Fluorescence intensity (FI) after 30 min was subtracted from bassline values and the resulting δFI was expressed as δFI/1x10^5 cells. The results are expressed as mean ± SD.

S9. Targeted metabolomics UHPLC-MS/MS analysis. Mobile phases were based on positive and negative detection ion modes and were performed in separated runs in scheduled multiple reaction monitoring (sMRM). Positive ion mode consisted of water and acetonitrile and both of them contained 0.5% formic acid, while the negative ion mode consisted of water containing 0.1% formic acid and 10 mM ammonium formate and acetonitrile. This targeted metabolomics analysis was able to detect and quantify more than 1,000 metabolites in a single short run using volumes as low as 2 µl of the bio-fluid samples. Metabolites were identified by using commercial standards if available or by using their predicted nominal masses, optimizing their fragmentation conditions and estimating their quantity by using the calibration curves of other structurally similar metabolites and isomers. Analytical validation was optimized by assessing the linearity of the calibration curves at 12 different concentration levels between 0.1-10,000 µg/L. More information about validation and analytic performance of the method can be found in previous publications [Behrendt et al 2022]. Quality controls composed by a pool of samples from the study were processed following the same procedures every 20 samples. Analyst 1.6.2 and Sciex OS software by Sciex were used for data acquisition and data processing, respectively. Finally, the coefficients of variation for areas, retention times and peak widths of the internal standards added to samples were calculated for analytical reproducibility assessment.

S10. Preprocessing of the metabolomics data. Metabolites with more than 30% of missing values were excluded from the analysis. For each metabolite, we calculated the fold change (FC) ratio between its concentration at the end of dietary intervention and its baseline measurement. Normal distribution of log_2FC in metabolites concentration was visually inspected. Afterwards, distances to the group centroid were computed based on Euclidean distances to remove outliers from the data matrix (±1.5×IQR). We used the R/Bioconductor package 'POMA' for preprocessing (10.1371/journal.pcbi.1009148).

S11. Basal expression of adhesion molecules on pancreatic cancer cells and secretion of cytokines. The expression of adhesion molecules such as integrins and selectins on cancer cells is one of the most important reasons of their migratory potential and therefore, their aggressivity. Circulating cancer cells were able to migrate across the endothelial barrier and settle down to establish a

secondary tumour. α- and ß-integrins, CAMs such as ICAM and VCAM as well as E-SEL (E-selectins) are targets for therapeutics to reduce migration and inhibit metastatic processes. Here, we investigated whether extracted plasma metabolites have an influence on expression levels of pancreatic cancer cells because we have previously shown, that only PANC-1 migration, but not AsPC-1 migration was reduced by incubating cells with plasma metabolites isolated from blood of volunteers who received a short-term ACN ingestion [Kuntz S et al 2017]. Comparing surface markers on the pancreatic cancer cell lines PANC-1 and AsPC-1, significant differences were observed. Compared to AsPC-1, PANC-1 expressed significantly higher levels of α3-integrin (398 ± 14), α4-integrin (117 ± 8), ß1-integrin (1623 ± 73), ß2-integrin (35 ± 2), ESEL (53 ± 3), ICAM-1 (361 ± 26) and VEGR-R (18 ± 2). In case of α3-integrin, ß1-integrin, and ICAM-1, the expression levels were 12-fold, 5-fold and 90-fold higher on PANC-1 than on AsPC-1 cells (Supplementary Figure 3). Adhesion of cancer cells to endothelial cells were not only influenced by the expression levels of CAMs, their secretion of cytokines and VEGF could also influence the capability of migration. As shown in Supplementary Figure 4, secretion of TNF-α, IL-1ß and VEGF from PANC-1 was significantly higher than the secretion from AsPC-1. After 36-h cultivation, TNF-α concentration in the supernatant of cultivated PANC-1 was 128 ± 11 pg/ml in comparison to that of AsPC-1 with 25 ± 2.9 pg/ml. This was also seen for IL-1ß (22 ± 1.9 to 15 ± 0.8) and VEGF (35 ± 1.2 to 19 ± 4.3), whereas IL-8 secretion was not different between both pancreatic cancer cell lines (52 ± 1.2 to 53 ± 4.8).

S12. Basal expression of adhesion molecules on endothelial cells and CYTOmix-induced expression. In addition to the expression of CAMs, the so-called microclimate of the tumour plays an essential role in the migration process of single tumour cells. In this context, the secretion of tumour cell associated cytokines which act on the endothelial barrier is another aspect that influences tumour aggressiveness. Binding of tumour cells with their CAMs to endothelial cells via the corresponding receptors could also be a result of the cancer cell specific microclimate. In order to investigate the effects of cytokines secreted from pancreatic cancer cells on HUVECs, HUVECs were exposed to a mixture of cancer cell specific cytokines (CytoMIX), which were detected before (see S11). Thereafter, expression levels of CAMs under basal und CytoMIX-stimulated cells were compared. As shown in Supplementary Figure 5, surface receptors on HUVECs under basal unstimulated conditions were expressed at very low levels. After a 36h stimulation with AsPC-1- CytoMIX (called `C1´) and PANC-1- CytoMIX (called ´C2´), only ß4-integrin and ICAM-1 expression were significantly enhanced compared to basal levels. AsPC-1- CytoMIX increased ß4-integrin and ICAM-1 0.2-fold and 2-fold, whereas the PANC-1- CytoMIX enhanced PANC-1 ß4-integrin and ICAM-1 0.3-fold and 9-fold. Concerning all other markers, AsPC-1- and PANC-1- CytoMIX have no significant effects on expression levels or other receptors on HUVECs (Supplementary Figure 5).

Supplementary Table 1: List of materials, biochemicals and kits used for cell culture assays

1290 Infinity UHPLC system	Agilent, XXX, U.S.A.
24-well plates	GreinerBioOne, Berlin, Germany
6-well plates	GreinerBioOne, Berlin, Germany
Accutase-solution	Promocell GmbH, Heidelberg, Germany
anti-human **REAfinity™ antibodies**	Miltenyi, Bergisch Gladbach, Germany
Ascent microplate fluorescence reader	ThermoScientific, Karlsruhe, Germany
AsPC-1	**ATCC (**LGC Standards GmbH), Wesel, Germany
Carboxy-H_2-DCFDA	Invitrogen GmbH, Darmstadt, Germany
CytoSelect™ 24-well Cell Migration Assay (8 µm), Colorimetric	CellBiolabs, San Diego, U.S.A.
Digicsan Reader	Asys, Eugendorf, Austria
DMEM (Dulbecco's modified Eagle's medium)	Invitrogen GmbH, Darmstadt, Germany
Endothelial growth medium II	Promocell GmbH, Heidelberg, Germany
FAK (Phospho) [pY397] Human ELISA Kit	ThermoScientific, Karlsruhe, Germany
Fetal bovine serum	PAA Laboratories GmbH, Cölbe, Germany
Fibronectin solution	Sigma-Aldrich Chemie GmbH, Taufkirchen, Germany
Formic acid	LGC Promochem, Wesel, Germany
GraphPad Prism Version 9	GraphPad Software, LLC, San Diego, U.S.A.
H1 microplate fluorescence reader	Biotec GmhH, Karlsruhe, Germany
HBSS	Invitrogen GmbH, Darmstadt, Germany
HUVECs	Promocell GmbH, Heidelberg, Germany
IgG1-REAfinity™ antibodies	Miltenyi, Bergisch Gladbach, Germany
Interleukin (IL-8) ELISA	ThermoScientific, Karlsruhe, Germany
Interleukin-1ß (IL-1ß) ELISA	ThermoScientific, Karlsruhe, Germany
Ion Drive Turbo V ion source	Sciex, XXX, U.S.A.

L-glutamine	Invitrogen GmbH, Darmstadt, Germany
Luna Omega Polar C18 column	Phenomenex, XXX, U.S.A.
MACS Running Buffer	Miltenyi, Bergisch Gladbach, Germany
MACS Quant 10 (MQ10)	Miltenyi, Bergisch Gladbach, Germany
Methanol	ThermoScientific, Karlsruhe, Germany
Micro-Spin Eppendorf filter (pore size 0.2 µm)	Eppendorf, Hamburg, Germany
Millicell® ERS volt-ohmmeter	Millipore Corporation, Bedford, U.S.A.
NF-kB InstantOne™ ELISA	ThermoScientific, Karlsruhe, Germany
SPE cartridge Oasis-HLB (5 mL/200 mg)	Waters, Inc., Eschborn, Germany
PANC-1	**ATCC (**LGC Standards GmbH), Wesel, Germany
PBS	Invitrogen GmbH, Darmstadt, Germany
Propidium iodide solution (PI)	Miltenyi, Bergisch Gladbach, Germany
R statistical software	R foundation, Vienna, Austria
RPMI 1640 medium (Roswell Park Memorial Institute)	Invitrogen GmbH, Darmstadt, Germany
Sodium pyruvate	Invitrogen GmbH, Darmstadt, Germany
TrypLE™ Express solution	ThermoScientific, Karlsruhe, Germany
Tumor necrosis factor-α (TNF-α) ELISA	ThermoScientific, Karlsruhe, Germany
Vascular endothelial growth factor (VEGF) ELISA	R&D Systems, Heidelberg, Germany

Supplementary Table 2: CONSORT 2010 checklist of information to include when reporting a randomised trial

Section/Topic	Item No	Checklist item	Reported on page No
Title and abstract			
	1a	Identification as a randomised trial in the title	1
	1b	Structured summary of trial design, methods, results, and conclusions (for specific guidance see CONSORT for abstracts)	2
Introduction			
Background and objectives	2a	Scientific background and explanation of rationale	2-3
	2b	Specific objectives or hypotheses	3
Methods			
Trial design	3a	Description of trial design (such as parallel, factorial) including allocation ratio	3, previously published [Behrendt et al 2022]
	3b	Important changes to methods after trial commencement (such as eligibility criteria), with reasons	No changes
Participants	4a	Eligibility criteria for participants	3, previously published [Behrendt et al 2022]
	4b	Settings and locations where the data were collected	3, previously published [Behrendt et al 2022]
Interventions	5	The interventions for each group with sufficient details to allow replication, including how and when they were actually administered	3, previously published [Behrendt et al 2022]
Outcomes	6a	Completely defined pre-specified primary and secondary outcome measures, including how and when they were assessed	4-5
	6b	Any changes to trial outcomes after the trial commenced, with reasons	No
Sample size	7a	How sample size was determined	3, previously published [Behrendt et al 2022]
	7b	When applicable, explanation of any interim analyses and stopping guidelines	
Randomisation:			
Sequence generation	8a	Method used to generate the random allocation sequence	3, previously published [Behrendt et al 2022]
	8b	Type of randomisation; details of any restriction (such as blocking and block size)	No block size
Allocation concealment mechanism	9	Mechanism used to implement the random allocation sequence (such as sequentially numbered containers), describing any steps taken to conceal the sequence until interventions were assigned	3, previously published [Behrendt et al 2022]
Implementation	10	Who generated the random allocation sequence, who enrolled participants, and who assigned participants to interventions	3, previously published [Behrendt et al 2022]
Blinding	11a	If done, who was blinded after assignment to interventions (for example, participants, care providers, those assessing outcomes) and how	3, previously published [Behrendt et al 2022]
	11b	If relevant, description of the similarity of interventions	no similarity
Statistical methods	12a	Statistical methods used to compare groups for primary and secondary outcomes	5
	12b	Methods for additional analyses, such as subgroup analyses and adjusted analyses	5
Results			

Participant flow (a diagram is strongly recommended)	13a	For each group, the numbers of participants who were randomly assigned, received intended treatment, and were analysed for the primary outcome	Supplemental Data
	13b	For each group, losses and exclusions after randomisation, together with reasons	Supplemental Data
Recruitment	14a	Dates defining the periods of recruitment and follow-up	3, previously published [Behrendt et al 2022]
	14b	Why the trial ended or was stopped	
Baseline data	15	A table showing baseline demographic and clinical characteristics for each group	6, previously published [Behrendt et al 2022]
Numbers analysed	16	For each group, number of participants (denominator) included in each analysis and whether the analysis was by original assigned groups	6-7, Supplements
Outcomes and estimation	17a	For each primary and secondary outcome, results for each group, and the estimated effect size and its precision (such as 95% confidence interval)	6-7, Supplements
	17b	For binary outcomes, presentation of both absolute and relative effect sizes is recommended	
Ancillary analyses	18	Results of any other analyses performed, including subgroup analyses and adjusted analyses, distinguishing pre-specified from exploratory	6-7, Supplements
Harms	19	All important harms or unintended effects in each group (for specific guidance see CONSORT for harms)	
Discussion			
Limitations	20	Trial limitations, addressing sources of potential bias, imprecision, and, if relevant, multiplicity of analyses	7
Generalisability	21	Generalisability (external validity, applicability) of the trial findings	7
Interpretation	22	Interpretation consistent with results, balancing benefits and harms, and considering other relevant evidence	7-8
Other information			
Registration	23	Registration number and name of trial registry	3
Protocol	24	Where the full trial protocol can be accessed, if available	3, previously published [Behrendt et al 2022]
Funding	25	Sources of funding and other support (such as supply of drugs), role of funders	1,8

Supplementary Table 3: MultiColor 8 x 8 compensation matrix. Anti-REA MACS Comp Bead Kit was used for compensation of fluorescence spillover of fluorochrome-conjugated REAfinity™ antibodies. Diluted (1:10 or 1:50) REAfinity™ fluorochrome-conjugated antibodies were incubated for 10 min in dark at room temperature with 50 µl anti-REA `Comp Beads´ or 50 µl blank `Comp Beads´. After incubation, 1 ml MACSQuant running buffer was added to the reaction and fluorescence spillover was automated measured with MQ10. Spillover matrix was saved as instrument settings for PANC-1, AsPC-1 and HUVEC. Individual fluorescence signals were organized in columns and fluorescence channels in rows (8x8).

	VioBlue	VioGreen	FITC	PE	PerCP-Vio770	PE-Vio770	APC	APC-Vio770
V1	1.0	0.0	0.0	0.0	0.0	0.0	0.0	0.0
V2	0.0	1.0	0.0	0.0	0.0	0.002	0.0	0.0
B1	0.0	0.0	1.0	0.029	0.0	0.007	0.0	0.0
B2	0.0	0.0	0.08	1.0	0.0	0.028	0.0	0.0
B3	0.0	0.0	0.016	0.207	1.0	0.0	0.013	0.001
B4	0.0	0.0	0.002	0.022	0.0	1.0	0.002	0.014
R1	0.0	0.0	0.0	0.0	0.0	0.003	1.0	0.053
R2	0.0	0.0	0.0	0.0	0.0	0.114	0.144	1.0

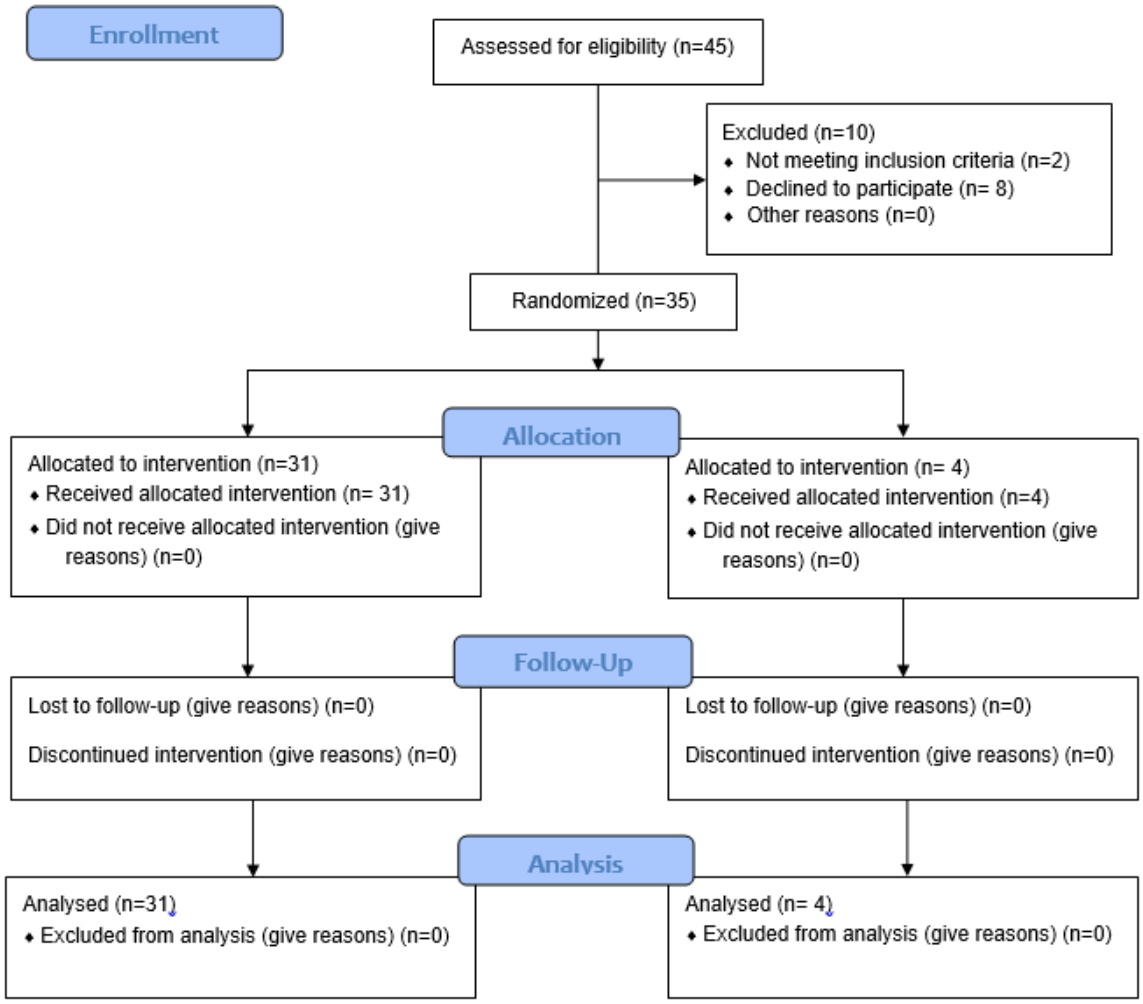

Supplementary Figure 1: CONSORT flowchart diagram.

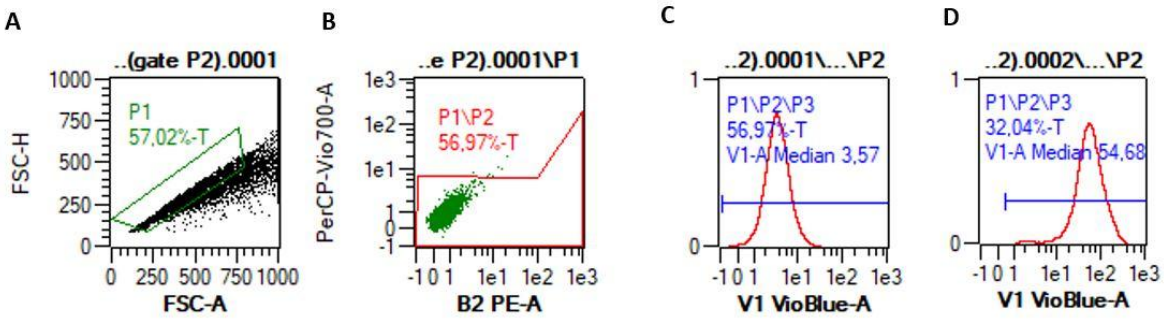

E

Path	V1 VioBlue-A Mean	B1 FITC-A Mean	B2 PE-A Mean	PE-Vio770-A Mean	R1 APC-A Mean	APC-Vio770-A Mean
P1\P2\P3	4,09	2,61	0,64	0,34	0,50	0,53
P1\P2\P4	4,09	2,61	0,64	0,34	0,50	0,53
P1\P2\P5	4,09	2,61	0,64	0,34	0,50	0,53
P1\P2\P6	4,09	2,61	0,64	0,34	0,50	0,53
P1\P2\P7	4,09	2,61	0,64	0,34	0,50	0,53
P1\P2\P8	4,09	2,61	0,64	0,34	0,50	0,53

F

Path	V1 VioBlue-A Mean	B1 FITC-A Mean	B2 PE-A Mean	PE-Vio770-A Mean	R1 APC-A Mean	APC-Vio770-A Mean
P1\P2\P3	63,21	12,93	30,70	31,44	10,15	37,89
P1\P2\P4	63,24	13,13	31,26	31,95	10,28	38,16
P1\P2\P5	64,21	14,57	35,89	36,04	11,43	39,82
P1\P2\P6	64,05	14,45	34,22	36,17	11,36	39,66
P1\P2\P7	64,29	14,70	34,90	36,50	11,75	40,03
P1\P2\P8	63,26	12,97	30,82	31,57	10,17	37,97

Supplementary Figure 2. Gating strategy and quantification. (A) Cells were gated by FSC(A) *vs.* FSC(H) plot: Gating the cells that have an equal area and height, thus removing clumps (greater FSC(A) relative to FSC(H)) and debris (very low FSC) [P1-marker]; **(B)** PerCP-Vio770 *vs.* B2-channal plot: broad selection of living cells (P2 marker) and exclusion of dead cells stained with propidium iodide [P2-marker]; **(C)** Histogram plots of unstained cells in V1-channel (CD104); **(D)** Histogram plots of unstained cells in V1-channel (CD104); Histogram markers were used to quantify the main fluorescence intensity (means with SD or median with SD) for **E)** unstained and **(F)** stained cells [representative staining panel 1].

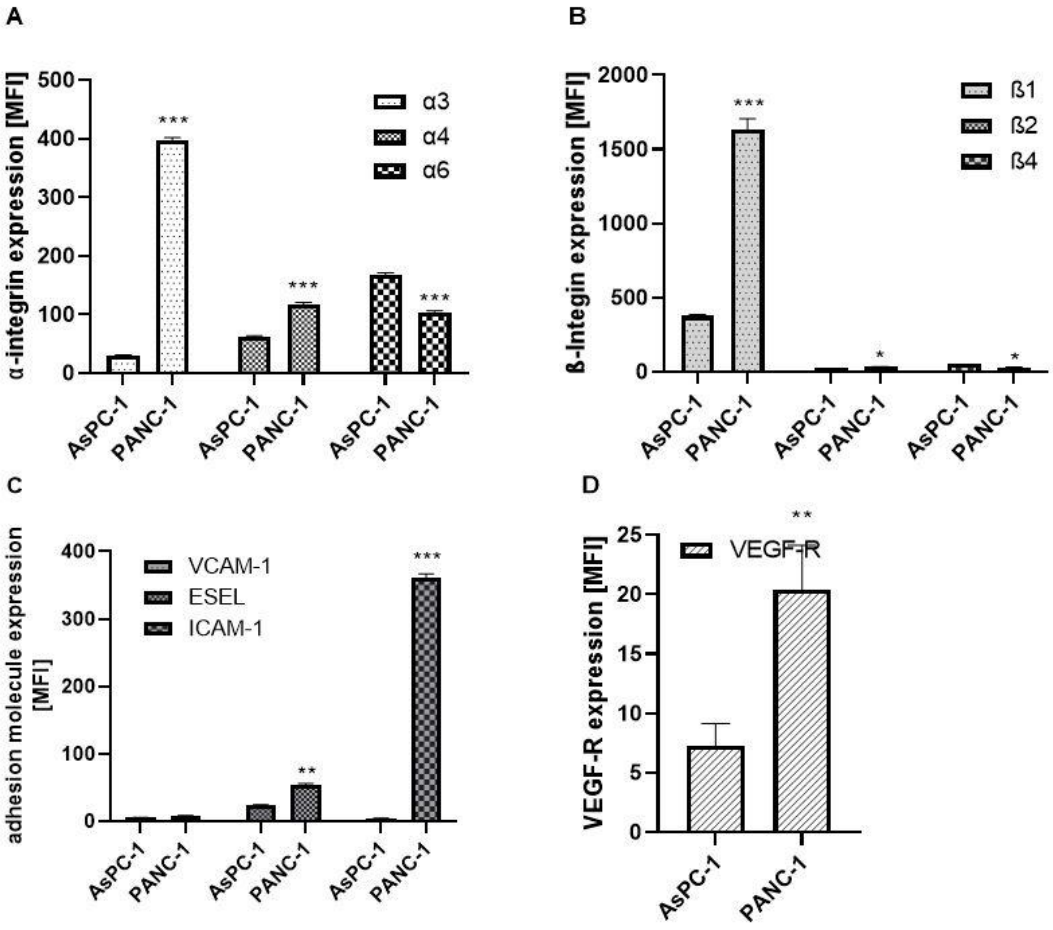

Supplementary Figure 3. Protein expression of adhesion molecules and markers on PANC-1 and AsPC-1 *in vitro*. Expression levels of α-integrins **(A)**, ß-integrins **(B)**, CAMs and E-SEL **(C)** and VEGF-R **(D)** on the cell surface of pancreatic cancer cells were measured under basal conditions. PANC-1 and AsPC-1 cells were seeded onto 6-well plates ($1x10^5$ cells/mL) and allowed to adhere for 24 h. Thereafter, medium was changed and cells grow for further 36h in corresponding medium. After incubation, medium was removed, cells were washed twice with PBS, detached with 1 ml TrypLE™ Express solution and centrifuged at 300xg for 5 min at RT. Cells were resuspended in MACS-Running buffer and expression levels were measured after cells were stained with anti-human REA-antibodies coupled with fluorochromes by flow cytometry as described in the Methods section (see 2.4.2.). Values are expressed as means of main fluorescence intensity (MFI) with standard deviation (means ± SD). Significant differences between the pancreatic cancer cell lines were calculated with One-way ANOVA and values were different with $P^* < 0.05$, $P^{**} < 0.01$ and $P^{***} < 0.001$ (n=3 in duplicates).

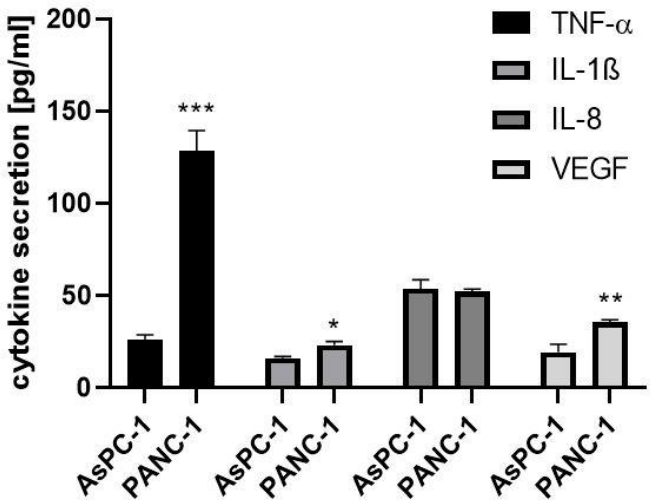

Supplementary Figure 4. Secretion of cytokines and VEGF from PANC-1 and AsPC-1 *in vitro*. PANC-1 and AsPC-1 were seeded onto 6-well plates (1 x 10^5 cells/mL) and allowed to adhere for 24h. Thereafter, medium was changed and cells grow for further 36h in corresponding medium. After incubation, supernatant was removed and centrifugated (1,500xg, 5 min, RT). Protein levels were measured by ELISA as described in the Methods section (see 2.4.2.). Values are expressed as means of secreted proteins as pg/ml ± standard deviation (means ± SD). Significant differences between the pancreatic cancer cell lines were calculated with One-way ANOVA and values were different with $P^* < 0.05$, $P^{**} < 0.01$ and $P^{***} < 0.001$ to corresponding controls (n=3 in duplicates).

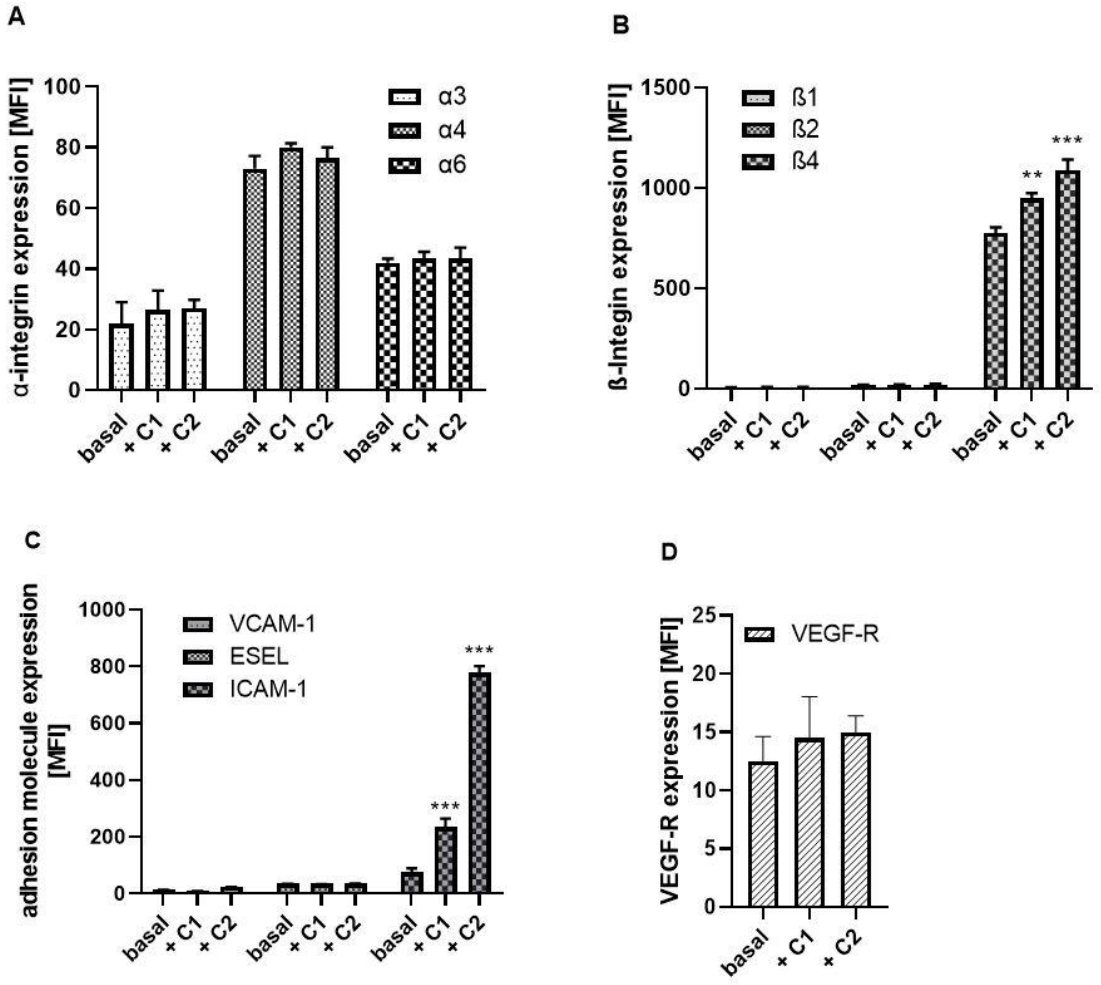

Supplementary Figure 5. Expression of adhesion molecules and markers on basal (unstimulated) and CYTOmix-stimulated HUVEC *in vitro*. Expression of α-integrins **(A)**, ß-integrins **(B)**, CAMs and ESEL **(C)** and VEGF-R **(D)** on cell surface of HUVECs were measured under basal (unstimulated) or stimulated conditions (´C1´ or ´C2´). HUVECs were seeded onto fibronectin (0.1%)-coated 6-well plates (5 x 10^5 cells/mL) and allow to grow to confluence. After reaching confluence, medium was changed and cells grow for further 36h in corresponding medium with AsPC-1-CYTOmix (C1: 25 pg/ml TNF-α, 15 pg/ml IL-1ß, 50 pg/ml IL-8, 20 pg/ml VEGF) or PANC-1-CYTOmix (C2: 130 pg/ml TNF-α, 25 pg/ml IL-1ß, 50 pg/ml IL-8, 35 pg/ml VEGF). Thereafter, cells were washed twice with PBS, detached with 1 ml accutase-solution and centrifuged at 220xg for 3 min at RT. Cells were resuspended in MACS-Running buffer and expression levels were measured after cells were stained with anti-human REA antibodies coupled with fluorochromes by flow cytometry as described in the Methods section (see 2.4.2.). Values are expressed as means of MFI ± standard deviation (means ± SD). Significant differences between basal and CYTOmix-stimulated cells were calculated with One-way ANOVA and values were different with *P**< 0.05, *P***< 0.01 and *P****< 0.001 (n=3 in duplicates).

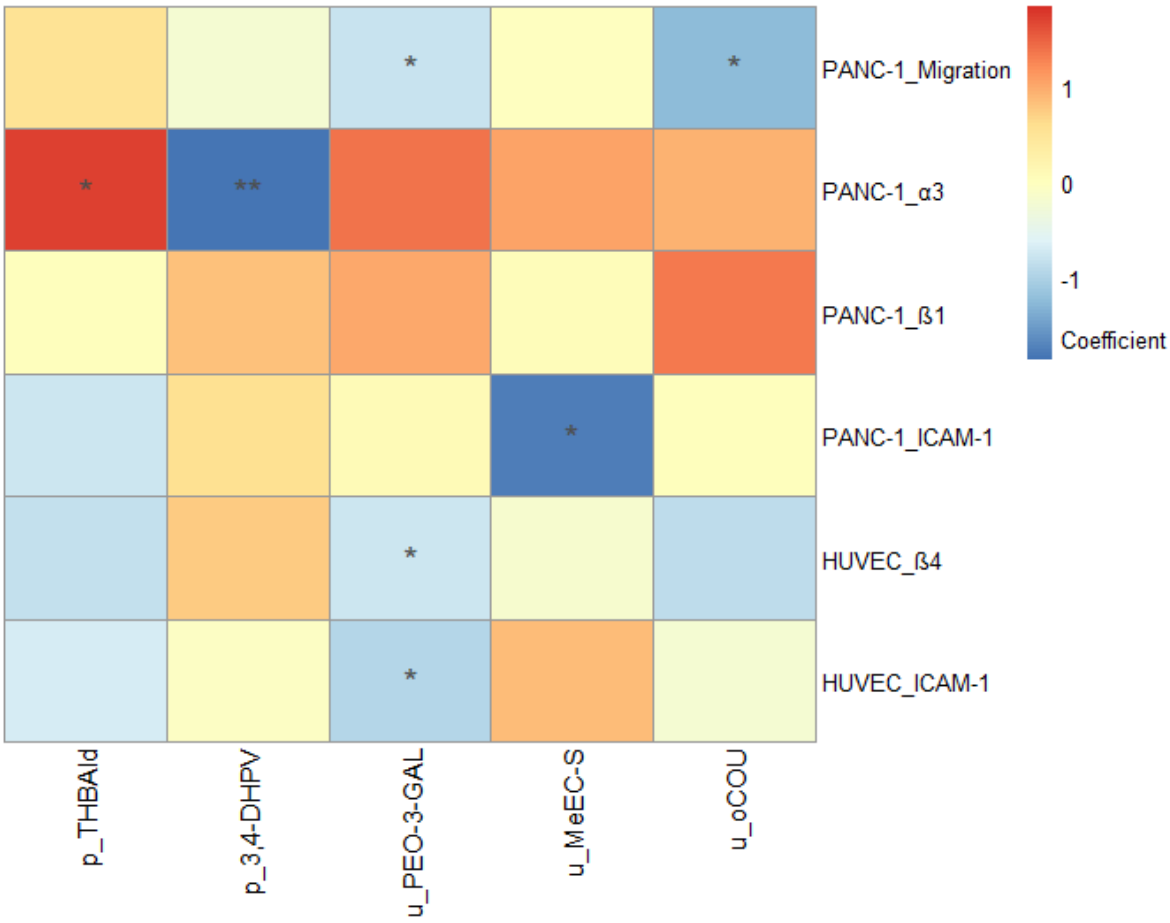

Supplementary Figure 6. Heatmap showing the association between cancer cells analyses and plasma and urine metabolites altered by the ACN-rich juice. Assessed using linear mixed models with participants as random effects adjusting by age, sex, and treatment. p_: plasma metabolite; u_: urine metabolite; THBAld: 2,4,6-trihydroxybenzaldehyde; 3,4-DHPV: 3',4'-dihydroxyphenyl-γ-valerolactone; PEO-3-GAL: peonidin 3-galactoside; MeEC-3-S: 3'-methyl(epi)catechin sulphate; oCOU: o-coumaric acid. *: *p*-value <0.05; **: P-value <0.01. Metabolites included in the heatmap are those with at least one statistically significant association.

Anhang C

Supplemental Material:

Grape/blueberry anthocyanins and their gut-derived metabolites attenuate LPS/nigericin-induced inflammasome activation by inhibiting ASC speck formation in THP-1 monocytes.

Behrendt I, Röder I, Will F, Michel G, Friedrich E, Grote D, Martin Z, Dötzer H.P., Fasshauer M, Speckmann M, Kuntz S. *Metabolites* **2024**, 14, 203. doi:10.3390/metabo14040203.

Journal impact factor: 4.1

Grape/Blueberry Anthocyanins and Their Gut-Derived Metabolites Attenuate LPS/Nigericin-Induced Inflammasome Activation by Inhibiting ASC Speck Formation in THP-1 Monocytes

Inken Behrendt [1,*], Isabella Röder [2], Frank Will [2], Gabriela Michel [3,4], Daniela Grote [1], Zoe Martin [1], Hanna Pauline Dötzer [1], Mathias Fasshauer [1], Martin Speckmann [3,4] and Sabine Kuntz [1]

[1] Institute of Nutritional Science, Justus-Liebig-University Giessen, 35390 Giessen, Germany; grote.d@outlook.de (D.G.); martin.zoe@gmx.de (Z.M.); hanna.doetzer@t-online.de (H.P.D.); mathias.fasshauer@ernaehrung.uni-giessen.de (M.F.); sabine.kuntz@nutr.jlug.de (S.K.)
[2] Department of Beverage Research, Hochschule Geisenheim University, 65366 Geisenheim, Germany; isabella.roeder@googlemail.com (I.R.); frank.will@hs-gm.de (F.W.)
[3] Institute for Clinical Immunology, Transfusion Medicine and Hemostaseology, Justus-Liebig-University Giessen, 35392 Giessen, Germany; gabriela.michel@immunologie.med.uni-giessen.de (G.M.); martin.speckmann@immunologie.med.uni-giessen.de (M.S.)
[4] Flow Cytometry Core Facility, Department of Medicine, Justus-Liebig-University Giessen, 35392 Giessen, Germany
* Correspondence: inken.behrendt@ernaehrung.uni-giessen.de; Tel.: +49 641 9939067

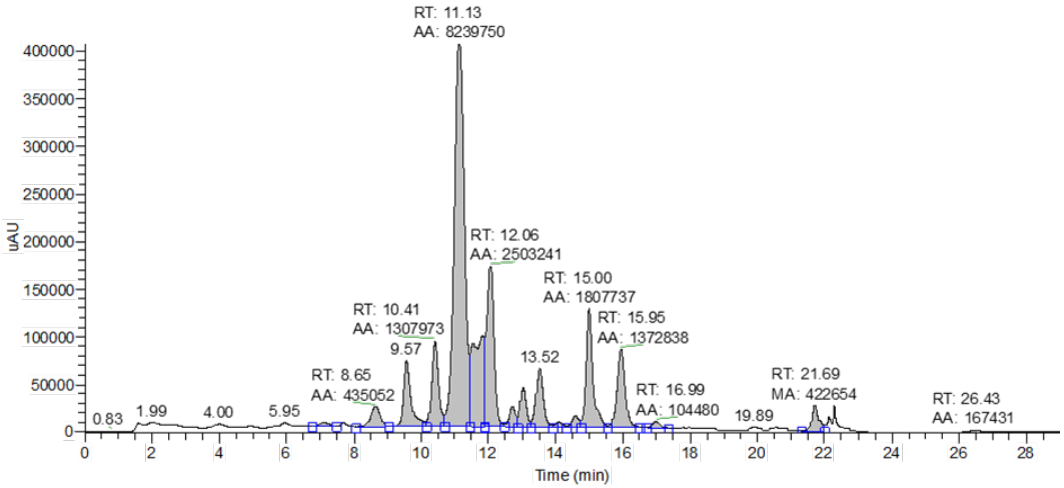

Figure S1. Representative HPLC-PDA/ESI-MS chromatogram of the powdered anthocyanin-rich grape/blueberry extract. Identified anthocyanins according to their retention times (RT): 7.10, Delphinidin-3,5-diglucoside; 8.65, Cyanidin-3,5-diglucoside; 9.57, Delphinidin-3-galactoside; 10.41, Delphinidin-3-glucoside; 11.13, Peonidin-3,5-diglucoside; 11.84, Delphinidin-3-arabinoside; 12.06, Malvidin-3,5-diglucoside; 12.72, Petunidin-3-galactoside; 13.03, Cyanidin-3-arabinoside; 13.52, Petunidin-3-glucoside; 14.10, Peonidin-3-galactoside; 14.59, Petunidin-3-arabinoside; 15.00, Peonidin-3-glucoside; 15.95, Malvidin-3-glucoside; 16.99, Malvidin-3-arabinoside; 21.69, Malvidin-3-(6"-coumaryl)-5-diglucoside.

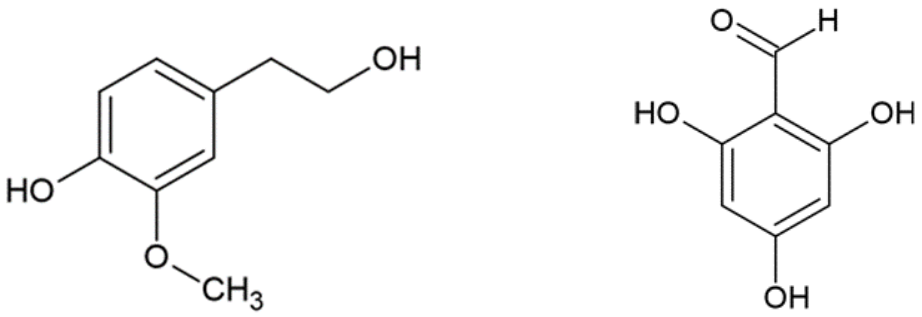

(**a**) (**b**)

Figure S2. Molecular structures of gut-derived anthocyanin metabolites. (**a**) Homovanillyl alcohol (HVA) and (**b**) 2,4,6-trihydroxybenzaldehyde (THBA). Molecular strtuctures were drawn with ChemSketch version 14.00, Advanced Chemistry Development, Inc. (ACD/Labs), Toronto, ON, Canada, www.acdlabs.com.

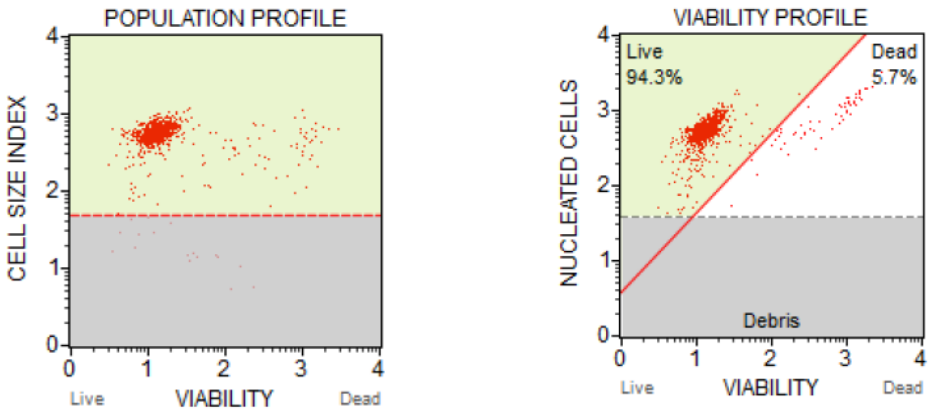

(**a**) (**b**)

Figure S3. Gating strategy to assess cell viability. (**a**) To exclude cellular debris cells were first gated based on their cellular size (horizontal line). (**b**) Then nucleated cells were gated (angled marker) for their staining with the membrane-permeant DNA staining dye, that stains all cells with a nucleus (nucleated cells), and a DNA-binding dye, that stains dead and dying cells which have lost their membrane integrity (viability), to discriminate live and dead cells.

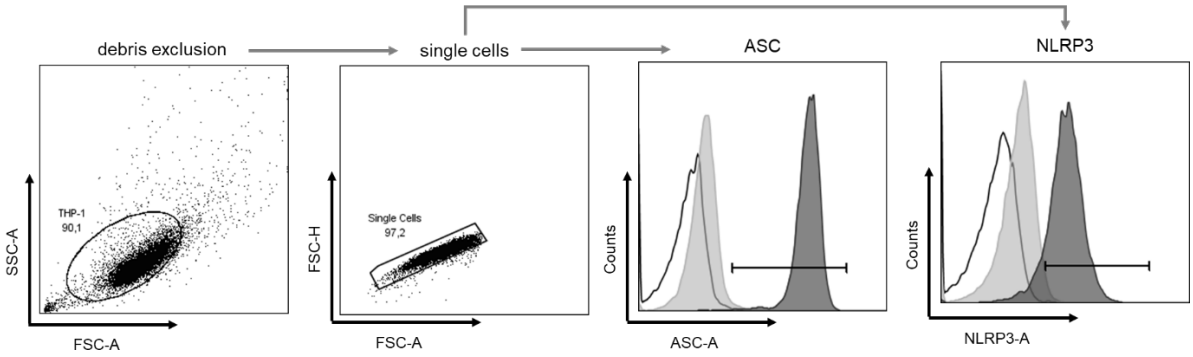

Figure S4. Gating strategy to assess ASC and NLRP3 protein expression. To exclude debris, cells were first gated using forward light scatter-area (FSC-A) versus side scatter-area (SSC-A). Next, FSC-A versus FSC-height (FSC-H) was used to perform doublet exclusion. Single cells were then gated for ASC and NLRP3 expression compared to the matching isotype control and median fluorescence intensity (MFI) was assessed. Open histogram unstained, light grey filled histogram matching isotype control, dark grey filled histogram stained.

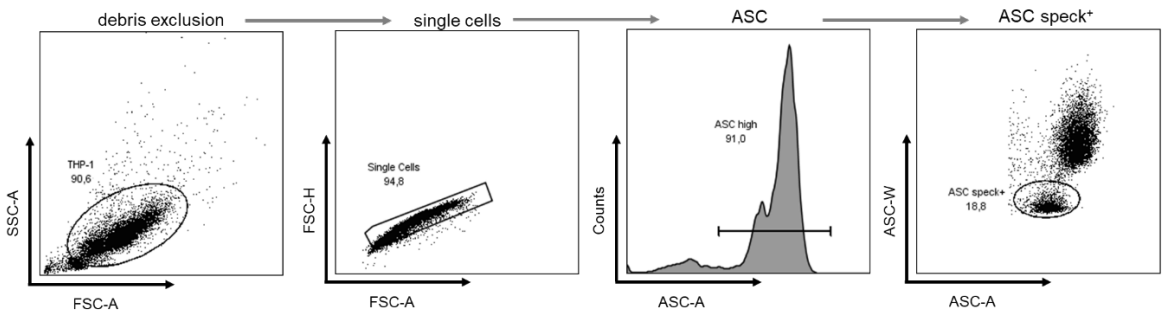

Figure S5. Gating strategy to assess ASC speck formation. ASC high expressing cells were gated as indicated in Figure S3. ASC high cells were further gated using ASC fluorescence pulse area (ASC-A) and ASC fluorescence pulse width (ASC-W). ASC speck forming cells were selected via the observed reduction in ASC-W and the percentage of ASC speck positive cells was quantified.

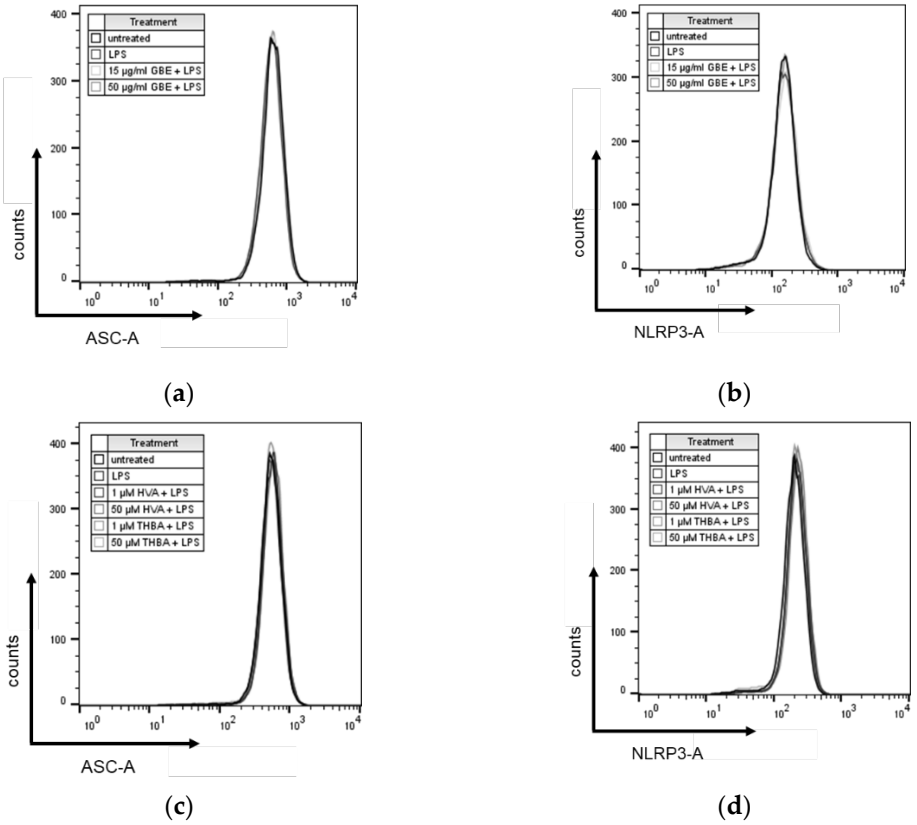

Figure S6. Effect of grape/blueberry anthocyanins and their gut-derived metabolites on ASC and NLRP3 protein expression in THP-1 cells. THP-1 monocytes were pretreated with the indicated concentrations of grape/blueberry anthocyanins and their gut-derived metabolites, before cells were primed with LPS as mentioned in the methods section. Protein expression of (**a,c**) ASC and (**b,d**) NLRP3 was assessed as median fluorescence intensity (MFI) by intracellular flow cytometry. The presented histogram overlays depict representative results from one of at least three replicated experiments.

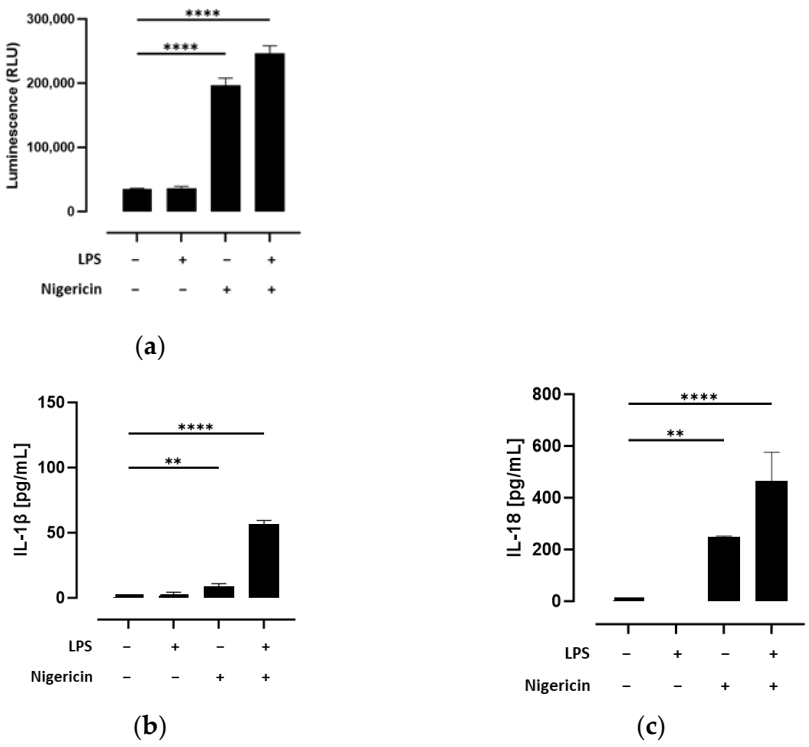

Figure S7. NLRP3 inflammasome activation in THP-1 cells. THP-1 monocytes were left untreated or primed with 10 ng/ml LPS for 4 h before the inflammasome was activated by adding 10 μM nigericin for further 40 min. (**a**) Caspase-1 activity was measured by using the Caspase-Glo® 1 Inflammasome Assay and luminescence was measured. Release of (**b**) IL-1β and (**c**) IL-18 into the cell culture supernatant were measured by ELISAs. Data are presented mean ± SD of at least three replicated experiments. Significant differences compared to the untreated control were calculated using one-way ANOVA, followed by Dunnett's multiple comparison test. $^{**}p < 0.01$ and $^{****}p < 0.0001$. RLU, relative light unit. RLU, relative light unit.